UNIVERSITÀ DEGLI STUDI DI MILANO
FACOLTÀ DI MEDICINA E CHIRURGIA

DOTTORATO DI RICERCA IN FISIOLOGIA
Settore scientifico disciplinare BIO-09

CICLO XXVI

EFFECTS OF GENERAL ANESTHETICS ON VISUAL CORTEX EVOKED AND RESTING ACTIVITY

Tesi di Dottorato di Ricerca di:
Dott. Alessandro Arena
matr. R09123

Tutor: Professor Antonio Malgaroli
Università Vista-Salute San Raffaele

Coordinatore: Professor Michele Mazzanti

Anno Accademico 2013-2014

CONSULTAZIONE TESI DI DOTTORATO DI RICERCA

Il sottoscritto Arena Alessandro n° matr. R09123

nato a Sesto San Giovanni (MI) il 30/09/1984

autore della tesi di Dottorato di Ricerca dal titolo:

EFFECTS OF GENERAL ANESTHETICS ON VISUAL CORTEX EVOKED AND RESING ACTIVITY

AUTORIZZA
la consultazione della tesi stessa, fatto divieto di riprodurre, in tutto o in parte, quanto in esso contenuto.

Data 07/05/2014 Firma .....

A Martina,

che l'immaginazione sia l'unico limite

ABSTRACT

Even though anesthetics are widely used in the medical practice, there are still unresolved issues which relate to their mechanisms of action and therefore to their ability to induce loss of consciousness. Since a large number of very different chemical molecules are used in general anesthesia, a large variety of potential molecular targets might exist. Some of these might relate to axonal conduction and membrane excitability. In some cases, this action could either occur at the presynaptic level, modifying the neurotransmitter release and reuptake machineries, or at the postsynaptic level, modifying the number and/or sensitivity of post-synaptic receptors. These functional alterations might also selectively affect one or more specific neuronal phenotypes.

Nevertheless, despite the complexity of their molecular targets, all general anesthetics induce a profound inhibition of the awake functions without suppressing the cortical EEG activity and sparing evoked cortical responses. Therefore, anesthetics should lead to the loss of consciousness by altering the signal processing of the brain, rather than by abolishing its activity. Based on these considerations, I began the investigation of the electrophysiological alterations induced by various classes of general anesthetics, on the activity of the rat visual system to uncover some aspects of their mechanisms of action.

In this project I compared the effects of three states of anesthesia induced by two different molecules, sevofluorane, a volatile general anesthetic, and propofol, which is intravenously injected. For these experiments rats were curarized, mechanically ventilated and the body temperature was controlled. During states of anesthesia, visual evoked potentials were recorded by means of superficial electrodes implanted in the skull. Two functional properties of the visual processing were evaluated: i) the sensitivity to stimuli of different brightness and ii) the dichotomy of the ON/OFF response, which is essential for contrast detection. Moreover, the EEG resting activity was recorded. The preliminary results showed that the overall basal cortical activity was reduced in a comparative manner between the two drugs throughout the three states of anesthesia. Otherwise, significant differences were found in the power of alpha and gamma EEG oscillations and in the effects on the visual evoked activity, suggesting the presence of two very distinct circuital mechanisms of action and providing novel information about the ability of anesthetics to induce loss of consciousness.

CONTENTS

1 INTRODUCTION

Drugs currently used to induce and maintain general anesthesia are known to provide three main effects, namely analgesia, muscle relaxation, and unconsciousness. The latter effect, which is sometimes referred to as "hypnotic", is of paramount importance, since relates to unconsciousness which is the main characteristic of general anesthesia and deep sedation. In all reports where the mechanism of action of general anesthetics has been addressed, the hypnotic effect proved to be the most elusive and difficult to study. This is not an unexpected finding, since the mechanism underlying consciousness itself is not clearly understood. In fact, the "perturbation" of consciousness induced by hypnotics may shed light on such mechanisms. Although some progress has been made, our knowledge of the molecular basis of the action of hypnotics (Herold & Hemmings, 2012) (Bertaccini & Trudell, 2012) and their site of action in the brain is still fragmented (Mhuircheartaigh et al., 2010) (John & Prichep, 2005) (Franks, 2008). In particular, the effects of general anesthetics on the responsiveness of brain to sensory stimuli are still incompletely described. It is well recognized how sensory stimuli produce activation of the cerebral cortex during anesthesia at surgical levels, when unconsciousness is clinically accepted. This observation added to the increasing consensus that anesthesia causes unconsciousness by blocking the brain's ability to integrate information, rather than by preventing information from reaching the brain (Alkire et al.,2008). Nevertheless cortical activation during general anesthesia differs in many respects from that occurring in awake subjects and these differences provide clues to understand the mechanism of action of general anesthetics.

At the present time, sensory evoked potentials are probably one of the most effective instruments to address this topic at both clinical and experimental level. Visual evoked potentials (VEPs) in the rat are particularly suitable for studying anesthetic effects, since rat responses to light stimuli are still robust during sleep and throughout several concentration of different anesthetic and narcotic drugs

(Meeren et al., 1998) (Hudetz & Imas, 2007) (Kuroda et al., 2009). The study of VEPs study also some practical usefulness in the clinical setting, since the reliability of using VEPs for intraoperative neurophysiological monitoring during surgical manipulation along the visual pathway has been well established (Ota et al., 2010) (Kodama et al., 2010). Nevertheless VEPs have been more extensively characterized in the experimental setting. Late potentials (> 100-200ms) in response to stimuli are commonly considered as an expression of signal integration and a possible hallmark of consciousness (Sergent et al., 2005). General anesthetics suppress this long-latency response in VEPs in a dose-dependent manner (Hudetz, et al., 2009). Conversely, the effect of general anesthetics on the early short-latency responses of VEP, that are the expression of sensory input processing of the cortex (Meeren et al., 1998), is somewhat more puzzling.

In the present work I analyzed the effect of general anesthetics onto resting EEG activity and on the early (<200ms) VEP response in rats and compared the effects of sevoflurane (1,1,1,3,3,3-hexafluoro-2-(fluoromethoxy)propane, an halogenated ether) with those of propofol (2,6-diisopropylphenol, an alkylphenol). I chose these two drugs because they are probably the most representatives of the inhalational and intravenous anesthetics respectively used in the clinical practice. Moreover, besides studying effects of these two drugs on the ON response to light pulses, I also investigated the effect on the OFF response occurring after the end of stimulation. To my knowledge, the results I'm presenting here are novel and some of the aspects, including the analysis of the effect of anesthetics on the OFF response of the VEP, has never been previously addressed.

1.1 ACTION OF GENERAL ANESTHETICS

1.1.1 Molecular targets

Since a large number of very different chemical molecules can produce general anesthesia, from simple gases to more complex barbiturates, a large variety of potential molecular targets might exist. Theoretically, the action of general

anesthetics might impact the following neuronal functional mechanisms: 1) the mechanisms underlying the resting membrane potential, 2) at the membrane excitability level, modifying the axonal conduction of the cell and therefore, its likelihood of generating and/or propagating action potentials, 3) at a presynaptic level, modifying the neurotransmitter release and reuptake machineries, 4) at the postsynaptic level, modifying the number and/or sensitivity of post-synaptic receptors. These functional alterations might be general or affect selectively one or more subsets of neuronal phenotypes. For example, to explain their silencing action we might envisage the inhibition of glutamatergic synapses or the enhancement of GABAergic synapses or other inhibitory networks. Over the years, a large numbers of putative target molecules have been proposed and intensely investigated, but interestingly, only a few of them were considered influent for the anesthetic action (Franks, 2008).

The $GABA_A$ receptor (γ-aminobutyric acid type A receptor) is one of the most reasonable candidate as an anesthetic target because of its widespread availability in the central nervous system, particularly at the post-synaptic level where it generates Cl^- currents in response to binding with GABA (γ-aminobutyric acid) neurotransmitter. $GABA_A$ receptor is a member of the ligand-gated ion channels family, it is composed by 5 sub-units (two α sub-units, two β and one γ) and the combination of the different sub-unit isoforms defines the properties of the channel, such agonist affinity or conductance. The most abundant combination presents the sub-unit isoforms α_1 β_2 γ_2. With the exception of small and apolar molecules such xenon, it's been found that the majority of general anesthetics, including sevoflurane and propofol, bind and potentiate and/or directly activate $GABA_A$ receptor (Nishikawa & MacIver, 2001) (Bieda & MacIver, 2004) (Franks, 2008) (de Sousa et al., 2000). By generating specific mutations in the sub-units, it's been found that the α sub-unit is the main binding region of volatile anesthetics, while modifications in the β sub-unit can somehow reduce the effect of both volatile and intravenous anesthetics (Mihic et al., 1997) (Franks, 2008).

Some reports show that the inhibitory action of volatile anesthetics is in part mediated also by the two-pore-domain K^+ channels (2PK). This transmembrane dimeric channel family contribute to control the resting potential and therefore the

cellular excitability. Five member of this family (TREK1, TREK2, TASK1, TASK3 and TRESK) are directly activated by volatile anesthetics such halothane, isoflurane, desflurane and sevoflurane, even if with different selectivity among the channels. Otherwise, intravenous anesthetic seems to modify the 2PK functioning only minimally (Liu et al., 2004) (Franks, 2008).

Another relevant mechanism by which general anesthetics could reduce the brain activity, is the inhibition of excitatory synapses. Indeed, it's been reported that the glutammategic synapses are important targets of some anesthetic molecules. Specifically, the NMDA (*N*-methyl-$_D$-aspartate) receptor, which mediate the late component of excitatory synaptic transmission, is inhibited by ketamine and volatile anesthetics, including sevoflurane (Solt et al., 2006) (Liu et al., 2001) (Hollmann et al., 2001) (Franks, 2008).

In all likelihood, general anesthetics affect the activity of other molecules, for example volatile anesthetics could reduce the release of glutamate by inhibiting voltage-gating Na^+ channels or other presynaptic machinery (Maclver et al. 1996) (Herold & Hemmings, 2012). Otherwise, since exposure to clinical doses of anesthetics is far from completely shutting down the electrical brain activity, the simple knowledge about their molecular mechanisms cannot fully account for their ability to induce the loss of consciousness.

1.1.2 Systemic alterations

Information that potentially clarifies the hypnotic effect of general anesthetics, comes from similarities between the anesthetized brain and other states of loss of consciousness which brain can assume, such as during the non-rapid-eye-movement (NREM) sleep. It is well known that during NREM sleep, the voltage oscillations of the electroencephalogram (EEG) recorded by scalp electrodes, change dramatically relative to those recorded during awareness state (Alkire et al., 2008). During waking, neurons of the ascending activating system, which origin from various nuclei of the upper brainstem, basal forebrain and posterior hypothalamus and which release various neurotransmitters (such as acetylcholine, norepinephrine and serotonin), depolarize persistently the relay cells of the

thalamus (thalamic-cortical, TC, neurons). This depolarization promotes the tonic activity of the TC neurons, which transmit the sensory information to the cortex. Cortical neurons, which also receive innervations from the ascending activating system, elaborate and integrate such sensory information by a sustained firing activity which can be recorded by EEG scalp electrodes, resulting in a low voltage and fast oscillation (20-80Hz) activity (Steriade et al., 1993). During both NREM sleep and general anesthesia, the EEG activity changes into a bi-stable pattern, where delta (1-4Hz) middle and fast oscillations are grouped by slow-waves (0,5-1Hz) into complex-wave sequences (Steriade, 2006) (Alkire et al., 2008). The resulting EEG activity is composed by a slow alternation (~1Hz) between down-state epochs, without cortical activity, possibly due to a reduction of extracellular Ca^{2+} in cortical and thalamic-cortical networks (Massimini & Amzica, 2001) and up-state epochs, characterized by sustained cortical activity which gives rise to groups of delta (1-4Hz), spindle (12-15Hz) and, less frequently, even gamma (~40Hz) waves (Steriade, 2006).

Spindles are an electroencephalographic landmark for the transition from wakefulness to sleep. These oscillation are generated when the ascending activating systems reduce both their excitatory action on TC neurons and their inhibitory action on the GABAergic neurons of the reticular thalamic nucleus (RT neurons). This change in the state of the thalamus, triggers a reverberating loop of activity among the RT neurons, TC neurons and cortical-thalamic neurons. RT neurons directly inhibit TC neurons and receive excitatory projections from TC cells, while cortical-thalamic neurons receive excitatory innervations from TC neuron and send feedback excitatory projections to both RT and TC neurons. In RT cells rhythmic inhibitory bursts at spindle frequency, are generated by low-threshold Ca^{2+} spikes. This periodic inhibition forces the activity of TC neurons into a bursting mode that is transferred directly back to the RT neurons, facilitating the rhythm, and forward to the cortex, where the excitatory postsynaptic potentials produce the EEG spindle waves (Steriade et al., 1993). TC neurons undergo progressive hyperpolarization and during the late stage of NREM sleep, spindles are reduced and single TC neurons generate the delta rhythm by the interplay of two intrinsic currents, the hyperpolarizing-activated cation

current (I_h) and the transient-low threshold Ca^{2+} current (I_t). This slow activity pattern is transferred to the cortex, which cortical-thalamic feedback synchronize and potentiate the oscillations, generating the large amplitude EEG delta waves (Steriade et al., 1993).

The administration of general anesthetics also produces similar EEG oscillations and it has been proposed that the thalamic inhibition and the resulting rhythmical activity could block sensory information flow, playing a key role in the loss of consciousness (Franks, 2008) (Alkire & Miller, 2005). This hypothesis is supported by neuroimaging studies which revealed similarities in the reduction of relative cerebral blood flow (rCBF) between states of loss of consciousness induced by general anesthetics with those seen during NREM sleep (Franks, 2008). Clearly, these kinds of functional brain imaging studies have some important limitations, like temporal and spatial resolution, but it is generally accepted that there is a substantial correlation between the amount of blood brain flow and the concomitant activity of related brain areas. Because of this neural-vascular coupling, the reduction of the blood flow should correlate with a reduction of neuronal activity (Shmuel et al., 2002). The largest reductions of rCBF during NREM sleep were observed in the thalamus, brainstem, basal ganglia and specific cortical regions, such as precuneus, posterior and anterior cingulate cortexes and orbito-frontal cortex (Kajimura et al., 1999). Analogue decreases in rCBF were found during both sevoflurane and propofol general anesthesia and the major corresponding changes were in the thalamus, posterior cingulate cortex, precuneus, cuneus and frontoparietal cortex (Kaisti et al., 2003) (Franks, 2008). Nevertheless, several findings challenge the idea of the switching role of the thalamus in the transition from the awake state to loss of consciousness. First, during ketamine general anesthesia, it was found that the cerebral blood fluid increased in a concentration dependent manner and also the glucose metabolic rate increased, exactly at the thalamic level, by suggesting an intense activity of the thalamus despite of the loss of consciousness (Långsjö et al., 2005). Moreover, EEG cortical responses evoked by sensory stimulations are always present during both general anesthesia and NREM sleep (Hudetz & Imas, 2007) (Meeren et al.,1998). This strongly suggests that thalamic rhythmic activity is not enough to block the

sensorial flow and also that the activity of the primary cortexes does not necessary correlate with conscious sensorial experience (Alkire et al., 2008). Since EEG slow-waves (0,5-1Hz) associated to NREM sleep and general anesthesia, seem to be cortically generated and largely independent from the thalamic action (they persisted also after thalamic disconnection and in preparation of cortical slices maintained *in vitro* (Steriade, Nuñez, & Amzica, 1993) (Sanchez-Vives & McCormick, 2000)) a primary role of the cortex in the loss of consciousness is suggested. However, extended damage to the frontal cortex, which is seen to be deactivated during NREM sleep and during sevoflurane and propofol anesthesia (Kajimura et al., 1999) (Kaisti et al., 2003), produces severe alterations to executive functions while the awareness remains uncompromised (Markowitsch & Kessler, 2000). Moreover the posterior mesial cortical areas (posterior cingulate cortex, and precuneus) which are deactivated during general anesthesia and during NREM sleep, remain deactivated also during REM sleep, where the vivid dream experience cannot be associated to the loss of consciousness (Maquet et al., 2000) (Alkire et al., 2008). Taken together, these data show how a localizationistic approach fails to fully understand how general anesthetic produce the loss of consciousness and that a new theoretical framework is needed in order to clarify this cardinal property of general anesthesia.

1.1.3 Signal processing alterations

It's been proposed that, instead of the simple deactivation of single brain areas, the hypnotic action of general anesthetics could arise from the ability of unbinding the exogenous and endogenous information, and therefore by interrupting long-range synchronization of neuronal ensembles which codify and bind such information in a conscious experience (John & Prichep, 2005). This unbinding action can be achieved at the cellular level, where the molecular action of anesthetics alters the informative content and the timing by which the information is transferred and it can be reflected at a systemic level, by preventing the integrated communication among brain cortical areas.

This hypothesis is coherent with the "Integrated information theory" of consciousness developed by Tononi and Edelman (Alkire et al., 2008). In the formulation of their theory, authors support the idea that neurons give rise to consciousness from two main properties of the brain signal processing, rather than from particular anatomical locations or biochemical properties. First, as the conscious experience is an indivisible unity of different features, the underlying neural process must be integrated. Second, the signal process must be informative in the sense of reduction of uncertainty, therefore a conscious brain must be able to assume a particular state of activity among several and different possibilities of functional states (Tononi & Edelman, 1998). According to this framework, the level of consciousness is a function of the integration and of the informative content of a system. Therefore, if the brain is highly connected and integrated but less able to differentiate in its possible states, it cannot produce conscious experience, such as during absence seizures of epilepsy where large groups of neurons fire together or are silenced together, without other possibilities. Otherwise, if the brain regions can differentiate amongst a high number of possible states, but lose their long-range functional connectivity, they also will not produce a conscious experience. An example of the latter case is the split-brain disconnected syndrome, where the two hemispheres are disconnected by the excision of the corpus callosum. In affected subjects, visual stimuli projected to the non-verbal hemisphere generate behavioral responses, but the verbal hemisphere is not conscious of them and therefore the subject cannot verbally describe them (Gazzaniga, 1995) (Tononi & Edelman, 1998).

The hypothesis that general anesthetics produce the loss of consciousness by avoiding the cortical integration of the electric signal, is confirmed by several reports. It was found that between the frontal and occipital regions in humans, the synchrony in all brain frequencies was cut down shortly after the loss of consciousness. Moreover spectral synchrony was restored between prefrontal and sensory cortexes when consciousness returned and the most striking coherent variations were ascribed to the gamma oscillation (~20-80Hz), which began to return several minutes before eye opening, by predicting the awareness (John & Prichep, 2005). Indeed, a putative marker of the cognitive binding and of the

integration of cortical information is the spectral power of the gamma oscillation and most importantly, its phase synchrony among cortical regions (Rodriguez et al., 1999), which increases during mental and perception tasks (John & Prichep, 2005). The same reduction in the synchrony of the gamma and lower frequencies was also seen in rats exposed to isoflurane anesthesia and the reduction of coherence was higher between long-range anterior-posterior cortical areas than within local anterior circuits, where no effect was detected (Imas et al., 2006).

Nevertheless, reports are not fully accordant and it has been observed that during propofol anesthesia in humans, the phase synchrony in the gamma, alpha and theta bands between the anterior and posterior cingulate cortexes could even increase relative to the awareness state (Murphy et al., 2011). Meanwhile another study reported that gamma activity occurred in a strong relation to the presence of large amplitude slow-waves during anesthesia induced by volatile anesthetics (Vanderwolf, 2000). Therefore the simple phase synchrony of the gamma band and its power may not be reliable parameters useful to discriminate between states of loss of consciousness and awareness. Otherwise the combination of high-density EEG recording (hd-EEG) and transcranial magnetic stimulation (TMS) could be used to detect some important features of the loss of consciousness. In a first report, Massimini and colleagues recorded the evoked potentials induced by transcranial magnetic pulses on the premotor cortex in awake and sleeping human subjects. During awareness, evoked potentials produced long lasting (>150ms) and long-range complex activity patterns, where variations of field potential could be detected at first, near the stimulation site and later, in other cortical locations following a complex sequence. Otherwise, during NREM sleep the same stimulation produced a short-time (<150ms) simple response and the variation of field potential, even if it was higher in voltage than during awareness, did not propagate far from the stimulation site. This data strongly suggests that the loss of consciousness during NREM sleep correlates with a breakdown of the cortical ability to integrate information (Massimini et al., 2005). Moreover the same results were obtained in response to TMS evoked potentials during loss of consciousness induced by midazolam, a benzodiazepine (Ferrarelli et al., 2010). This suggests that anesthesia could generate loss of consciousness by similar mechanisms of the

physiological NREM sleep, that is by avoiding integrated processing of information. The authors propose that this breakdown of connectivity could be related to the neuronal mechanisms that produce the cortical slow-wave activity during NREM sleep. A depolarization-dependent K^+ current and the reduction of extracellular Ca^{2+} seem to be involved in the transition from the up-state epoch to the down-state epoch of the slow-wave pattern and therefore could have a role in the generation of loss of consciousness (Sanchez-Vives & McCormick, 2000) (Massimini & Amzica, 2001). Of course, the thalamus also plays an important role in the generation of NREM sleep and also its hyperpolarized state can contribute to block the integration of the signal. Moreover, it has been found that a slow TMS stimulation (<1Hz) over the sensory-motor cortex during NREM sleep, produces a different activity pattern. The stimulation of this cortical area (and not of the premotor cortex) leads to a high-voltage, long lasting and stereotypic global response, which expands far from the stimulation site (Massimini et al., 2007). This is interesting because this activity pattern is also predicted from the integrated information theory as a cause of loss of consciousness: the loss of informative content of the signal processing, where a system oscillates between only two or very few possible states. Importantly the sensory-motor cortex is an important hub of the cortical connectivity, which receives, elaborates and sends much information from many other cortical areas. Therefore it is a maximally connected area and this could help to explain this dramatic change of response and suggests its role as cortical generator of slow-waves.

Similar signal processing alterations could occur also in response to more physiological stimulations, such visual stimulation. Therefore in this study, I tried to clarify some aspects of the hypnotic action of sevoflurane and propofol by analyzing the evoked responses to light pulses in anesthetized rats. Since the adopted model is the visual system, a brief introduction is needed. The main focus will be on the visual signal processing, specifically on the ON / OFF dichotomy, how the retinal output is generated and how it is interpreted in the lateral geniculate nucleus of the thalamus and in the visual cortex. The coding of motion and colors will not be discussed.

1.2 THE VISUAL SYSTEM

1.2.1 The eye

The eye is an extremely efficient and reliable optical system. It is composed of several parts, each one is fundamental to form image perception. It can be subdivided into three main layers: the outer layer, formed by the sclera and the cornea; the intermediate layer, or *uvea*, comprised of an anterior part (the iris) an intermediate part (the ciliary body) and a posterior part (the choroid); and the inner layer, the retina (Purves et al., 2004) (Rodieck, 1973) (Yamada, 1969).

The first lens in the light pathway of the visual system is the cornea, a transparent and avascular tissue which is in contact with the sclera, the outermost layer of the eye globe. Posterior to the cornea there is the anterior chamber, a space filled with aqueous umor, with both trophic and a refractive function, which separates the cornea from the iris (Purves et al., 2004). The iris is a thin membrane made of stroma, melanocites, vessels and muscular tissue. In the middle of the iris, there is the pupil, a circular hole whose diameter can be either increased through the action of the sympathetic nervous system via the iris dilator muscle (mydriasis) or reduced through the action of the parasympathetic nervous system via the iris sphincter muscle (miosis). These variations occur mainly in response to variations in light intensity, therefore by regulating the amount of light which enters the eye and the depth of field. Posterior to the iris there is the lens, a fibrous and transparent structure which can modify its curvature, by means of the ciliary muscle, in order to focalized objects at different distances on the retina (accommodation reflex). In rats, the lens occupies a great part of the vitreous chamber and differently from other mammals, the lens can't change its curvature. Indeed, rats have a poorly developed ciliary muscle and relaxing agents like atropine do not change the focus. The space between the lens and the iris is called the posterior chamber and it is filled with aqueous umor produced by the ciliary bodies, also located in this space (Purves et al., 2004). Behind the lens there is the vitreous umor, a gel like substance delimited by the hyaloid membrane. The vitreous umor fills the vitreous chamber and has both a trophic and a structural

function (Purves et al., 2004). Directly behind the vitreous there are the retina (see below) and the choroid, the posterior part of the uvea. This is a layer of connective tissue very rich in blood vessels, therefore it provides a blood supply for the outer and intermediate layer of the retina. The outermost layer of the eye bulb is the sclera, a thick connective tissue which encloses every internal structure of the eye; it is covered with a stratified columnar epithelium, the conjunctiva, that together with the lacrimal glands provide protection and lubrication secreting mucus and lacrimal fluid (Purves et al., 2004).

1.2.2 Structure and neurons of the retina

The retina is the first neural network involved in processing of the visual information. It is able to detect the light stimuli, converting them to electrical signals and encoding them in a spike frequency mode. It is a complex circuit that is not fully understood, but it is clear that the retina is not a simple transducer, but instead is able to carry out a huge amount of local computation.

Basically, the retina is a disk of neural tissue that can be dived in three layers containing neuronal cell bodies and two layers of synaptic connections (both containing vertical and horizontal connections) (Purves et al., 2004):

1) *The outer nuclear layer*, which contains the nuclei and cell bodies of photoreceptors (rods, for scotopic vision, and cones, for color vision).

2) *The outer plexiform layer,* where the synaptic connections between photoreceptors and second order neurons (bipolar cells) take place together with horizontal interactions between different photoreceptors via horizontal cells.

3) *The inner nuclear layer,* which contains the nuclei and the cell bodies of bipolar cells (the neurons interposed between photoreceptors and ganglion cells), horizontal cells and amacrine cells (these are usually inhibitory interneurons).

4) *The inner plexiform layer*, where the synaptic connections between bipolar cells and ganglion cells take place, together with horizontal connections mediated by amacrine cells.

5) *The ganglion cell layer,* which contains the cell bodies of the output neurons, the ganglion cells, and the cell bodies of the displaced amacrine cells.

Since photoreceptors lie in the outer part of the retina and the output ganglion cells are in the inner part, light must pass through the full thickness of the retina to trigger the visual response. Therefore, in the central part of the retina of higher mammals, there is a specialized region, the fovea, where cellular bodies of the cells of the inner layers are in an oblique position relative to the photoreceptor layer, by reducing the thickness of the retina and therefore by reducing scattering. The fovea is also the region with higher visual acuity and great sensibility to colors. Indeed, this region has only cone photoreceptors organized in a very efficient packing way, with the lower output convergence compared to the peripheral retina by increasing the resolution capability. The ganglion cell axons then, run radially toward the optic nerve, avoiding to covering the fovea and transfer the information out from the retina. Otherwise rats do not have a structure similar to the fovea (Paxinos, 2004). In the retina the spatial organization reflect the functional role of the cells, therefore cells which make "vertical" connections (photoreceptors, bipolar and ganglion cells) are responsible to give rise to the transduction of the irradiance energy into a spike-rate code sent to the central nervous system. Meanwhile cells that make "horizontal" connections (horizontal and amacrine cells) give rise to parallel pathways with regulatory functions.

Photoreceptors transduce radiant energy into electric signals and even if they are not able to make action potentials, they respond with graduate potentials. There are two kinds of photoreceptors: cones (responsible for the color vision, subdivided into long wavelength or L, medium wavelength or M and short wavelength or S, according to the wavelengths to which they are sensitive) and rods (specific for scotopic or night vision). Rats have rods also but only two types of cones: green and blue. Therefore, rats are unable to see the red color. Green cones, that account for 88% of the total cones, have a peak sensitivity around 510 nm, while for blue cone, the peak sensitivity is around 359 nm, which means that rats can see ultraviolet light (Jacobs, 2001). Both cones and rods are composed by four compartments: the outer segment, containing photo-pigments, the inner segment, containing the Golgi apparatus and packed with mitochondria, the cell body and the synaptic terminal. The membrane of the outer segment, at the base of the photoreceptor, creates a stack of invaginations (membrane discs) where the

photo-pigments (rhodopsin or cone pigments) are embedded. Cone discs are in communication with the extracellular fluid, while rod discs are completely integrated in the cell outer segment. The photo-pigment is made of two components, an opsin, a G protein-coupled receptor, and a chromophore, 11-cis-retinal (each opsin binds 11-cis-retinal in different ways, making it sensible to different wavelengths). When a photon reaches the cis-retinal molecule it changes its state into all-trans-retinal. This leads to conformational changes in the opsin which activates a G-protein (transducin). This activates a cGMP-phosphodiesterase leading to a decrease in intracellular cGMP and therefore to the closure of cGMP-dependent ion channels. These channels are normally open in dark conditions causing constant depolarization of the photoreceptors (the "dark current", prevalently a Na^+ current but also involving Ca^{2+} and Mg^{2+}) and continuous release of glutamate from the synaptic terminal. The closure of these channels causes the hyperpolarization of the photoreceptor which ceases to release glutammate. The whole process is stopped by phosphorylation of the proteins involved and by a rapid restoring of the intracellular cGMP by Guanylate Cyclase (GC) (Kandel, et al., 2000). Then, the synaptic terminals make contact with two kinds of neurons: bipolar cells and horizontal cells.

Bipolar cells: receive visual inputs from photoreceptors plus other inputs from amacrine and horizontal cells and transfer the information to the ganglion cells. Bipolar cell respond in a graded manner to light inputs and generally, are not able to make action potentials, although in some cases they have shown some non-linear responses. Their voltage responses are mediated by depolarizing Ca2+ currents and release glutamate (Dreosti, et al., 2011) (Protti, et al., 2000). Bipolar cells give rise to 2 important channels of the visual system: the ON pathway, which responds preferably to changes in light conditions from dark to light and the OFF pathways, which responds preferably to light-to-dark changes. These different responses are mediated by the expression of two different glutamate receptors. AMPA and Kainate receptors are expressed on OFF bipolar cells therefore, depolarize in dark conditions, when glutamate is released and hyperpolarize in light conditions, when concurrently with the hyperpolarization of photoreceptors. Otherwise, ON bipolar cell express the hyperpolarizing metabotropic receptor

mGluR6 (Vardi, et al., 2000) (Wu, et al., 2000) (Nakajima, et al., 1993) (Waêssle & Boycott, 1991). The ON bipolar response to glutamate is therefore, inverted. In dark conditions, photoreceptors release glutamate and the ON bipolar cells are hyperpolarized. Meanwhile, recent reports showed that in light conditions, when glutamate unbinds from mGluR6, a pathway mediated by a G0 protein it is triggered and leads to the activation of a non-selective cation channel, TRPM1, thus depolarizing the ON bipolar cells. (Vardi, 1998) (Dhingra et al., 2000) (Koike et al., 2010) (Xu et al., 2012). Bipolar cells also receive inhibitory inputs from horizontal and amacrine cells. These connections shape their receptive fields and modify the temporal responses to light. Amacrine cells also make electrical synapses onto ON bipolar cells which are important for retinal ON/OFF circuitry (Manookin, et al., 2008).

Retinal ganglion cells (RGCs): RG cells can be divided into several subtypes based on their morphology and connectivity which in higher mammals, varies with the distance from the center of the retina: small cells are more abundant near the fovea while ganglion cells with large bodies and dendritic arbors are more abundant in the peripheral retina (Kandel et al., 2000). RG neurons are the output cells from the retina; they codify the visual graduate signal into action potentials by a frequency code and send visual information to the central nervous system through the optic nerve. They have a spontaneous firing rate that can be modulated by synaptic inputs from the upper retinal circuits, especially from the contacts with bipolar cells. Therefore, RGCs can be ON (responding to light stimuli), OFF (responding to dark stimuli) or mixed ON-OFF. The main difference is that the ON-OFF ganglion cells respond with burst activity at the onset and offset of light stimuli and with very low firing activity in between, while ON or OFF RG cells maintain a higher-than-basal firing rate for the whole duration of their preferred stimulus (Hartline, 1969).

Horizontal cells: are GABAergic neurons which make connections with photoreceptors and also with bipolar cells in the outer plexiform layer. Horizontal cells of the same subtype (at least two main sub-types exist) are widely linked together by gap junctions. This creates a giant electrical syncytium that allows them to spread over a wide surface of the retina (Bloomfield & Völgyi, 2009). They

are part of the photoreceptors' synapses and make feedback signaling onto the photoreceptors and feedforward signaling onto the bipolar cells. Although the way which they act is still unclear they seem to contribute importantly to visual perception, by shaping the receptive fields of bipolar cells and of RG cells (next section) (Kolb, 1974) (Ahnelt & Kolb, 1994).

Amacrine cells: compose a wide class of heterogeneous neurons which can release different neurotransmitters like GABA, glycine, substance P, dopamine or acetylcholine (Kolb, et al., 1990) (Masland, 1988) (Pourcho & Goebel, 1988). As horizontal cells, most of them are interconnected via gap junctions (Bloomfield & Völgyi, 2009). The amacrine cell sub-type AII is particularly important for the communication between the ON and OFF pathways. Amacrine cells-AII are glycinergic and are able to make action potentials. They make chemical synapses onto other amacrine cells, OFF ganglion cells and OFF cone bipolar cells and are linked to ON cone bipolar cells via gap junctions (Strettoi, et al., 1992).

1.2.3 Circuitry and signal processing of the retina

The main characteristic of the retina is the ability to detect contrasts, defined as the detection of spatial variations of lightness within an object and/or between objects. To solve this computational problem, the retinal circuitry give rise to the typical round shaped receptive field of the RG cells, with center-surround antagonism. In the visual system the receptive field is the portion of visual space that can alter the release of neurotransmitter from a neuronal cell. Specifically, the receptive field of an ON-ganglion cells is organized such as a light stimulation to the center of the receptive field produces an excitation, while a light stimulation to the periphery produces an inhibition (ON-center receptive field). While the receptive field of an OFF-ganglion cell works in the opposite way (OFF-center receptive field). This organization is usually modeled as a Difference of Gaussians (DOG) function (reversed for the OFF-ganglion cells), which is a band-pass filter able to enhance the edges and discontinuities of an image. If the "polarity" (ON- or OFF-center) of the ganglion receptive field is defined by the kind of glutamate receptor that is expressed by the bipolar cell which connects the RG cell, the

center-surround architecture takes origin from retinal network connections. The mechanism is not fully understood, but it is thought that the horizontal cells have a key role in such shaping, through a mechanism of lateral-inhibition. In the outer plexiform layer, multiple cones are connected with the same horizontal cell, which receives excitation signals from cones and makes inhibitory feed-back connections with the same cones. Therefore, cones are interconnected by means of horizontal cells. When the light hits a cone, possibly at the surround of a receptive field, it hyperpolarizes and interrupts the glutamate release, by reducing the excitation of the horizontal cell which is contacted. Thus, the horizontal cell reduces the release of GABA and the hyperpolarizing currents in cones which lie at the center of the receptive fields, by increasing the release of glutamate and by leading to a hyperpolarization in an ON bipolar cell or to an depolarization in an OFF bipolar cell. This implies that also bipolar cells have a receptive field with a center-surround antagonism analogue to the ganglion receptive field. Otherwise, RG cells exhibit properties of their receptive fields by modulating their firing rate rather than simple membrane depolarization. The maximum of the firing rate of an ON-ganglion cell is evoked by a central spot stimulation and the surround elicits an active inhibition of the center when stimulated, while the opposite occurs for an OFF-ganglion cell. However, a wide stimulation of the whole receptive field does not simply evoke a smaller firing rate, but can also shift the behavior of the ganglion cell from tonic to phasic as the stimulus is displaced from the center. Normally, the receptive fields of the same kind of RG cells form a highly structured mosaic with minimal overlaps between dendrite branches. While, RG cells of different kinds seem to have a mutually independent spatial distribution (Wassle, et al., 1981). Otherwise, this organization is not static and can be modulated, for example during dark adaptation, the surround inhibition becomes weaker, possibly by means of a selective inhibition of the surround via amacrine cells (Wassle, et al., 1981). Moreover, rod bipolar cells and even some RG cells seem to have a receptive field without a center-surround opponency, but with a center-only organization (Bloomfield & Xin, 2000) (Kandel et al., 2000).

Differently from higher mammals, the rat retina has a highly convergent synaptic organization. This means that each ganglion or bipolar cell in the rat

retina has a much wider receptive field than those of the human retina, increasing sensitivity at the expense of acuity. Specifically, the receptive fields of the rat ganglion cells are an order of magnitude larger than those of the human fovea.

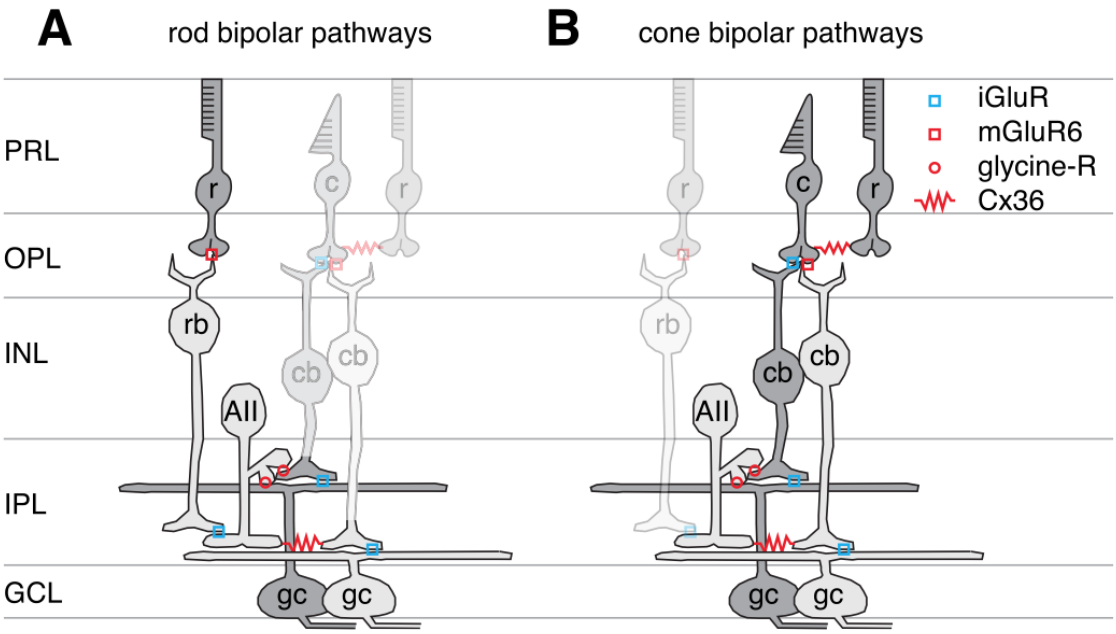

Fig. 1 Rode and cone bipolar pathway of the mammalian retina. **A)** The light hyperpolarizes rod (r) which stops releasing glutamate. ON-rode bipolar cell (rb) is excited and releases glutamate onto an AII amacrine cell (AII), which inhibits OFF-cone bipolar (cb-dark grey) and OFF-ganglion (gc) cells by chemical synapses and excites the ON-cone bipolar cell (cb-light gray) by electric synapses. **B)** The light hyperpolarizes cone (c) which stops releasing glutamate and communicates with rode by electrical synapses. OFF-cone bipolar cell (cb-dark grey) is more inhibited because expresses iGluR and does not excite the OFF-ganglion cell (gc-dark grey). Otherwise, ON-cone bipolar cell (cb-light gray) is excited and release glutamate onto ON-ganglion cell (gc-light gray), while exciting AII amacrine cell (AII) by electrical synapses, which inhibits OFF-cone bipolar (cb-dark grey) and OFF-ganglion cells (gc-dark gray) by chemical synapses. PRL = photoreceptor layer; OPL = outer plexiform layer; INL = inner nuclear layer; IPL = inner plexiform layer; GCL = ganglion cell layer. iGluR = ionotropic glutamate receptors (AMPA, Kainate); mGluR6 = metabotropic glutamate receptor type 6; glycine-R = inhibitory glycine receptor; Cx36 = electric synapse connexin 36. (From Manookin et al., 2008).

Importantly, cones and rods pathways differ in many aspects (Fig. 1). Cones are involved in color and high resolution vision during daylight. They make synapses with both ON- and OFF-cone bipolar cells, which converge onto the dendritic arbors of ON-center and OFF-center ganglion cells respectively. With the

contribution of the horizontal and amacrine cells, this pathway gives rise to the classical organization of the center-surround receptive field of the RG cells. Rods are more sensitive to light than cones, therefore are involved in scotopic vision, with dim light conditions. Rods make synapses only with horizontal cells' axons and rod bipolar cells which express mGluR6 receptor, thus being all ON bipolar cells. Moreover, rod bipolar cells do not contact RGCs directly but synapse onto two kinds of amacrine cells: A17 and AII. AII amacrine cells express ionotropic glutamate receptors, therefore are excited by ON-rod bipolar cells and make chemical glycinergic synapses onto OFF-cone bipolar cells and OFF ganglion cells, inhibiting them. AII amacrine cells also make Cx36-gap junctions with ON-cone bipolar cells by providing a direct electrical bridge to transfer information with the same polarity to ON-ganglion cells. It is important to note that electrical synapses are bidirectional in signal transmission, therefore when an ON-cone bipolar cell depolarizes because of the hyperpolarization of cone, it excites the AII amacrine cell as well. This has an important functional consequence: the ON pathway (both rode and cone) always inhibits the OFF pathway, when it is excited. Recently it has been proposed that this lateral inhibition could improve the ability of the OFF pathway to detect negative contrasts (from light to dark) by a mechanism of removal of inhibition (Manookin et al., 2008) (Liang & Freed, 2010) (Liang & Freed, 2012).

1.2.4 The lateral geniculate nucleus of the thalamus

The visual information is transferred out of the eye through the optic nerve, which collect the myelinated axons of RG cells. Right below the hypothalamus, the optic nerves from the two eyes form the optic chiasm. At this point axons from the nasal part of each retina cross to reach cerebral contralateral structures, while axons from the temporal emi-retina follow a straight path and connect to ipsilateral structures. After the fiber crossing, axons form the optic tract. Axons of RG cells have several parallel targets: the pretectum (which controls the papillary reflex), the suprachiasmatic nucleus of the hypothalamus (which controls circadian rhythms), the superior colliculus (which controls saccadic movements of

the eye and head rotation in response to visual stimuli; it also projects diffusely to the cortex by participating in the spatial localization of visual stimuli) and the lateral geniculate nucleus (LGN) of the thalamus, which is the first true image-forming region of the central nervous system and is the most important relay nucleus from the retina to the primary visual cortex. Ninety percent of the retinal output reaches the LGNs, by generating a retinotopic representation of the visual field, where the retinal regions with higher ganglion cell density are more represented and occupy a larger portion of the LGN surface (Kandel et al., 2000).

The LGN of primates is subdivided into six laminae (numbered from 1 to 6 on the ventro-dorsal axis) interleaved by fiber layers. These laminae are grouped in two classes, based on the cell body diameter: M or magnocellular cells and P or parvocellular cells. These two classes of cells receive axons respectively from M and P ganglion cells of the retina and maintain their physiological properties: M cells are highly sensitive to contrasts but poorly to color changes, respond mainly to low spatial frequencies and have high temporal resolution; on the contrary P cells are very sensitive to colors but respond poorly to luminance contrast, respond to high spatial frequencies and have low temporal resolution. A third class of cells, koniocellular cells, have been identified. These cells are located between the LGN laminae, have small cell bodies and intermediate characteristic between the first two classes and receive axons from koniocellular ganglion cells.

Each lamina receives inputs from one eye only: contralateral input fibers contact laminae 1, 4 and 6, while ipsilateral input fibers contact laminae 2, 3 and 5. Moreover, each laminae includes both ON-center and OFF-center relay neurons which reproduce the center-surround receptive field of their input RG cells. Otherwise, the functional circuitry of the LGN is not yet fully understood, indeed only 10-20% of the presynaptic connections onto geniculate relay cells come from the retina. The majority of inputs come from other parts of the central nervous system such as from the activating ascending systems of the brain stem, from the reticular nucleus of the thalamus and feedback projections from the cortex. These connections may control the flow of information from the retina to the cortex by interacting with several internal control systems, based on inhibitory interneurons

(Kandel et al., 2000) (Dubin & Cleland, 1977). Therefore, the LGN is likely to solve more complex functions than a simple relay nucleus.

The LGN of rat shows great differences from other mammals. It is a bean shaped nucleus and can be subdivided into three functionally distinct sub-nuclei on the coronal plane: the dorsal LGN (dLGN), the ventral LGN (vLGN), and the intergeniculate leaflet (IGL). Whereas the dLGN receives image-forming retinal input, the vLGN and IGL receive non-image-forming input from ipRGCs. Moreover, the LGN receives only a small part of the retinal output which in rats is mainly directed to the superior colliculus (Huberman, et al., 2010) (Kim, et al., 2010) (Su et al., 2011) (Hattar, et al., 2002).

The vLGN can be further subdivided into two portions, the parvocellular part (medially) and the magnocellullar part (laterally). Only the magnocellular part receives inputs from RG cells from both eyes and is involved mainly in the perception of luminance, but not in the perception of contrasts. The parvocellular part receives inputs from nonvisual nuclei and its function is still unclear. The IGL projects to the suprachiasmatic nucleus, it is involved in the regulation of the circadian rhythm and its neurons gradually increase their firing rate as a function of the overall luminance. The dLGN is the only image forming region of the LGN of the rat, it lacks laminations and it has a peculiar organization that only partially reproduces the general features of the LGN in other mammals. It has two main groups of axons: the first running from the posterior to the anterior pole of the nucleus, mainly constituted by the geniculo-cortical projections and the second, which runs transversely, including retinal-geniculate axons and cortical-geniculate fibers (which represent cortical feedback fibers from the layer 6 of the V1). Neurons of dLGN could be subdivided in relay cells (or Golgi A type) and interneurons (or Golgi B type). Relay cells are big, have highly ramified dendritic arbors and project outside the LGN, mainly to the visual cortex, while interneurons represent 20% of the total number of neurons and are mostly GABAergic interneurons. Neurons of dLGN also have large receptive fields and respond in a phasic mode when light stimuli are turned both ON and OFF. Moreover, the properties of relay cells can be regulated by the feedback projection from the visual cortex (Paxinos, 2004).

1.2.5 The primary visual cortex

Axons of relay cells from the LGN organize themselves into the optic radiations and reach the primary visual cortex (V1) or Brodmann's area 17, which is located in the occipital lobe and like the LGN, V1 receives information only from the contralateral half of the visual field. The primary visual cortex consists of six layers of cells (layers 1-6) dorsal-ventrally organized. The principal input layer from the LGN is layer 4, which is subdivided into four sublaminae: 4A, 4B, 4Ca, and 4Cb. In primates it has been shown that M and P cells of the lateral geniculate nucleus terminate in different sublaminae: M cells project principally in sublamina 4Ca, while axons of most P cells terminate in sublamina 4Cb. Thus, parvocellular and magnocellular pathways continue to be segregated. Axons from koniocellular cells terminate in layers 2 and 3, where they innervate ensembles of cells called blobs. The visual cortex contains two main classes of cells: pyramidal cells, which are large, with long spiny dendrites and project to other brain regions or interconnect neurons in local areas; nonpyramidal cells, which have a small and stellate shape and based on their dendritic arbor, are divided in spiny or smooth stellate cells. The pyramidal and spiny stellate cells are excitatory neurons and many release glutamate or aspartate, while the smooth stellate cells are inhibitory and many are GABAergic (Kandel et al., 2000).

The main inputs of the LGN project onto the spiny stellate cells, which predominate in layer 4. These cells distribute the input to the cortex and the pyramidal cells send axon collaterals upward and downward by integrating the signal processing within V1. The output connections depart from all layers of V1, except for 4C and the pyramidal cells are the principal output cells. Cells in layers 2 and 3 send outputs to other visual cortical regions, such as V2, V3, and V4. They also make connections to contralateral symmetric cortical areas of the other brain hemisphere. Cells in layer 4B project to the V5 cortex, or middle temporal area. Cells in layer 5 project to the superior colliculus, pons, and pulvinar. Cells in layer 6 project back to the LGN and to the claustrum (Kandel et al., 2000).

Most of the cortical cells have a substantially more complex receptive field than the circular center-surround field of retinal and thalamic cells. Instead of circular

stimuli, cells of V1 respond better to stimuli that have a linear shape, such as lines or bars, with a preferred spatial orientation. Therefore, at the cortical level, the ability to represent different orientations of a bar stimulus (or of a border) emerges. These cells can be subdivided in two main groups: simple and complex. The simple cells have a strictly oriented receptive field, composed by ON and OFF sub-regions which lay parallel and adjacent to one other. Like center-surround sub-regions, also the oriented ON and OFF sub-regions of the simple cells have a mutually antagonistic relationship, therefore bar stimuli of reverse contrasts evoke "push-pull" responses. That is, a light bar projected along the ON sub-region evokes an excitation (push) and a light bar projected along the OFF sub-region evokes an inhibition (pull). Meanwhile, opposite responses are evoked by a dark bar. Moreover, the most vigorous response is obtained by bar stimuli which are oriented along the same orientation of the receptive field, while the weaker response is obtained by bar stimuli which are perpendicularly oriented. Receptive fields of complex cells are less oriented and have less defined or substantially overlapped ON and OFF sub-regions. Because of this organization, the fields of complex cells have a "push-push" or a "push-null" structure. Therefore both stimuli with opposite polarities evoke an excitation (push-push) or there is a strong preference for stimuli with only one polarity, so that stimuli with the opposite polarity cannot evoke any response (push-null) (Hirsch & Martinez, 2006). The oriented organization of the receptive fields of the simple cells takes origin mostly from feedforward projections of the LGN. Therefore the convergence inputs from many circular fields of ON and OFF relay cells with an appropriate arrangement, build the sub-regions of the field of simple cells. Otherwise, because thalamic projections are excitatory, the pull response must originate from other mechanisms. Some reports provided evidence that this suppression of activity was cortically generated and comes from the mirrored interposition of local interneurons between thalamic inputs and simple excitatory cells. These interneurons also have simple receptive fields with ON and OFF sub-regions, which resemble those of their excitatory partners, but the overlapped sub-regions have opposite polarities. Therefore, when a light bar is projected along the OFF sub-region of the receptive field of an excitatory simple cell, is projected also along

the ON sub-region of the field of the mirroring interneuron, which is excited and inhibits the simple cell (Fig. 2) (Hirsch & Martinez, 2006).

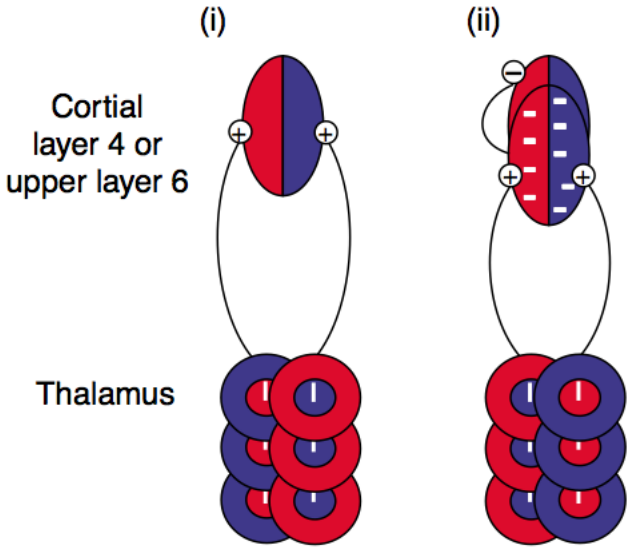

Fig. 2 Push-pull circuitry of a simple cell of V1. Red=ON sub-region; blue=OFF sub-region; cells are represented as their receptive fields; interneuron is marked by white dashes; excitatory connections are marked by +; inhibitory connection is marked by -. **i)** The push response of the simple cell is generated by ON-center and OFF-center neurons of the thalamus, which are properly laid so that their receptive fields give rise to parallel rows in visual space. Therefore a light bar projected along the ON sub-region of the simple cell, excites the ON-center relay cells, which in turn excite the corresponding simple cell. **ii)** The pull response is produced by the interposition of an inhibitory intereuron with an overlapped simple field with opposite polarity, among the thalamic projections to the simple cell. Therefore the projection of a dark bar along the ON sub-region of the simple cell, excites the OFF-center relay cells of the thalamus, which in turn excite the interneuron with the mirrored and opposite receptive field, which inhibits the simple cell.
(From Hirsch & Martinez, 2006)

Otherwise this model could be an over simplification for at least two reasons. First, the number of excitatory neurons in the cortex greatly exceed that of interneurons, therefore single interneurons should supply several simple cells. Second, this model considers the ON and OFF field sub-regions as spatially segregated, but some evidence suggests that they could be only functionally segregated and that interneuronal microcircuits or the excitatory/inhibitory balance could play a key role in their modulation. Indeed it was found that the typical push-pull receptive field of simple cells could be converted into a push-

push receptive field of complex cell by blocking GABA receptors, suggesting that a more complex model is needed (Liu et al., 2010) (Abbott & Chance, 2002) (Sillito, 1975). Nevertheless, it seems that there is a convergent pathway along the whole visual system: groups of photoreceptors converge onto bipolar cells, which in turn converge onto ganglion cells. RG cells converge onto relay cells of thalamus, LGN cells converge onto cortical simple cells, which finally contact complex cells. At each step, the optimal stimulus properties for the recipient cells become more and more specific. Retinal ganglion and LGN neurons respond primarily to the contrast. Cortical simple cells convert it into line segments. This is essential for detecting boundary, which is the most important information in visual coding.

Moreover, the primary visual cortex is organized into functional domains that take the form of columns of cells along the cortical thickness. Specifically, each orientation columns contains cells in layer 4C with concentric receptive fields and above and below there are simple cells whose receptive fields receive input from closely spaced retinal regions and have similar axes of orientation. Columns are then grouped in an orderly arrangement with other columns with different orientations in a circular space so that a complete cycle of changes in the orientation axis is contained in less than a millimeter. This precise organization is sometimes interrupted by blobs, groups of cells in layer 2 and 3 whose receptive fields are not orientated and are sensitive to different color stimuli, since they receive inputs from koniocelluar LGN cells. A third system of alternating columns consists of the the ocular dominance columns. These are a consequence of a regular arrangement of cells that receive inputs preferentially from the left or right eye and are important for binocular vision. A complete sequence of ocular dominance columns, orientation columns and blobs is repeated regularly over the surface of the primary visual cortex. This clearly shows the modular architecture of the visual cortex. Each module completely processes a part of the visual field (including orientation, binocular interaction, color, and motion) and corresponds to the hypercolumn. Moreover, hypercolums are not segregated, but are interconnected by horizontal connections that link cells within the same layer. Axon collaterals of individual pyramidal cells in layers 3 and 5 run long distances through paths parallel to the cortical layers, effectively coupling the firing of

distant cells coding similar information in different modules (Kandel et al., 2000). Rodent primary visual cortex lacks the proper columnar organization of higher mammals, but it contains an ordered retinotopic map, where neurons show selectivity for stimuli parameters such as orientation and ocular dominance and simple and complex cells can be found (Schuett, et al., 2002) (Horton & Adams, 2005) (Niell & Stryker, 2008) (Liu et al., 2010).

1.3 AIM OF THE STUDY

A putative useful tool which could be used to clarify how general anesthetics modify the information processing of the brain is the quantitative analysis of the sensory evoked potentials, cortical population responses that are recorded by scalp electrodes. When an appropriate sensory stimulation is presented, an electrical potential is triggered by sensory receptors and transmitted to the central nervous system. If the electrical potential reaches the cortex, it will generate a variation in the activity of a neuronal ensemble which will be reflected in a variation in the local field potential that could be recorded by scalp electrodes. This variation in the field potential is the evoked sensory response and corresponds to the coordinated cortical computation of the sensory event. Despite the complex meaning of the response, it's been proposed that the later component of the evoked potential (>100-200ms) could be associated to the long-range integrative function of the cortex, essential to the conscious experience (Pascual-Leone & Walsh, 2001) (Supèr et al., 2001)(Sergent et al., 2005), while the earlier component (<200ms) could be associated to the thalamic-cortical interaction and to the first steps of the signal processing (Creel et al., 1974) (Coenen, 1995) (Meeren et al., 1998). By confirming the hypothesis that general anesthetics induce the loss of consciousness by breaking the long-range integration of the signal, it has been observed in rats, that during anesthesia, the late component (>100-200ms) of the evoked response was selectively lost, while the earlier response was conserved (Hudetz et al., 2009). However, because of the systemic action of the anesthetic drugs, the earlier steps of cortical computation should be also modified.

Therefore, the earlier response of the evoked potential offers a putative useful window to observe how general anesthetics modify the signal processing of the sensory event, by shedding light on their mechanism of action.

In this exploratory study I analyzed the visual evoked response and the resting EEG activity of rats exposed to both sevoflurane and propofol. Specifically, in order to detect functional alterations in the sensory computation related to the anesthesia, I focused my investigation on 2 functional properties of the visual system: the brightness sensitivity and the ability to detect contrasts by analyzing both the ON and the OFF responses to the light/dark stimulation. Then, I analyzed the variations of these two functions in relation to 3 progressive deeper states of anesthesia induced by both anesthetics. Moreover, I compared the variations of the evoked potentials to a quantitative analysis of the resting EEG activity related to the same states of anesthesia.

2 METHODS

2.1 ANIMAL MODEL

Adult male Sprague Dawley rats (weight 350-540g) were used in the whole set of experiments. All animals were individually caged with free access to food and water ad libitum and were exposed to 12 hour light/dark cycles, at a constant room temperature of 23°C. In order to reduce inter-animal variability, rats were exposed to more than one experimental condition, when it was possible, therefore all responses could be compared to control condition in every single animal. In these cases, rats were left to rest for at least 3 days between experiments. The rat care and all the surgical and experimental procedures were approved by the Institutional Committee for Good Animal Experimentation of S. Raffaele Scientific Institute, in agreement with the Italian law.

2.2 SURGICAL PROCEDURE

The electrical activity of the cortex was recorded by 3 electrodes made up of steel screws (length: 4,5mm, caliber: 1,4mm, head diameter: 2,5mm) and a gold pin (length: 1cm, caliber: 1mm) soldered onto the head of the screw. Two electrodes were grafted into the thickness of the skull at the level of left and right primary visual cortex (X=±4,6mm; Y=-7,00mm from bregma) and the third one was placed at the level of right motor cortex (X=-1,82mm; Y=2,4mm from bregma) (Fig. 3). These coordinates were determinated by using the stereotaxic atlas: "The rat brain in stereotaxic coordinate", G. Paxinos (Paxinos & Watson, 2007). During the surgical operation, the animal was deeply anesthetized with sevoflurane (Sevorane, Abbvie) and additionally, received an intraperitoneal injection of gentamicin (1,5mg/kg, Italfarmaco) and two subcutaneous injections, one of carprofen (5mg/kg) and the second one of dexamethasone (0,2 mg/kg, Hospira) to prevent an inflammatory response and/or swelling of the brain, respectively. The

operating area was sterilized by wiping the skin with three alternating swipes of 2% chlorhexidine (Esoform) and betadine (Esoform). Rats were placed into a stereotaxic frame and the skin over the top of the skull was removed in order to expose the sites of interest. At this point a drop of lidocaine (Astra Zeneca) + epinephrine (S.A.L.F.) solution was applied onto the skull to avoid excessive bleeding and post-surgical pain. Once the recording sites were chosen, 3 holes were drilled in the bone and the electrodes were positioned. Particular care wass taken to avoid any damage to the brain. Methylmethacrylate cement (SPD-Salmoiraghi Produzione Dentaria) was applied over all of the exposed skull surface, covering also the screws and the soldered parts of the gold pins, to secure the electrodes. During the following three days, animals were left in cages with free access to food and water and received two intraperitoneal injections of gentamicin sulfate (1,5 mg/kg) each day. (The surgical procedure was modified slightly from Mostany & Portera-Cailliau, 2008).

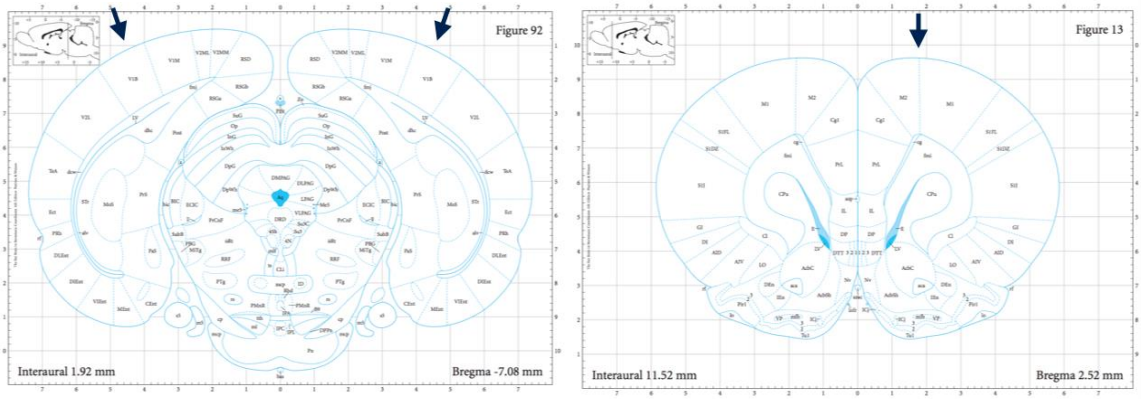

Fig. 3 Positions of the EEG electrodes (arrows) on the cortical surfaces. 2 electrodes are symmetrically grafted at the level of the primary visual cortexes (X=±4,6mm; Y=-7,00mm from bregma) (left) and another electrode is grafted at level of the motor cortex (X=-1,82mm; Y=2,4mm from bregma) (right). (Brain panels are from the stereotaxic atlas Paxinos & Watson, 2007).

2.3 EXPERIMENTAL PROCEDURE

2.3.1 Experimental setting

The day of the experiments rats were deeply anesthetized with sevoflurane, intubated with a polyethylene 16GA catheter and artificially ventilated with a mixture of air and 2,5% sevoflurane (3,7-4% for induction) by using a ventilator (SERVO900C-Siemens). The volume-controlled ventilation delivered a tidal volume of 6ml with respiratory rate of 80-85 breath/min and volume/min of 0,5 l/min. A gas analyzer (Vamos-Dräger) was used to monitor the inspiratory and the expiratory concentrations of the anesthetic and the pCO2. Animals were placed on an anti-vibration table on a heating pad in order to maintain a stable body temperature set between 36 and 37°C. Curare was delivered into the tail vein in one bolus of atracurium, 5mg/kg (Glaxo Smith Kline) each 18' by using a syringe pump (Pump11 elite–Harvard Apparatus), in order to guarantee the muscular relaxation (Mayer & Fink, 2001). Rats were maintained in complete darkness condition with their left eye covered by a black tape. For light stimulation their right eye was exposed to trains of light pulses of various irradiance[1] and duration values, with a rate of 0,1Hz. The flash stimulation was produced by using a white, high-brightness, light-emitting diode (LED) placed at 2cm from the eye on an imaginary axis which passed perpendicularly through the fundus of the eye and crossed the rostral-caudal axis with an angle of 60° from the nose on the horizontal plane. On the elevation axis, the LED pointed at the pupil from 2cm above the eye. Animals were electrically grounded by means of a hook electrode placed on their skin. The evoked response was recorded using a custom-built instrumentation amplifier (the left occipital electrode was connected to the positive input and the right occipital or the right frontal electrode was connected to the negative one) featuring a total gain of 5000 and band-pass filtering (0.1 – 3000 Hz); the signal

[1] LED irradiance is calculated making reference to the 509nm wavelength, where the M-cones (middle-wavelengths sensitive) of the rat show the peak in their absorbance function (Jacobs, 2001).

was digitalized at 20kHz (16 bit) using the ITC-18 data acquisition interface (HEKA Elektronik) and custom acquisition software developed in LabView®.

2.3.2 Stimulation protocols

Animals were subjected to different experimental protocols. 5 rats were exposed to 2 recording sessions, one under sevoflurane anesthesia, the other one under propofol (Astra Zeneca) anesthesia. The session order was randomized between animals and at least 3 days passed between the 2 sessions. Each session consisted of 3 types of stimulations, which were sequentially repeated for 3 increasing concentrations of anesthetic. The first concentration used was the minimal dose required to keep the animal anesthetized, evaluated by the absence of pain reflexes, the second one was 150% of the first and the third was 200% of the first concentration. In the sevoflurane condition, the minimal alveolar concentration (MAC) to keep animal anesthetized was 2,5% (Benito et al. 2010) and the other 2 states of anesthesia are induced by sevoflurane 3,75% and 5%. In propofol anesthesia, the minimal systemic dose needed was 1mg/kg/min, with the second and third being 1,5mg/kg/min and 2mg/kg/min, respectively. In the propofol condition the drug was administrated by a cannula into the tail vain and the induction of anesthesia was obtained by a bolus of propofol 10mg/kg (Brammer et al., 1993). The stimulation started 3min after a stable value of the desired expired concentration of sevoflurane was reached or 3min after the beginning of the propofol infusion at the desired concentration rate. The first type of stimulation consisted of a randomized train of 20ms light pulses of 7 irradiance values: 0,9 6,5 24,8 67,7 150,8 288,8 and 327,9µW/cm^2. For all irradiance values there was 19-20 pulses presented, with the exception of the first 2 lower irradiance values, in which the number of pulses was 24-23[2], in order to obtain a better estimation of the evoked response function in relation to the light irradiance. The electrode derivation used to record the brain activity was the inter-hemispheric occipo-

[2] In the propofol condition, one rat has been stimulated by a train of 15 randomized light pulses for each irradiance value.

occipital one. The second recording was performed by the inter-hemispheric coccipito-frontal derivation and consisted of a resting activity recording of 110 seconds, in a complete darkness condition. The inter-hemispheric occipital-occipital derivation was used to record the evoked brain response to the third stimulation, which was composed of a train of 19 light pulses of 300ms and 150,8μW/cm^2.

In order to evaluate the OFF component of the VEP, 7 rats were stimulated by a randomized sequence of light pulses of 150,88μW/cm^2 at 3 different durations: 300, 500, 800ms. For all durations 19 pulses at the basal state of anesthesia induced by sevoflurane 2,5% were presented and the inter-hemispheric occipito-occipital derivation was used for recording.

With the purpose of better understanding the relation between the OFF and the ON component of VEP, 3 rats were exposed to a randomized train of light pulses of 300ms and 7 irradiance values: 0,9 6,5 24,8 67,7 150,8 288,8 and 327,9μW/cm^2. For all irradiance values 19-21 pulses were presented and the electrode derivation used to record the brain activity was the inter-hemispheric occipo-occipital one. In these experiments the anesthesia was induced by sevoflurane 2,5%.

In another set of experiments, 5 rats were exposed to a train of 59 light pulses of 300ms and 150,88μW/cm^2 before and 10min after the intravitreal injection of the mGluR$_6$ agonist L-AP4 (L-2-amino-4-phosphonobutyric acid) (Tocris Bioscience) diluted as follows: 3 μl [100 mM] L-AP4, 11 μl Tyrode solution (containing 2mM CaCl2, 2mM MgCl2 and 6 g/L Glucose), 1 μl [1M] HEPES Buffer (Lonza). Based on the assumption of a vitreous volume of 50μl, the injection volume was 5μl in order to obtain a final concentration of 2mM, pH7.4. The whole experiment was performed under sevoflurane anesthesia 2,5% and the brain activity was recorded by the inter-hemispheric occipito-occipital electrode derivation.

In order to clarify the effect of sevoflurane specifically on the OFF component of VEP, an additional 4 animals anesthetized by sevoflurane 2,5%, were stimulated by trains of 24 light pulses of 300ms and 150,88μW/cm^2 before and immediately after the intravitreal injection of L-AP4 [2-8mM]. Subsequently, the same stimulation was repeated at sevoflurane 3,75%, 5% and in a second control stimulation at sevoflurane 2,5%. The L-AP4 injection induces the inhibition of the

ON pathway in the retina (Slaughter & Miller, 1981) sparing the OFF pathway, therefore only the rats that did not show the ON component of the VEP after the intravitreal injection were considered reliable and all animals that exhibited the ON response during the second control stimulation at sevoflurane 2,5%, were excluded from the analysis. To avoid any putative bias related to the injection damage to the vitreous or to the retina, animals that did not show a clear OFF response after injection, were rejected. The brain activity related to all stimulations was recorded by the inter-hemispheric occipito-occipital electrode derivation.

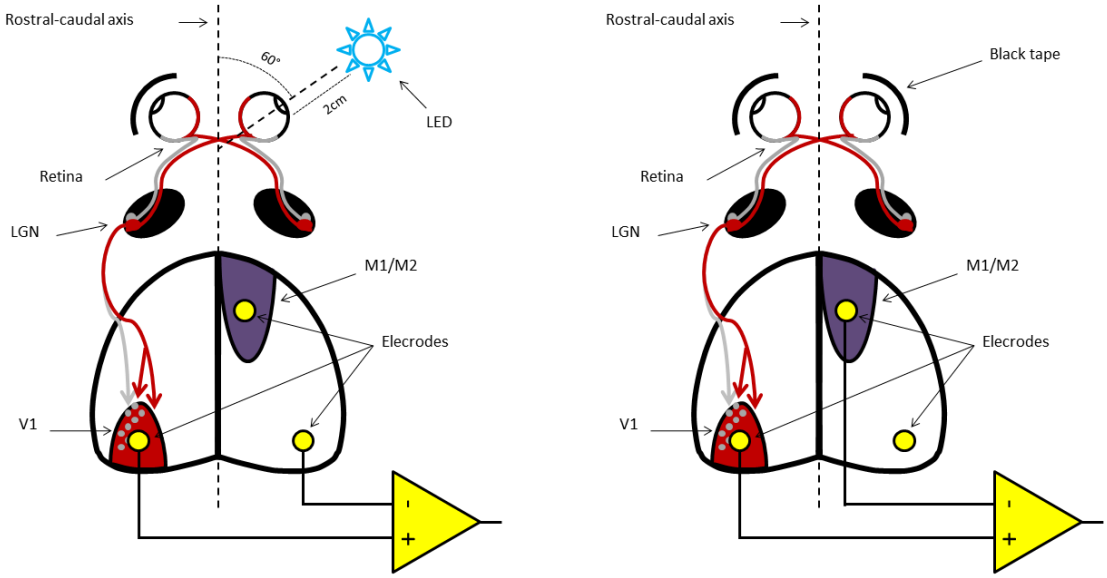

Fig. 4 Schematic representation of the visual pathway and the experimental setting: in the light pulses conditions (left), the visual evoked potentials are recorded by the inter-hemispheric occipital-occipital derivation and only the right eye is stimulated. This kind of differential recording removes the common mode electrical noise while sparing the evoked response, enhancing the signal to noise ratio. Otherwise, in the darkness condition (right), both eyes are covered by a black tape and the EEG resting activity is recorded by the inter-hemispheric occipital-frontal derivation, probing a large area of cortex. (Cartoons are modified from Gordon & Stryker, 1996).

2.4 SIGNAL PROCESSING AND DATA ANALYSIS

The VEP and resting EEG recordings were analyzed by using MicrocalTM Origin® 9.1 and MathWorks MATLAB® softwares. Non-parametric statistics were applied to evaluate significance levels. Friedman test was applied to test any putative principal effect across more than 2 levels of treatment in the repeated measure designs. Wilcoxon test was used in the groups comparison and multiple comparisons contexts, for the repeated measure designs; Mann-Whitney test was chosen for a non-repeated measure design. Bonferroni-Holm correction was adopted for multiple hypothesis testing. The statistical significance was represented as follow: $p<0,05$ $*$; $p<0,01$ $**$; $p<0,001$ $***$. Error bars represent the standard error of the mean (SEM).

2.4.1 Visual evoked potential analysis

For each condition, VEPs were analyzed by using the following procedure: the ensemble average of single sweeps was computed and 1 temporal index and 2 magnitudes were considered: the VEP latency, the VEP amplitude and the VEP area. The VEP latency coincided with the temporal location of the first positive peak (P1) found after the stimulus onset. The VEP amplitude was obtained by the difference between the amplitudes of the first positive and of the first negative peaks (N1) of the VEP. The first negative peak was the first lower and negative peak detected after P1, so that the N1 latency was always bigger than the P1 latency. The VEP peaks were identified automatically by using the first derivative method which is implemented in Origin software: if a point of the raw signal locates in a position $t = x_p$ where the first derivative at $t = x_p - 1$ is positive, while the first derivative at $t = x_p + 1$, is negative, than it would be considered as a positive peak. Otherwise, if a point stands in a position $t = x_p$ where the first derivative at $t = x_p - 1$ is negative while the first derivative at $t = x_p + 1$ is positive, than it will be considered as a negative peak. The VEP area was obtained by the integration of the first 150ms of the raw and absolute signal from the stimulus onset. The VEP latency, the VEP amplitude and the VEP area of an OFF evoked

response were referred to the end of the stimulus. In order to avoid any offset errors, the amplitude values were referred to a baseline identified as a horizontal line with intercept that is the mean amplitude value of 1,05 seconds of raw data (from 50ms before the stimulus onset to 1sec after the stimulus onset).

For representative reasons, the means of VEP latencies, of VEP amplitudes and of VEP areas from stimulations of light pulses with different irradiance values were plotted together and fitted by an algorithm which is implemented in Origin software, which weighted the error bars. The function which fitted the data with the highest adjusted R^2 value was chosen.

2.4.2 Resting EEG analysis

For estimating the power spectral density (PSD) of the raw EEG signal, the averaged periodogram was computed, as follows. The 110sec raw signal of the resting brain activity of one animal in a single condition was divided into 11 successive sweeps of 10 seconds each. The signal was then band-pass filtered between 0,5 and 90Hz and, in order to suppress 50Hz power-line noise, band-block filtered between 49 and 51Hz. Each sweep was then windowed with a hamming window before fast Fourier transform (FFT) was performed. The resulting power spectrum, computed as the square magnitude of the FFT, was divided by the number of samples N and by the sampling frequency F_s, for time-integral normalization (Origin algorithm). The ensemble average of the 11 power spectra was taken as the final estimation of the PSD for the 110sec raw signal and this PSD was divided into 6 wavebands of interest: delta (0,5-6Hz), theta (6-8Hz), alpha (8-12Hz), sigma or spindle (12-15Hz), beta (15-25Hz) and gamma (25-80Hz) (the chosen wavebands were the same as those used for human studies (Murphy et al., 2011), but were corrected for the theta band, which is the only one that increments its frequency with a decrease of the cerebral dimension (Buzsáki & Watson, 2012) and for the gamma band, which was extended to its cortical whole narrower spectrum (Crone, et al., 2011) (Buzsáki & Wang, 2012) (Cardin et al., 2009) (Sohal, et al., 2009)). The integral of the PSD on each waveband was divided by the corresponding bandwidth to obtain mean power densities for each

band and the sum of all mean band power densities was taken as total PSD (0,5-80Hz) of the resting EEG activity of one animal in a single condition.

At the higher states of anesthesia induced by both sevoflurane and propofol, the EEG activity assumed a burst-suppression pattern, where transient high-voltage oscillations followed intervals of low-voltage resting activity in a quasi-periodic alternation (Fig. 23). These transient events could be clearly discriminated by band-pass filtering the raw signal within middle frequencies, therefore bursts were detected automatically by using a custom algorithm implemented in Matlab software, which was adapted from a published protocol used to detect spindles (Ferrarelli et al., 2007) (Fig. 5). The burst detection was based on the amplitude and on the duration of the transient event (Lewis et al., 2013). Each 10 second-long sweep from the 110sec raw signal was down-sampled to 5kHz, band-pass filtered between 12-15Hz and rectified (absolute value of the filtered signal). If the amplitude of a local maximum of an event of the resulting signal was above an upper threshold, the same event is considered a putative burst. The duration of the event was defined by the identification of 2 points detected when the amplitude of the event decreased below a lower threshold (the starting point precedes the local maximum and the ending point comes after the local maximum). If the duration of the identified event was ≥500ms, it was considered to be a burst. Moreover, all the identified events with inter-event distance ≤300ms, were considered as parts of one single event. For the middle states of anesthesia (sevoflurane 3,75% and propofol 1,5mg/kg/min), the upper threshold was set at 2,3 times the standard deviation (SD) of the filtered and rectified signal, while the lower threshold was set at the SD. Otherwise, for the deeper states of anesthesia (sevoflurane 5% and propofol 2mg/kg/min), the upper threshold was set as 5,1 times the SD of the filtered and rectified signal, while the lower threshold was set at 1,3 the SD[3]. The burst analysis has been realized on the corresponding events of the down-sampled raw signal and the duration and the maximum peak amplitude of the rectified bursts have been evaluated. The PSD analysis was performed on each burst by

[3] For 2 rats the upper threshold was set at 5,8 times the SD and the lower threshold was set at 1,4 times the SD, in both middle and deeper states of anesthesia induced by both anesthetics.

using the same (non-averaged) periodogram estimation procedure described above, but without filtering the raw signal. In this case, delta waveband has been redefined between 4-6Hz, due to the very short signals. Short-time Fourier transform (STFT) was also performed on each raw recording, with Hamming windows of 120ms, overlapped for 99%, in order to obtain spectrograms of the EEG resting activity and of the bursts.

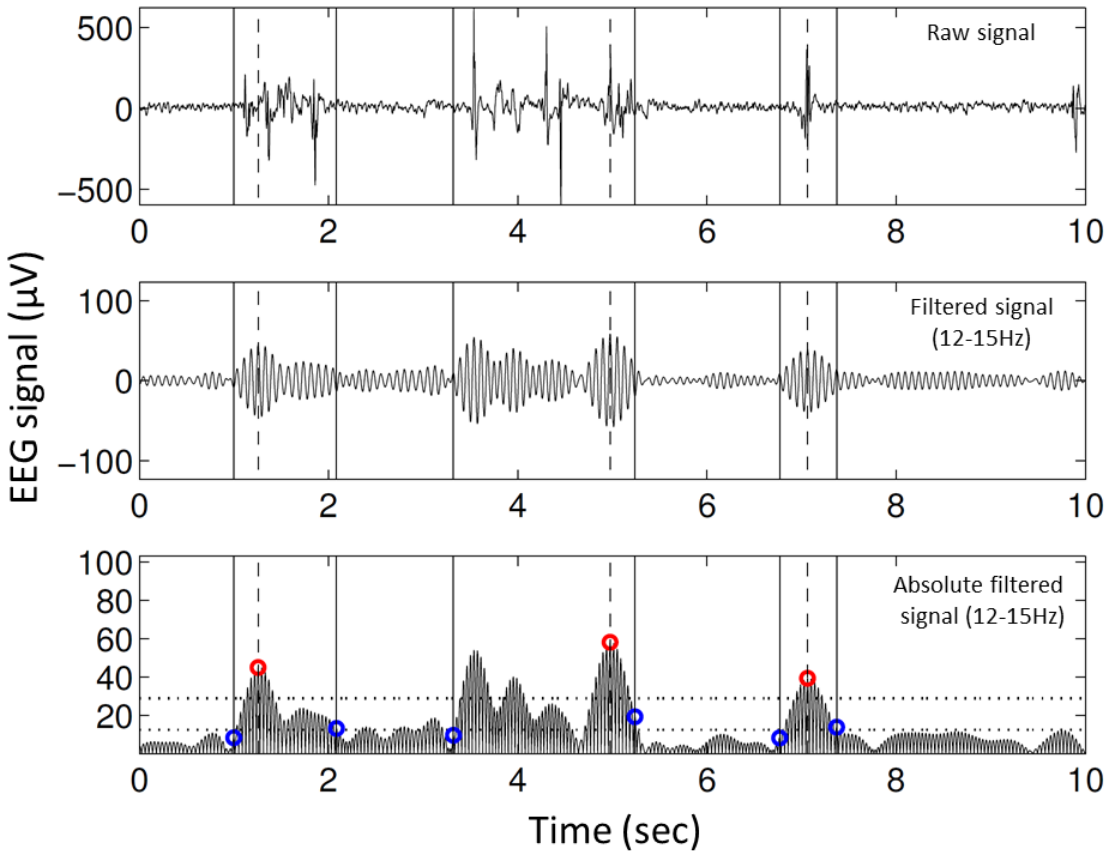

Fig. 5 Example of the burst detection from a representative animal exposed to sevoflurane 3,75%. The raw signal (top) is band-pass filtered between 12-15Hz (middle) and rectified (bottom). If the amplitude of a local maximum of an event is above an upper threshold (red circles), the event is considered a putative burst. The duration of the event is defined by a lower threshold (blue circles are the beginning or the end of a burst) ; only bursts which last ≥500ms are selected. Events with distances ≤300ms are considered as one.

3 RESULTS

3.5 THE ELECTRICAL RESPONSE OF THE VISUAL CORTEX TO LIGHT

A light pulse stimulation (flash duration 20ms and irradiance 24,8μW/cm²) induced an evoked response in the rat visual cortex, which was composed of a sequence of several positive and negative deflections of the electric field, up to 150-200ms from the stimulus onset (Fig. 6). The first positive and the first negative peaks of the VEP (P1 and N1 respectively) were the most reliable in both amplitude and latency. Both peaks were always clearly detectable even within single recordings (or sweeps), nevertheless their reproducibility was not very high within single animal recordings, as it was suggested by the coefficients of variation (CV) of the P1 amplitude from a single animal stimulated by light stimuli of different irradiance values (or brightness), which mean is higher than 0,5 (Fig. 6).

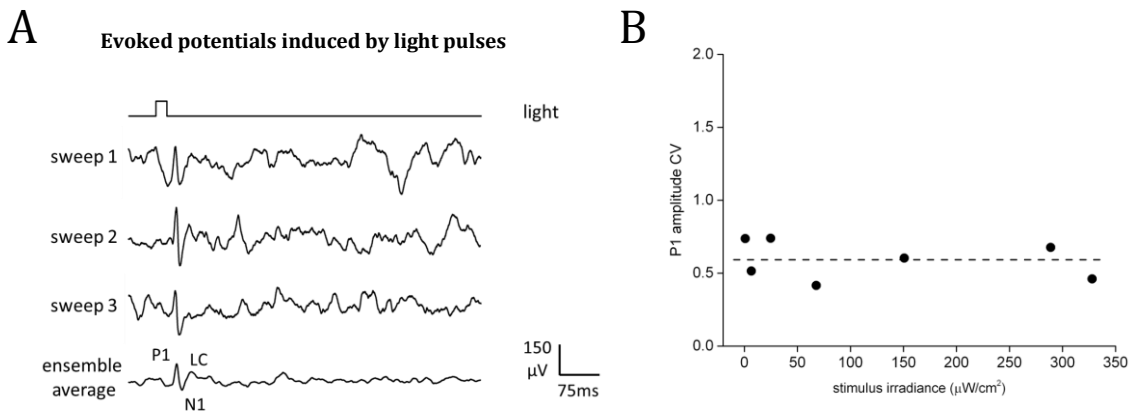

Fig. 6 A) Single recordings and ensemble average of 20 VEPs from a representative rat exposed to light pulses of 20ms and 24,8μW/cm² at sevoflurane 2,5%. **B)** Coefficients of variation (CV) of the first positive peak (P1) amplitude of VEPs obtained by stimulating the same animal with light pulses of different irradiance values and same duration of 20ms (dashed line represents the mean CV = 0,592). Amplitudes of the first positive and of the first negative peaks (P1, N1 respectively) are quite variable at each tested irradiance value, nevertheless VEP is always clearly detectable in each single recording at each irradiance value. Otherwise, the amplitudes of the subsequent peaks which represent the later complex of the VEP (LC) (up to 150-200ms from the stimulus onset), are more variable.

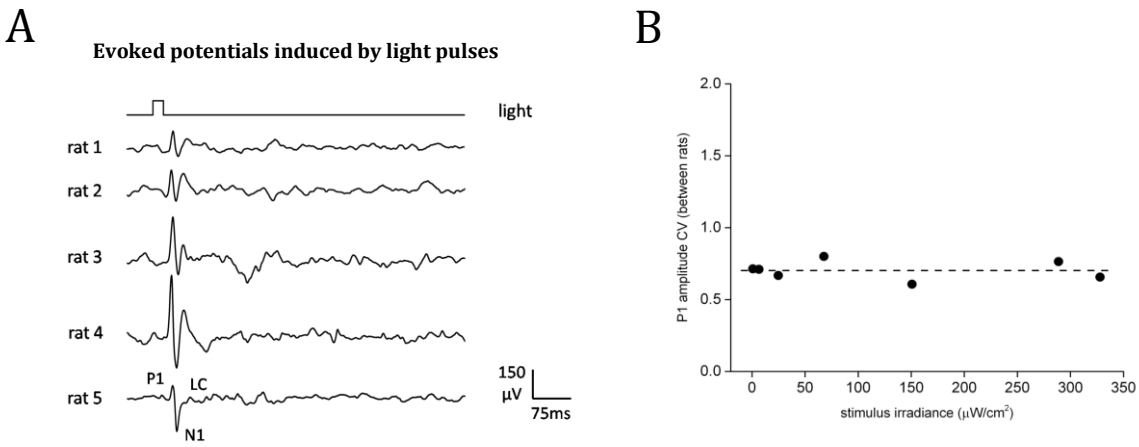

Fig. 7 **A)** Ensemble averages of 20 VEPs from 5 rats exposed to light pulses of 20ms and 24,8µW/cm^2 at sevoflurane 2,5%. **B)** Coefficients of variation (CV) of the first positive peak (P1) amplitude of the mean VEPs between rats, obtained by stimulating the same animals with light pulses of different irradiance values and same duration of 20ms (dashed line represents the mean CV = 0,702). Amplitudes of the first positive peaks are not very reproducible between rats, but this variability is stable among the tested irradiance values. The amplitudes of the subsequent peaks which represent the later complex of the VEP (LC) (up to 150-200ms from the stimulus onset), are even more variable.

Moreover, the following deflections, which represent the later complex of the VEP (LC), were even less reproducible within the same recording session. This variability probably were generated from the high voltage resting activity of the cortex, therefore to increase our ability to compare VEPs, ensemble averages of many single recordings were aways computed whithin each animal and condition.
Another source of variance were inter-individual differences such the exact position of electrodes or idiosyncrasies in the cortical response, indeed the shape of mean VEPs was not very reproducible between animals exposed to same conditions, even if first two peaks (P1 and N1) were always clearly detectable (Fig. 7). Nevertheless, this variability was stable among different stimuli, such different brightness, as it could be seen from Fig. 7-B, were CVs of the P1 amplitude of VEPs from rats exposed to light pulses of different irradiance values, were relatively stationary around their mean (CV = 0,702; n = 5). In order to reduce any bias due to this source of variability, the repeated measure design was always preferred for experiments, when it was possible.

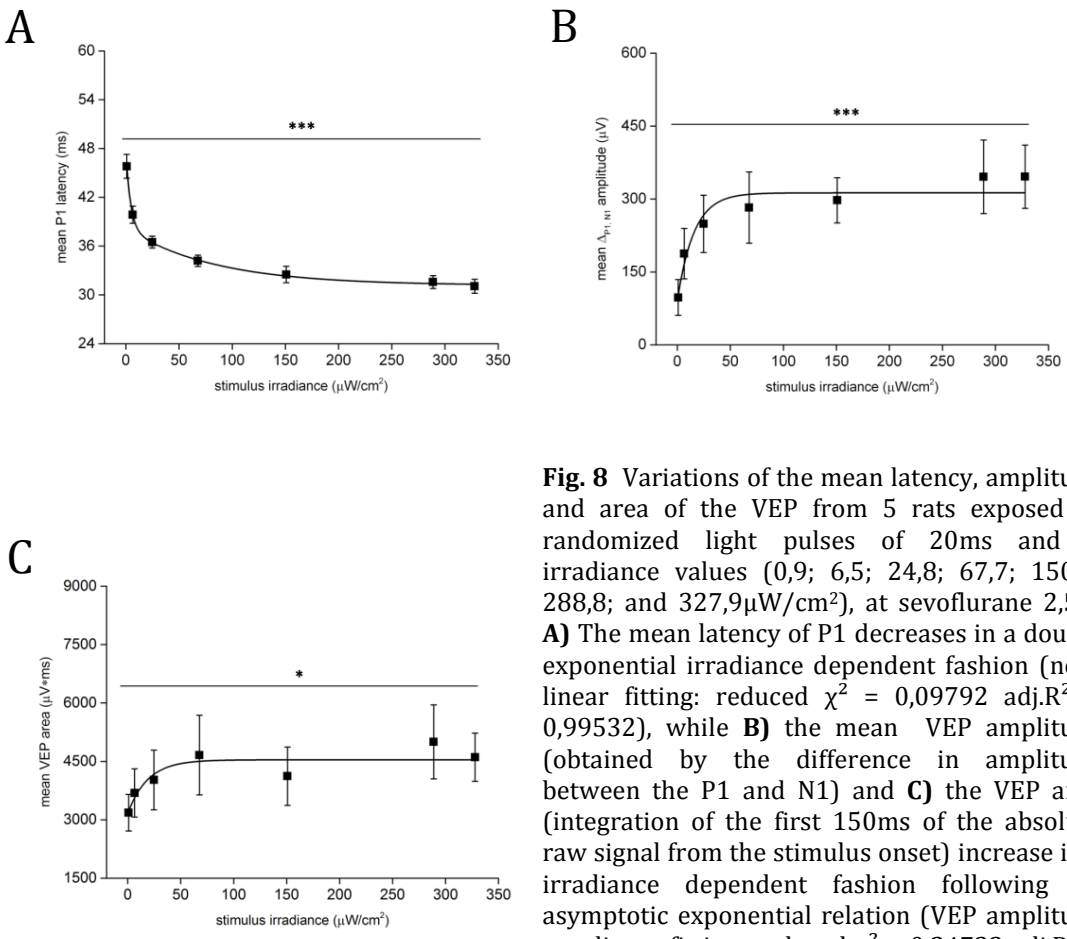

Fig. 8 Variations of the mean latency, amplitude and area of the VEP from 5 rats exposed to randomized light pulses of 20ms and 7 irradiance values (0,9; 6,5; 24,8; 67,7; 150,8; 288,8; and 327,9µW/cm²), at sevoflurane 2,5% **A)** The mean latency of P1 decreases in a double exponential irradiance dependent fashion (non-linear fitting: reduced χ^2 = 0,09792 adj.R^2 = 0,99532), while **B)** the mean VEP amplitude (obtained by the difference in amplitude between the P1 and N1) and **C)** the VEP area (integration of the first 150ms of the absolute raw signal from the stimulus onset) increase in a irradiance dependent fashion following an asymptotic exponential relation (VEP amplitude non-linear fitting: reduced χ^2 = 0,24733 adj.R^2 = 0,93184) (VEP area non-linear fitting: reduced χ^2 = 0,16767 adj.R^2 = 0,82501).
(Friedman test: principal effect of irradiance p<0,05∗ ; p<0,001∗∗∗).

Fig. 8 shows how the visual evoked response were strictly influenced by the light brightness (here measured as irradiance) in both its latency and magnitude. When animals were exposed to light pulses of same duration (20ms) and 7 different irradiance values, the mean latency of P1 exponentially decreased as the light came brighter (n=5; Friedman test: irradiance principal effect χ^2=30 df=6 p<0,001) (Fig. 8-A), while both the VEP amplitude and the VEP area quickly increased in an irradiance dependent fashion, until a plateau level was reached for brighter stimuli (n=5; Friedman test: irradiance principal effect on VEP amplitude χ^2=24,34286 df=6 p<0,001) (n=5; Friedman test: irradiance principal effect on VEP

area χ^2=15,25714 df=6 p<0,05) (Fig. 8-B,C). These physiological functions describe the relations between the stimulus intensity and brain activity and modifications in their shape could be ascribed to alterations in the computational properties induced by a particular state of the nervous system. Therefore, these stimulus-response functions could be used to clarify some aspects of the mechanism of action of drugs which modify the brain activity, like general anesthetics.

3.6 EFFECTS OF ANESTHETICS ON THE VISUAL EVOKED RESPONSE

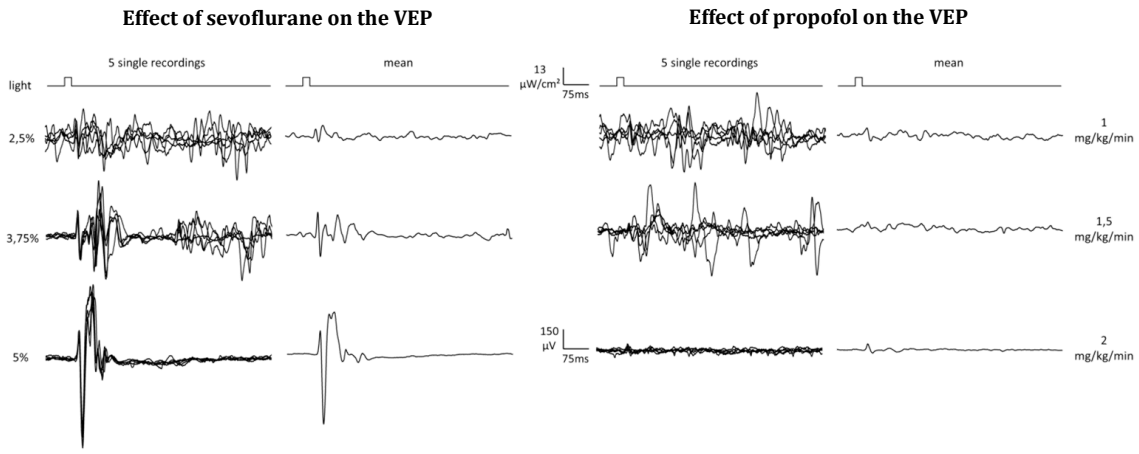

Fig. 9 Single recordings and ensemble averages of VEPs from representative animals exposed to the same light pulses (20ms, 6,5µW/cm^2) at increasing expiratory concentrations of sevoflurane (2,5%, 3,75%, 5%) (left) and propofol (1mg/kg/min, 1,5mg/kg/min, 2mg/kg/min) (right).

In this study the same 5 rats were exposed to different states of anesthesia induced by sevoflurane and propofol at 3 increasing concentrations (sevoflurane: 2,5 , 3,75 and 5 %; propofol: 1 , 1,5 and 2 mg/kg/min). In both sevoflurane and propofol conditions, the first concentration was the minimal dose required to keep the animal anesthetized, the second one was 150% of the first and the third was 200% of the first concentration. Therefore the anesthesia levels were considered comparable between the two drugs. At each state of anesthesia, visual evoked responses to different light pulse stimulations were evaluated in order to uncover some aspects of the action of these drugs.

A dim light pulse stimulation (20ms, 6,5μW/cm^2) immediately revealed how sevoflurane and propofol modify the computational properties of the brain in very different ways, even if their action results in the general anesthesia and in the loss of consciousness (Fig. 9). The resulting VEP area changed in opposing directions as the level of anesthesia increased between these two drugs. In the sevoflurane condition the VEP area increased its dimension (n=5; Friedman test: principal effect of sevoflurane χ^2=10 df=2 p<0,01), while in the propofol condition it became smaller (n=5; Friedman test: principal effect of propofol χ^2=10 df=2 p<0,01) (Fig. 10-C, D). P1 latency also changed and increased in a concentration dependent fashion with sevoflurane (n=5; Friedman test: principal effect of sevoflurane χ^2=10 df=2 p<0,01) (Fig. 10-B).

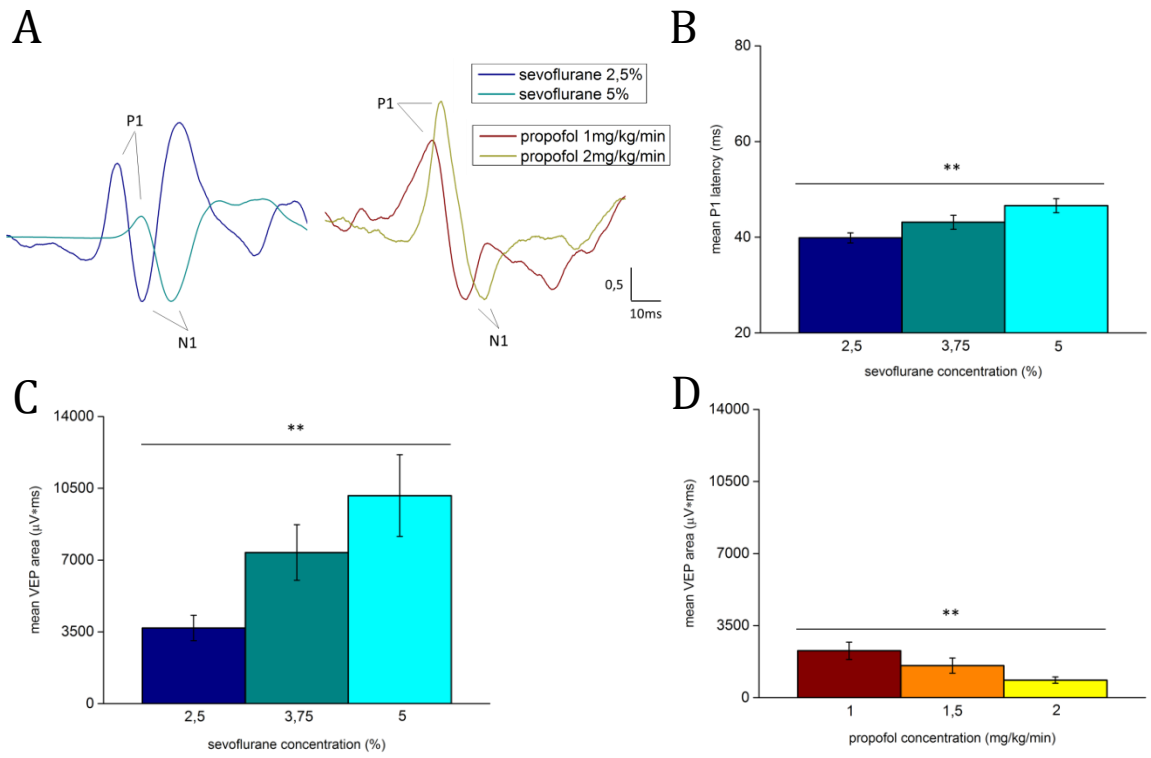

Fig. 10 **A)** Superimposition of normalized VEPs at sevoflurane 2,5-5% (left) and at propofol 1-2mg/kg/min (right) which were reported in Fig. 9 (normalization is made for N1 amplitude). **B)** Variations of the mean latency of P1 in relation to the increase of the sevoflurane concentration and variations of the mean VEP area in relation to the increase of concentration of sevoflurane **(C)** and propofol **(D)**. The mean values are obtained from 5 rats exposed to the same experimental condition of Fig. 9. The variation of the P1 latency in the propofol condition was omitted because at least one animal at each concentration condition did not show the evoked response; in particular at propofol 1mg/kg/min 2 of 5 rats did not exhibit the VEP, at propofol 1,5mg/kg/min 3 of 5 rats did not exhibit the VEP and at propofol 2mg/kg/min the VEP was not detectable for 4 of 5 rats.
(Friedman test: principal effect of drug concentration; p<0,01**).

In the propofol condition, P1 latency was not evaluated because the dim light stimulation failed to drive an evoked response in at least one animal at each concentration condition. Nevertheless, when the VEP could be detected, P1 latency was higher at the highest concentration of propofol relative to the lowest concentration, as it can be seen from the superimposition of the normalized evoked responses in Fig. 10-A.

When the same pool of animals (n=5), in the same anesthesia conditions, were exposed to light pulses (20ms) of 7 different brightness values, the relation between the irradiance and the evoked response could be evaluated. P1 latency was reduced by the intensification of the light pulse irradiance in both anesthesia conditions (Friedman test: irradiance principal effect in sevoflurane condition χ^2=84,6 df=6 p<0,001; irradiance principal effect in propofol condition χ^2=18,24 df=4 p<0,01) and the same effect was observed at each concentration condition (Table 1 for statistics) (Fig. 11-A, B; the significant marks relative to the irradiance effects are omitted because of expositive clarity). Moreover, P1 enhanced its latency in relation to the increase of the dose of both anesthetics, even if the propofol effect was detectable only by multiple comparisons (Friedman test: principal effect of sevoflurane concentration χ^2=60,33 df=2 p<0,001. Wilcoxon test: sev. 2,5 < 3,75% p<0,001 Z=-5,15236; sev. 2,5 < 5% p<0,001 Z=-5,15133; sev. 3,75 < 5% p<0,001 Z=-4,35729) (Wilcoxon test: prop. 1 < 1,5mg/kg/min p<0,05 Z=-1,84329; prop. 1 < 2mg/kg/min p<0,01 Z=-3,18861; prop. 1,5 < 2mg/kg/min p<0,05 Z=-2,44853) (Fig. 11-A, B; the significant marks relative to multiple comparisons are omitted to improve expositive clarity) (Table 1 lists statistics for each irradiance value). By enhancing the light pulse irradiance**,** the VEP area increased in both anesthesia conditions (Friedman test: irradiance principal effect in sevoflurane condition χ^2=22,2 df=6 p<0,01; irradiance principal effect in propofol condition χ^2=29,73 df=6 p<0,001) and the same effect was observed at each concentration condition (Table 2 for statistics) (Fig. 11-C, D; the significant marks relative to the irradiance effects are omitted to improve expositive clarity). Furthermore, VEP increased its area by the enhancement of the concentration of

sevoflurane (Friedman test: principal effect of sevoflurane concentration χ^2=43,56 df=2 p<0,001. Wilcoxon test: sev. 2,5 < 3,75% p<0,001 Z=-5,1021; sev. 2,5 < 5% p<0,001 Z=-5,15124; sev. 3,75 < 5% p<0,01 Z=-3,08747); while decreased its area by the enhancement of the dose of propofol (Friedman test: principal effect of propofol concentration χ^2=9,65 df=2 p<0,01. Wilcoxon test: prop. 1 > 2mg/kg/min p<0,01 Z=3,08747; prop. 1,5 > 2mg/kg/min p<0,01 Z=2,56334). In the sevoflurane condition the same relation is detected for all irradiance values but not for the lowest. While in the propofol condition, the principal effect of the anhestetic is detectable only for the 2 lower irradiance values (Fig. 11-C, D; the significant marks relative to multiple comparisons are omitted to improve expositive clarity) (Table 2 for statistics of each irradiance value).

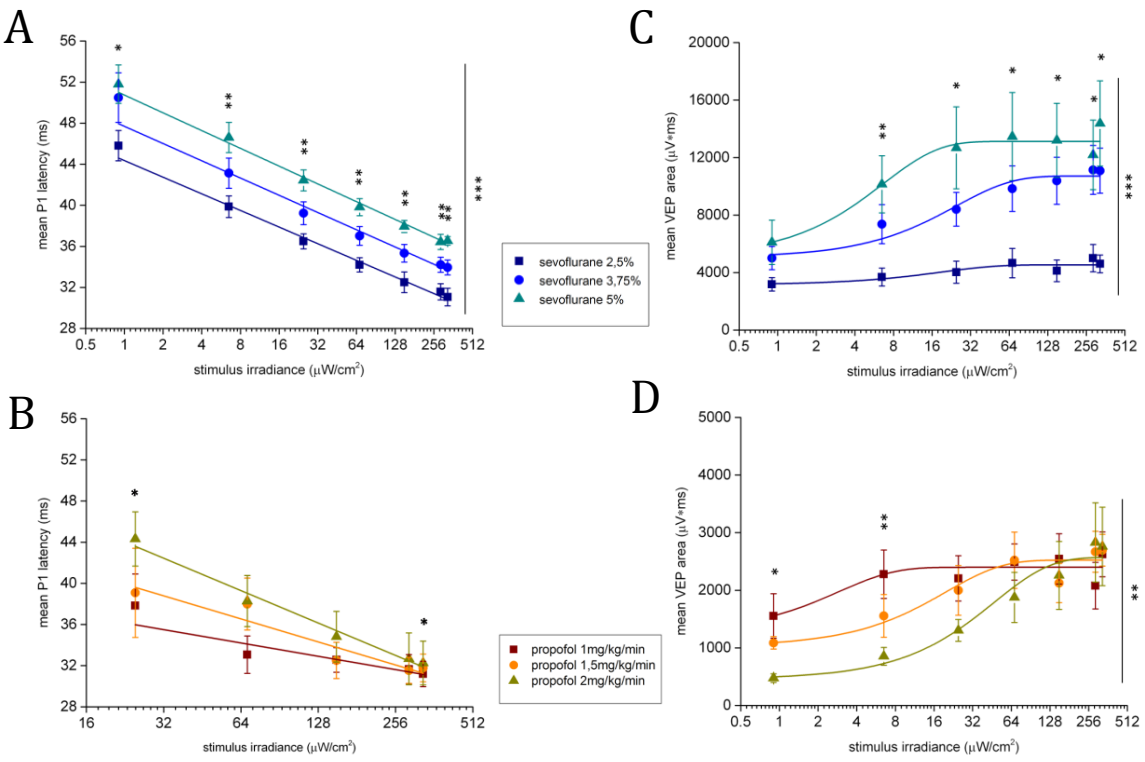

Fig. 11 A, B) Variations of the mean latency of the first positive peak of the VEP (P1) and **C, D)** variations of the area of the first 150ms of the VEP from 5 rats stimulated by randomized light pulses of 20ms and 7 irradiance values related to the increase of the expiratory concentration of sevoflurane (2,5 3,75 5%) (up) and to the increase of the endovenous concentrations of propofol (1 1,5 2mg/kg/min) (bottom). The irradiance values were: 0,9 6,5 24,8 67,7 150,8 288,8 and 327,9μW/cm². In panel B, the P1 latencies relative to the first 2 irradiance values are omitted because at each concentration condition, at least one rat did not show the evoked response. (Friedman test: principal effect of drug concentration; p<0,05 ∗ ;p<0,01 ∗∗ ; p<0,001 ∗∗∗).

Irradiance principal effect on P1 latency (Friedman test; df=6)

Sevoflurane (%)	2,5	3,75	5
χ^2	30	22,11429	17,91429
p	<0,001	<0,01	<0,01

Irradiance principal effect on P1 latency (Friedman test; df=4)

Propofol (mg/kg/min)	1	1,5	2
χ^2	13,12	9,96	19,04
p	<0,05	<0,05	<0,001

Principal effect of sevoflurane concentration on P1 latency (Friedman test; df=2)

Irradiance ($\mu W/cm^2$)	0,9	6,5	24,8	67,7	150,8	288,8	327,9
χ^2	7,6	10	10	10	10	10	10
p	<0,05	<0,01	<0,01	<0,01	<0,01	<0,01	<0,01

Principal effect of propofol concentration on P1 latency (Friedman test; df=2)

Irradiance ($\mu W/cm^2$)	0,9	6,5	24,8	67,7	150,8	288,8	327,9
χ^2	-	-	7,6	4,8	2,8	1,2	11,46667
p	-	-	<0,05	>0,05	>0,05	>0,05	<0,05

Table 1 Statistics of the irradiance principal effects on the P1 latency variation, in sevoflurane and propofol conditions (up) and statistics of the anesthetic concentration principal effects on the P1 latency variations in each irradiance condition (bottom). Statistics are from Fig. 11, pannels A and B.

Irradiance principal effect on VEP area (Friedman test; df=6)

Sevoflurane (%)	2,5	3,75	5
χ^2	18,17143	22,11429	17,91429
P	<0,01	<0,01	<0,01

Irradiance principal effect on VEP area (Friedman test; df=6)

Propofol (mg/kg/min)	1	1,5	2
χ^2	14,31429	19,71429	25,54286
P	<0,05	<0,01	<0,001

Principal effect of sevoflurane concentration on VEP area (Friedman test; df=2)

Irradiance ($\mu W/cm^2$)	0,9	6,5	24,8	67,7	150,8	288,8	327,9
χ^2	3,6	10	7,6	7,6	7,6	7,6	8,4
p	>0,05	<0,01	<0,05	<0,05	<0,05	<0,05	<0,05

Principal effect of propofol concentration on VEP area (Friedman test; df=2)

Irradiance ($\mu W/cm^2$)	0,9	6,5	24,8	67,7	150,8	288,8	327,9
χ^2	7,6	10	5,2	2,8	2,8	1,6	0,4
p	<0,05	<0,01	>0,05	>0,05	>0,05	>0,05	>0,05

Table 2 Statistics of the irradiance principal effects on the VEP area variation, in sevoflurane and propofol conditions (up) and statistics of the anesthetic concentration principal effects on the VEP area variations in each irradiance condition (bottom). Statistics are from Fig. 11, pannels C and D.

3.7 CHARACTERIZATION OF THE OFF COMPONENT OF THE VEP

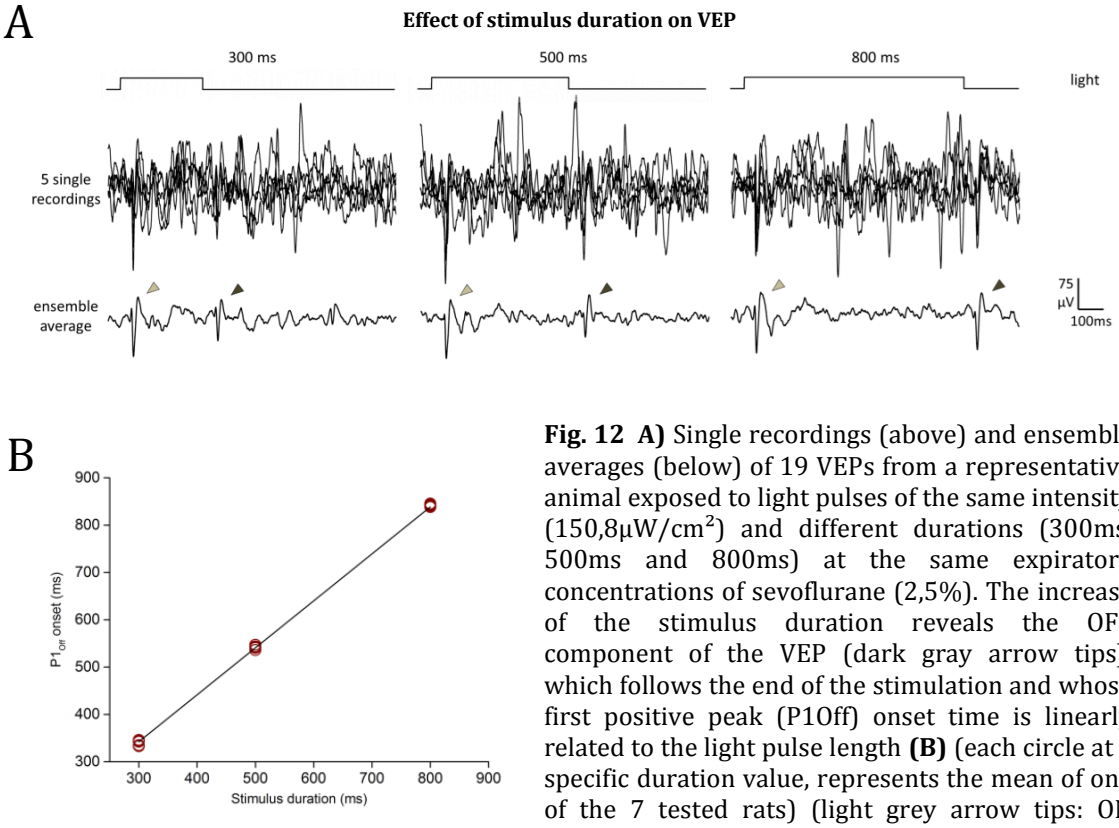

Fig. 12 A) Single recordings (above) and ensemble averages (below) of 19 VEPs from a representative animal exposed to light pulses of the same intensity (150,8µW/cm^2) and different durations (300ms, 500ms and 800ms) at the same expiratory concentrations of sevoflurane (2,5%). The increase of the stimulus duration reveals the OFF component of the VEP (dark gray arrow tips), which follows the end of the stimulation and whose first positive peak (P1Off) onset time is linearly related to the light pulse length **(B)** (each circle at a specific duration value, represents the mean of one of the 7 tested rats) (light grey arrow tips: ON component of the VEP).

When rats (n=7) were exposed to randomized light pulses of the same irradiance (150,8µW/cm^2) and 3 different durations (300, 500 and 800ms), a response which followed the end of the stimulation (VEPOff) could be detected (Fig. 12). The OFF response followed the end of the stimulation and its first positive peak (P1Off) onset time was linearly related to the light pulse length (Fig. 12-B). In this study no difference was found among the P1Off latencies and the VEPOff areas of the evoked responses relative to the different durations of light pulses (Fig. 13), whereas some differences were found in relation to the ON component of the VEP (VEPOn). The latency of P1Off seemed to be always higher than the latency of P1On, independently from the light pulse duration (Wilcoxon test: P1On 300ms < P1Off 300ms p<0,05 Z=1,94385; P1On 500ms < P1Off 500ms p<0,01 Z=2,28192; P1On 800ms < P1Off 800ms p<0,01 Z=2,28192) (Fig. 13-A).

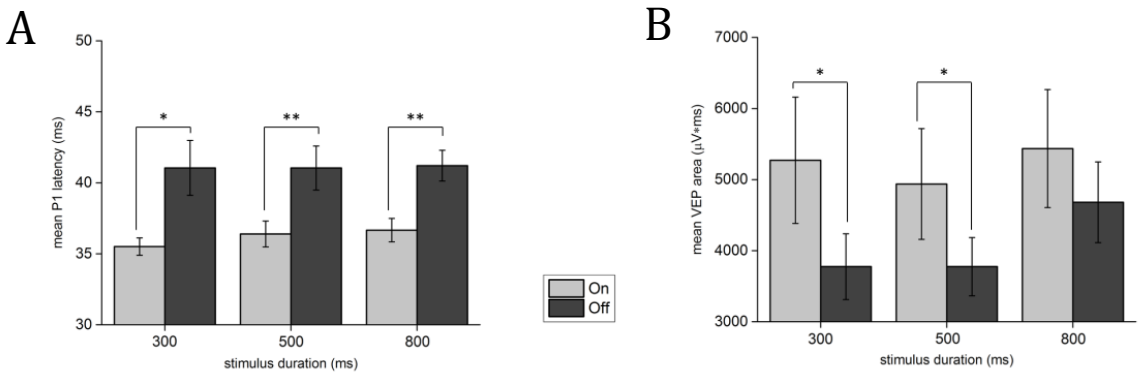

Fig. 13 Variations of mean P1Off latency and VEPOff area from 7 rats exposed to to light pulses of the same intensity (150,8µW/cm^2) and different durations (300ms, 500ms and 800ms) at the same expiratory concentrations of sevoflurane (2,5%). **C)** The mean P1Off latency from the end of the stimulus, does not change among the light pulses of different durations and it is always longer compared to the latency of the first positive peak (P1On) of the ON component of the VEP. **D)** The mean VEPOff area (obtained by the integration of the rectified first 150ms of the raw signal from the stimulus offset) also does not change among the light pulses of different duration, but it is smaller than the VEPOn areas induced by light pulses of 300ms and 500ms.
(Wilcoxon test; p<0,05 ∗ ; p<0,01 ∗∗).

Otherwise, the VEPOff area was smaller than the area of the On component of the VEP in 2 of the 3 tested light pulse durations (300 and 500ms) (Wilcoxon test: VEPOn 300ms > VEPOff 300ms p<0,05 Z=-1,77482; VEPOn 500ms > VEPOff 500ms p<0,05 Z=-1,77482) (Fig. 13-B).

In order to verify if the OFF component of the VEP seen in Fig. 12-13 were effectively related to the OFF pathway of the retina by reflecting the activity of a distinct population of cells, animals were subjected to an intravireal injection of L-AP4 (L-2-amino-4-phosphonobutyric acid) 2mM (Fig. 14). L-AP4 is an agonist of mGluR6 inhibitory receptors which are expressed at the synaptic membrane of the ON bipolar cells, but are absent at the synaptic membrane of the OFF bipolar cells. Therefore, L-AP4 is able to selectively cut down the activity of the ON pathway, sparing the OFF pathway activity (Slaughter & Miller, 1981) (Manookin et al., 2008). As it would be expected, after the injection of L-AP4, the ON component of the VEP were suppressed while the OFF response were preserved and increased in area dimension (n=4; Wilcoxon test: VEPOn before L-AP4 > VEPOn with L-AP4 p<0,05 Z=1,88776; VEPOff before L-AP4 < VEPOff with L-AP4 p<0,05 Z=1,88776) (Fig 14-B).

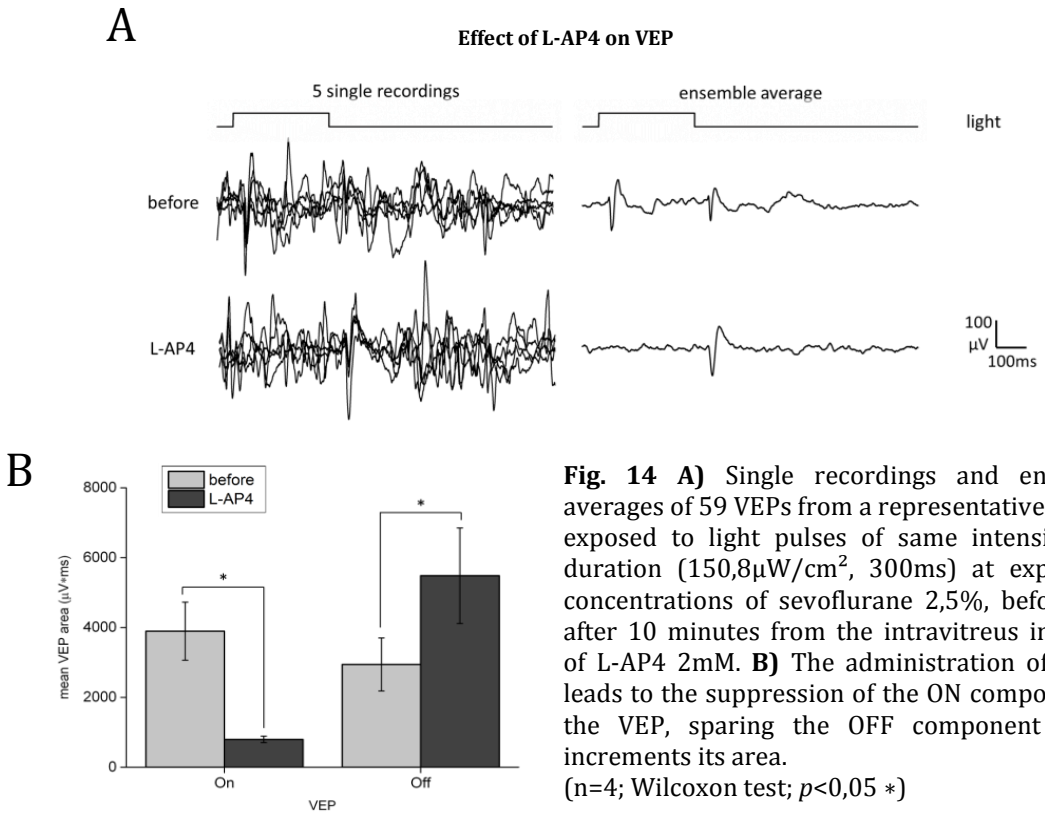

Fig. 14 A) Single recordings and ensemble averages of 59 VEPs from a representative animal exposed to light pulses of same intensity and duration (150,8µW/cm^2, 300ms) at expiratory concentrations of sevoflurane 2,5%, before and after 10 minutes from the intravitreus injection of L-AP4 2mM. **B)** The administration of L-AP4 leads to the suppression of the ON component of the VEP, sparing the OFF component which increments its area.
(n=4; Wilcoxon test; p<0,05 ∗)

Since a negative relation exists in the retina from the ON to the OFF pathway, it was important to test if this cross inhibition could affect the ability of the OFF pathway to discriminate different light intensities. If the OFF discrimination was affected by the negative interaction, for example due to the exceeding of the cross inhibition farther the duration of the light stimulation, the OFF response should be inversely dependent on the excitation level of the ON pathway, by decreasing its area dimension as the ON response increases. In order to test this possibility, rats were exposed to light pulses of 7 different brightness end adequate duration (300ms) to detect the OFF response (n=3) (Fig 15). The OFF component of the VEP was always smaller in area dimension then the ON component of the VEP (Wilcoxon test: VEPOn area > VEPOff area p<0,001 Z=3,99713). Otherwise, both the ON and OFF VEP areas increased in a irradiance dependent fashion (Friedman test: irradiance principal effect on the VEPOn χ^2=14 df=6 p<0,05) (Friedman test: irradiance principal effect on the VEPOff χ^2=16 df=6 p<0,05) (Fig. 15-B).

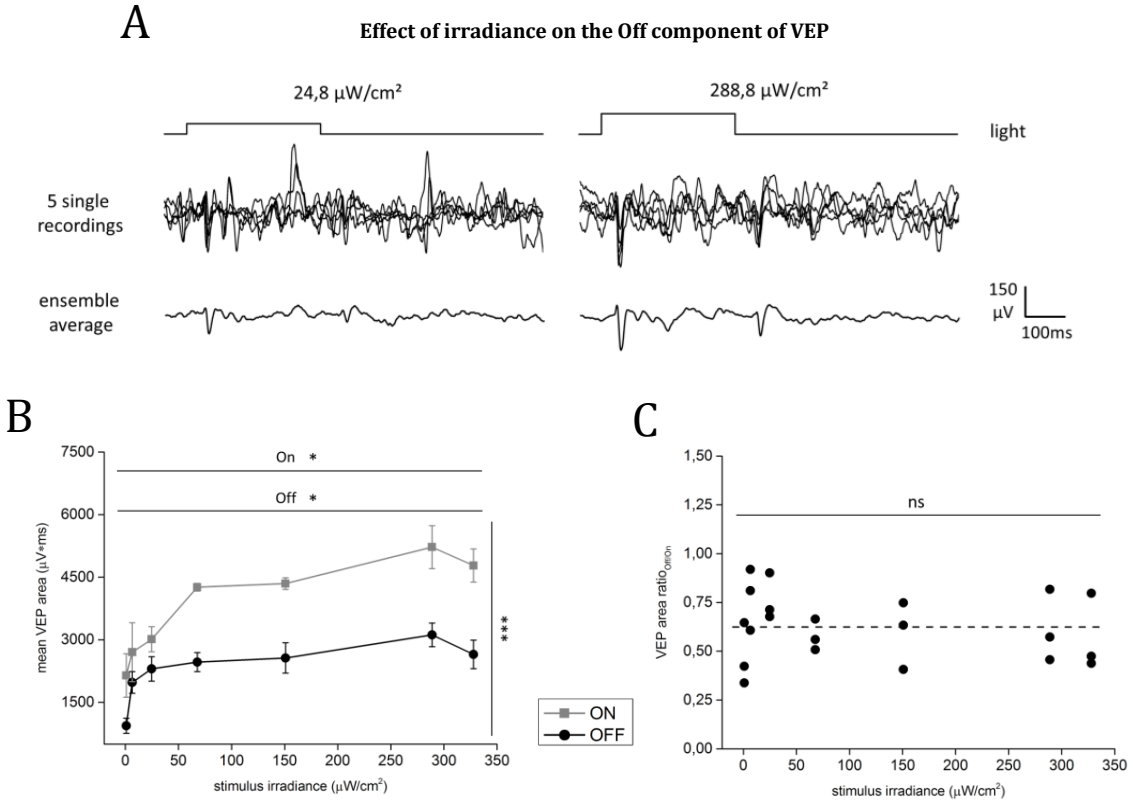

Fig. 15 **A)** Single recordings and ensemble averages of 21 VEPs from a representative animal exposed to light pulses of same duration 300ms and different irradiance: 24,8µW/cm² (left) and 288,8µW/cm² (right) at same expiratory concentrations of sevoflurane 2,5%. **B)** variations of VEP area of both ON and OFF first 150ms from rats in the same experimental conditions and exposed to randomized light pulses of 7 irradiance values (0,9 6,5 24,8 67,7 150,8 288,8 and 327,9µW/cm²). Both OFF and ON components of the VEP increase the area in an irradiance dependent fashion. Moreover, the VEPOn area is bigger than the VEPOff. **C)** By confirming of the same relation with which the areas of the ON and OFF components of VEP increase in an irradiance dependence fashion, the ratio VEPOff area/VEPOn area does not seem to change on varying of light irradiance (each circle is the mean VEP area ratio value of a single animal in a single condition and the dashed line is the mean value between animals and conditions: 0,6243).
(n=3; Friedman test: principal effect of irradiance $p<0,05$ ∗ ; $p>0,05$ ns; Wilcoxon test $p<0,001$ ∗∗∗)

Moreover the relative area increments of the VEPOn and of the VEPOff in relation to the brightness were the same, as no irradiance effect was found throughout the VEP area ratio of the OFF to ON responses (Friedman test: irradiance principal effect on the VEPOff area/VEPOn area $\chi^2=5,28571$ df=6 $p>0,05$) (Fig. 15-C).

3.8 EFFECT OF ANESTHETICS ON THE OFF COMPONENT OF THE VEP

Towards the ON response, the OFF evoked potential origins from a distinct and fairly independent population of cells, therefore the assessment of the effects of sevoflurane and propofol on this later component of the VEP could be informative about the action of these drugs (Fig. 16).

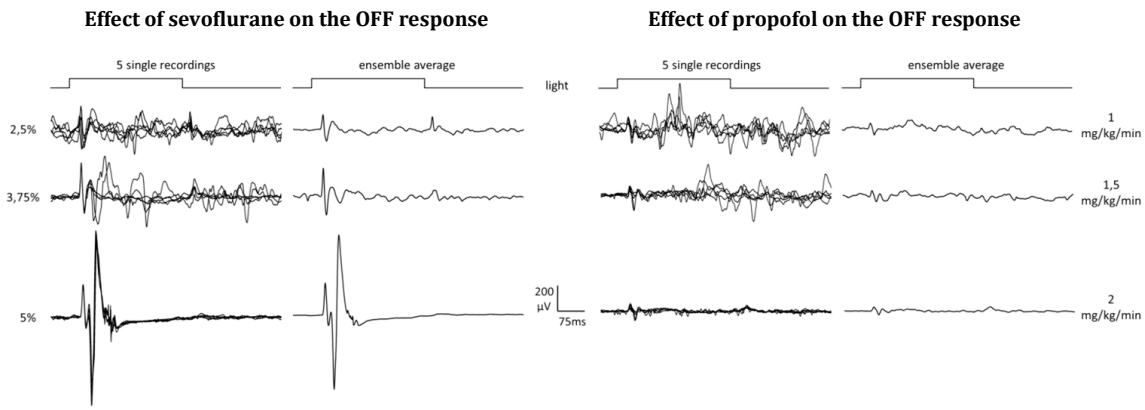

Fig. 16 Single recordings and ensemble averages of 19 VEPs from representative animals exposed to the same light pulses (300ms, 150,8µW/cm^2) at increasing expiratory concentrations of sevoflurane (2,5%, 3,75%, 5%) (left) and at increasing systemic concentrations of propofol (1mg/kg/min, 1,5mg/kg/min, 2mg/kg/min) (right).

When the same rats were stimulated by prolonged light pulses of fixed irradiance (300ms, 150,8µW/cm^2) at increasing and comparable concentrations of sevoflurane (2,5 , 3,75 and 5%) and propofol (1 , 1,5 and 2mg/kg/min), a significant difference between the trends of the OFF and ON responses was detected only with the sevoflurane anesthesia (n=5) (Fig. 16, 17). Each anesthetic leaded to the increase of the P1 latency in a dose dependent fashion, in both the ON and the OFF components of the VEP (Friedman test: principal effect of sevoflurane on the ON component of the VEP χ^2=10 df=2 p<0,01; Wilcoxon test: sev. 2,5% OFF < sev. 3,75% OFF Z=-1,88776 p<0,05) (Fig. 17-A); (Friedman test: principal effect of propofol on the ON component of the VEP χ^2=8,4 df=2 p<0,05; principal effect of propofol on the OFF component of the VEP χ^2=8,4 df=2 p<0,05) (Fig. 17-B).

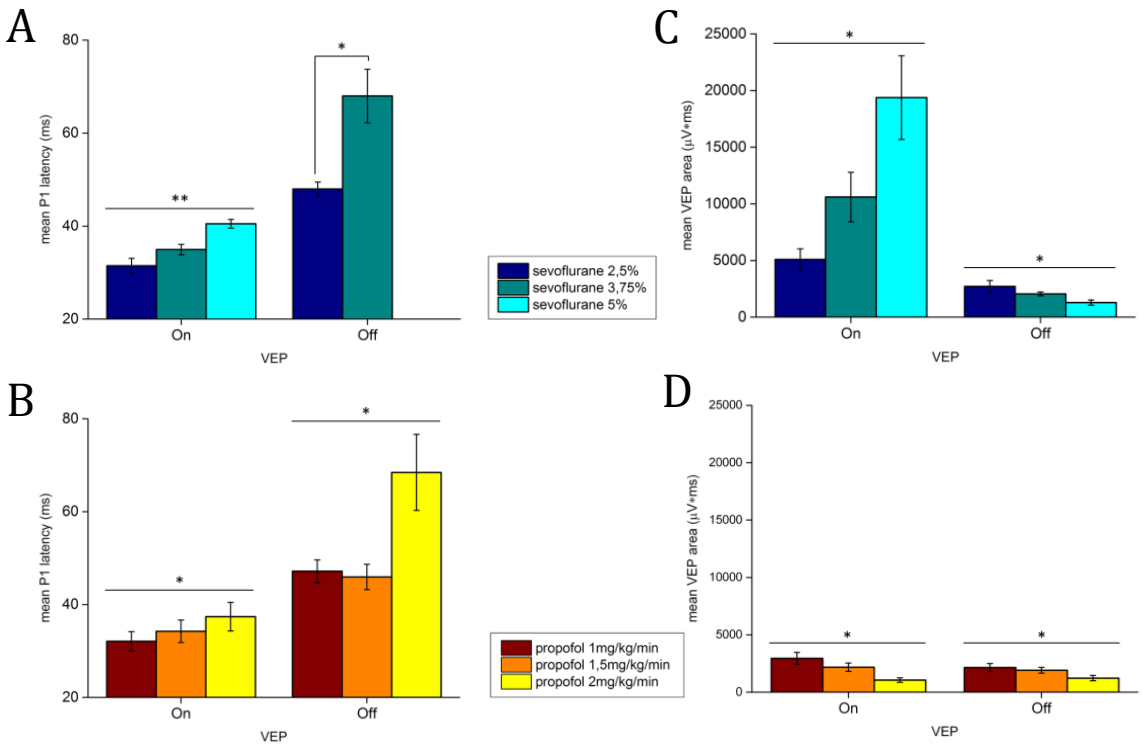

Fig. 17 A, B) Variations of the mean latency of the first positive peak (P1) of both the ON and the OFF components of the VEP and **C, D)** variations of the area of the first 150ms of both the ON and the OFF components of the VEP from rats stimulated by the same light pulses of 300ms and 150,8µW/cm^2 relative to the increase of the expiratory concentration of sevoflurane (2,5 3,75 5%) (up) and to the increase of the endovenous concentrations of propofol (1 1,5 2mg/kg/min) (bottom). In panel A, the P1 latency relative to the OFF response at sevoflurane 5% is omitted because none rat showed the evoked OFF response. Therefore, in panel C, the area of the OFF response at sevoflurane 5% is referred to the integration of 150ms of the rectified resting oscillation after the stimulus offset. (n=5; Friedman test: principal effect of drug concentration; p<0,05 ∗ p<0,01 ∗∗; Wilcoxon test: p<0,05 ∗).

The enhancement of the concentration of sevoflurane induced an increase in the area of the ON component of the VEP trace, while the area of the OFF response decreased in a dose dependent manner, until its disappearance at the highest concentration (Friedman test: principal effect of sevoflurane on the ON component of the VEP χ^2=8 df=2 p<0,05; principal effect of sevoflurane on the OFF component of the VEP χ^2=6,5 df=2 p<0,05) (Fig. 16, 17-C). Otherwise, propofol induced a reduction of the area of both the ON and the OFF components of the VEP trace in a dose dependent fashion (Friedman test: principal effect of propofol on the ON

component of the VEP χ^2=8,4 df=2 p<0,05; principal effect of propofol on the OFF component of the VEP χ^2=8,4 df=2 p<0,05) (Fig. 17-D).

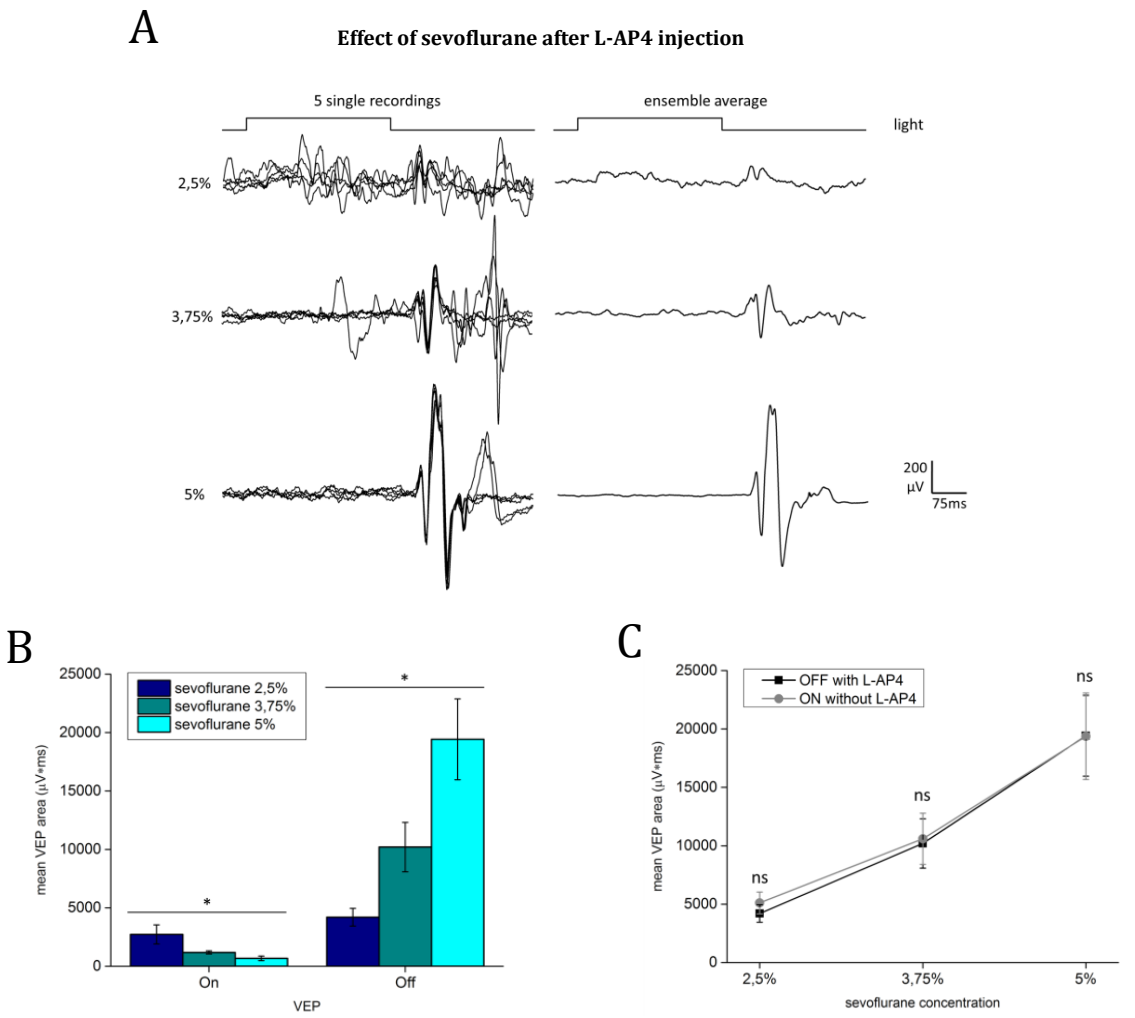

Fig. 18 **A)** Single recordings and ensemble averages of 24 VEPs from a representative animal exposed to the same light pulses (300ms, 150,8µW/cm^2) at increasing expiratory concentrations of sevoflurane (2,5%, 3,75%, 5%) immediately after the intravitreal injection of L-AP4 2-8mM and **B)** variations of the area of both ON and OFF first 150ms of the VEP from rats in the same experimental conditions (n=4). After the intravitreal injection of L-AP4, the ON component of the VEP is no more detectable and the decrease of its area among the sevoflurane concentrations could be ascribed to the reduction of the brain resting activity. **C)** Comparison throughout the increasing expiratory concentrations of sevoflurane, between the variations of the VEPOff area after the L-AP4 administration from the same 4 rats and the variations of the VEPOn area from another group of 5 animals never treated with L-AP4 and exposed to the same light stimulation.
(Friedman test: principal effect of drug concentration p<0,05 ∗ ;Mann-Whitney test: p>0,05 ns).

In order to test the action of sevoflurane on the OFF response isolated from the ON pathway, rats were exposed to the same concentrations of sevoflurane (2,5 - 3,75 - 5%) and were stimulated by the same light pulses of the experiment reported in Fig. 15-16 (300ms, 150,8μW/cm^2) immediately after an intravireal injection of L-AP4 2-8mM (n=4) (Fig. 18). The L-AP4 suppressed the ON response and the decrease of its area among the sevoflurane concentrations could be ascribed to the reduction of the brain resting activity. Otherwise, the OFF component of the VEP increased its area in a dose dependent fashion (Friedman test: sevoflurane principal effect on the ON component of the VEP χ^2=6,5 df=2 p<0,05; sevoflurane principal effect on the OFF component of the VEP χ^2=8 df=2 p<0,05) (Fig. 18-B). Moreover, none difference was detectable by comparing the variations of the VEPOff area with L-AP4 to the variations of the VEPOn area from another group of animals never treated with L-AP4 and exposed to the same light stimulation and sevoflurane concentrations (n=5) (Mann-Whitney test: sev. 2,5% VEPOn without L-AP4 ≠ VEPOff with L-AP4 p>0,05 Z=-0,61237; sev. 3,75% VEPOn without L-AP4 ≠ VEPOff with L-AP4 p>0,05 Z=0,12247; sev. 5% VEPOn without L-AP4 ≠ VEPOff with L-AP4 p>0,05 Z=0) (Fig. 18-C).

3.9 EFFECTS OF SEVOFLURANE AND PROPOFOL ON RESTING EEG ACTIVITY

To better understand the mechanism of action of this two anesthetics on the cortical circuit and on the thalamic-cortical connection, the EEG resting activity was recorded from animals exposed to the same increasing and comparable concentrations of sevoflurane (2,5%, 3,75%, 5%) and propofol (1mg/kg/min, 1,5mg/kg/min, 2mg/kg/min), by means of the occipital-frontal derivation (see methods) (n=5). This derivation was selected to improve the collection of the different basal rhythms. During the 110 seconds of recording for each condition, no stimulation was presented and rats were kept completely in the dark. Even if the visual evoked response changed in opposite directions with anesthesia depth, the amplitude of the resting oscillations decreased as a function of the anesthetic concentration in both sevoflurane and propofol conditions (Fig. 19).

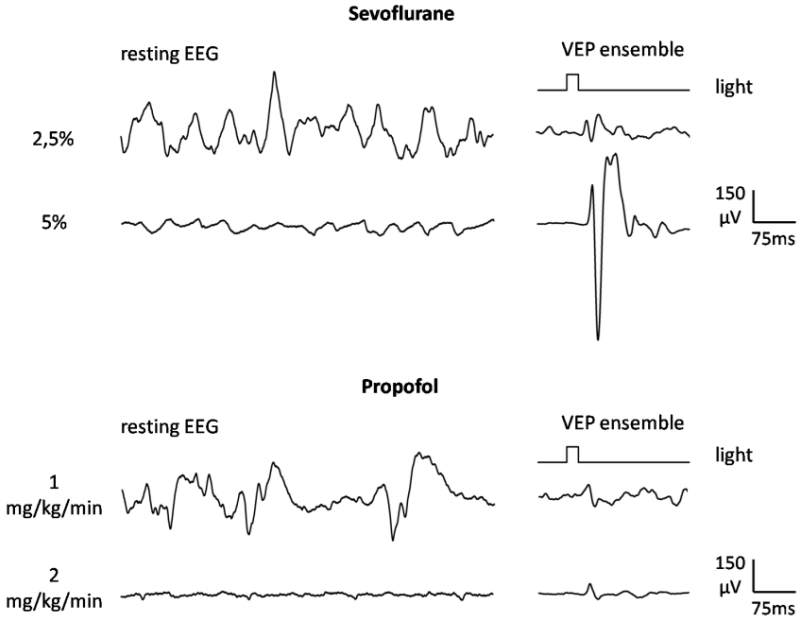

Fig. 19 Ensemble averages of VEPs and corresponding single recordings of resting EEG activity from representative animals exposed to low and high expiratory concentrations of sevoflurane (2,5 - 5%) (up) and at low and high endovenous concentrations of propofol (1 - 2mg/kg/min) (bottom).

This was confirmed by the variations of the power spectral densities (PSDs). In both anesthetic conditions, the PSD of the total frequency band of interest (broadband: 0,5-80Hz) decreased in a concentration dependent fashion (Friedman test: principal effect of sevoflurane concentration χ^2=7,6 df=2 p<0,05; principal effect of propofol concentration χ^2=10 df=2 p<0,01). The same trend was followed by each single waveband for both anesthetics, with the exception of the gamma band (25-80Hz) in the sevoflurane anesthesia, which seemed to increase even if no significant difference was detected among the concentrations (Fig. 20) (Table 3 for statistics of each waveband).

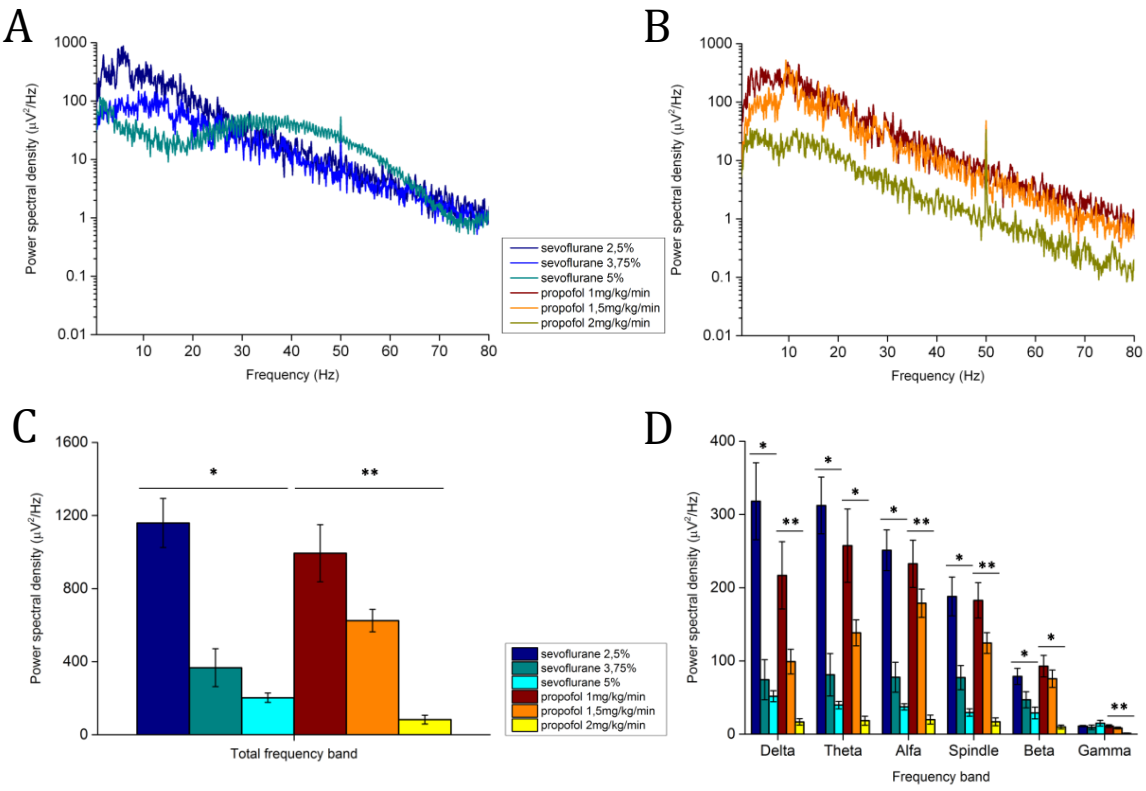

Fig. 20 **A, B)** Average periodograms from unfiltered EEG recordings (length 110 seconds) in resting condition from 2 representative experiments. Rats were exposed to the increasing expiratory concentration of sevoflurane (2,5 - 3,75 - 5%) (left) and to the increasing endovenous concentrations of propofol (1 - 1,5 - 2mg/kg/min) (right). **C)** Variations of the mean power spectral density (PSD) of the total frequency band (from 0,5 to 80 Hz) and **D)** of each frequency band of interest relative to the increase of the anesthetics concentrations. (n=5; Friedman test: principal effect of drug concentration; p<0,05 ∗ p<0,01 ∗∗).

Principal effect of sevoflurane concentration on PSD (Friedman test; df=2)

Wave band (Hz)	Delta (0,5-6)	Theta (6-8)	Alpha (8-12)	Spindle (12-15)	Beta (15-25)	Gamma (25-80)
χ^2	7,6	7,6	8,4	8,4	8,4	5,2
p	<0,05	<0,05	<0,05	<0,05	<0,05	>0,05

Principal effect of propofol concentration on PSD (Friedman test; df=2)

Wave band (Hz)	Delta (0,5-6)	Theta (6-8)	Alpha (8-12)	Spindle (12-15)	Beta (15-25)	Gamma (25-80)
χ^2	10	8,4	10	10	8,4	10
p	<0,01	<0,05	<0,01	<0,01	<0,05	<0,01

Table 3 Statistics of the anesthetic concentration principal effect on the PSD variations for each wave band, in sevoflurane (up) and in propofol (bottom) conditions. Statistics are from Fig. 20, panel D.

Nevertheless, it is important to note that the relative contribution of each waveband was not always stable for all anesthesia conditions (Fig. 21). The normalization of each waveband power for the broadband PSD of the corresponding condition, revealed that in the lighter states of anesthesia induced by both drugs, the relative contribution of the beta activity (15-25Hz) was lower than in the deeper states of anesthesia (Friedman test: sevoflurane principal effect for beta band χ^2=7,6 df=2 p<0,05; propofol principal effect for beta band χ^2=7,6 df=2 p<0,05). Moreover, for the sevoflurane conditions, the relative activity in the spindle band (12-15Hz) was higher in the middle state of anesthesia and the relative gamma power increased as a function of the dose (Friedman test: sevoflurane principal effect for spindle band χ^2=6,4 df=2 p<0,05; sevoflurane principal effect for gamma band χ^2=10 df=2 p<0,01).

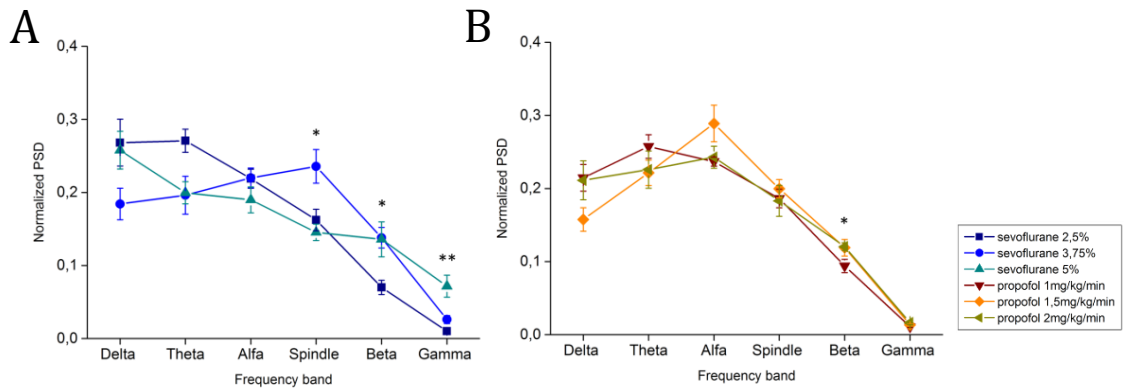

Fig. 21 Contribution of each wave band in relation to the power of the total frequency band. **A)** In the sevoflurane condition, the relative contribution of each frequency band among the 3 concentrations seems to be stable only for the slower frequencies; at the intermediate concentration, the contribution of the spindle band (12-15 Hz) is higher than at the other concentrations, while the beta (15-25 Hz) power contribution is smaller at the lowest concentration and the relative gamma power increases in a dose dependent fashion. **B)** In the propofol condition, only the beta band contribution seems to change among the 3 concentrations, increasing its relative power at the higher concentrations.
(n=5; Friedman test: principal effect of drug concentration; $p<0,05$ ∗ $p<0,01$ ∗∗)

It is interesting to observe that the spectra of the lightest states of anesthesia with sevoflurane and propofol exhibited the same pattern of relative powers, dominated by lower frequencies. Otherwise, at the 2 higher concentrations, when the relative beta power increased within each anesthetic (Fig. 22), some differences between the spectra of this two drugs could be detected. The relative contribution of the alpha activity (8-12Hz) was higher in the propofol anesthesia (Wilcoxon test for alpha band: sev. 3,75% < prop. 1,5mg/kg/min $p<0,05$ Z=-1,88776; sev. 5% < prop. 2mg/kg/min $p<0,05$ Z=-1,88776), while the relative gamma power was higher in the sevoflurane conditions (Wilcoxon test for gamma band: sev. 3,75% > prop. 1,5mg/kg/min $p<0,05$ Z=1,88776; sev. 5% > prop. 2mg/kg/min $p<0,05$ Z=1,88776) (n=5) (Fig. 22).

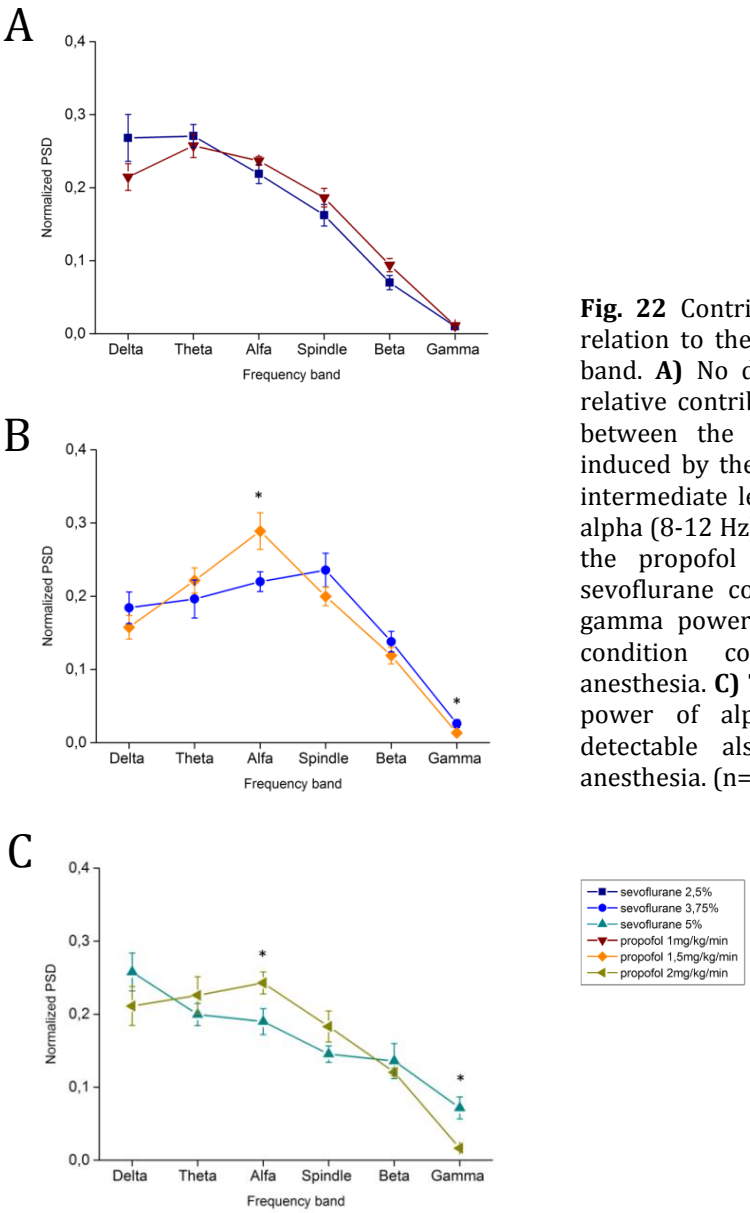

Fig. 22 Contribution of each wave band in relation to the power of the total frequency band. **A)** No difference is found among the relative contributions of all frequency bands between the lightest states of anesthesia induced by the 2 drugs **B)** Otherwise, at the intermediate level of anesthesia, the relative alpha (8-12 Hz) band contribution is higher in the propofol condition compared to the sevoflurane condition, whereas the relative gamma power is higher in the sevoflurane condition compared to the propofol anesthesia. **C)** The same variations in relative power of alpha and gamma bands are detectable also at the highest level of anesthesia. (n=5; Wilcoxo test: $p<0,05$ ∗).

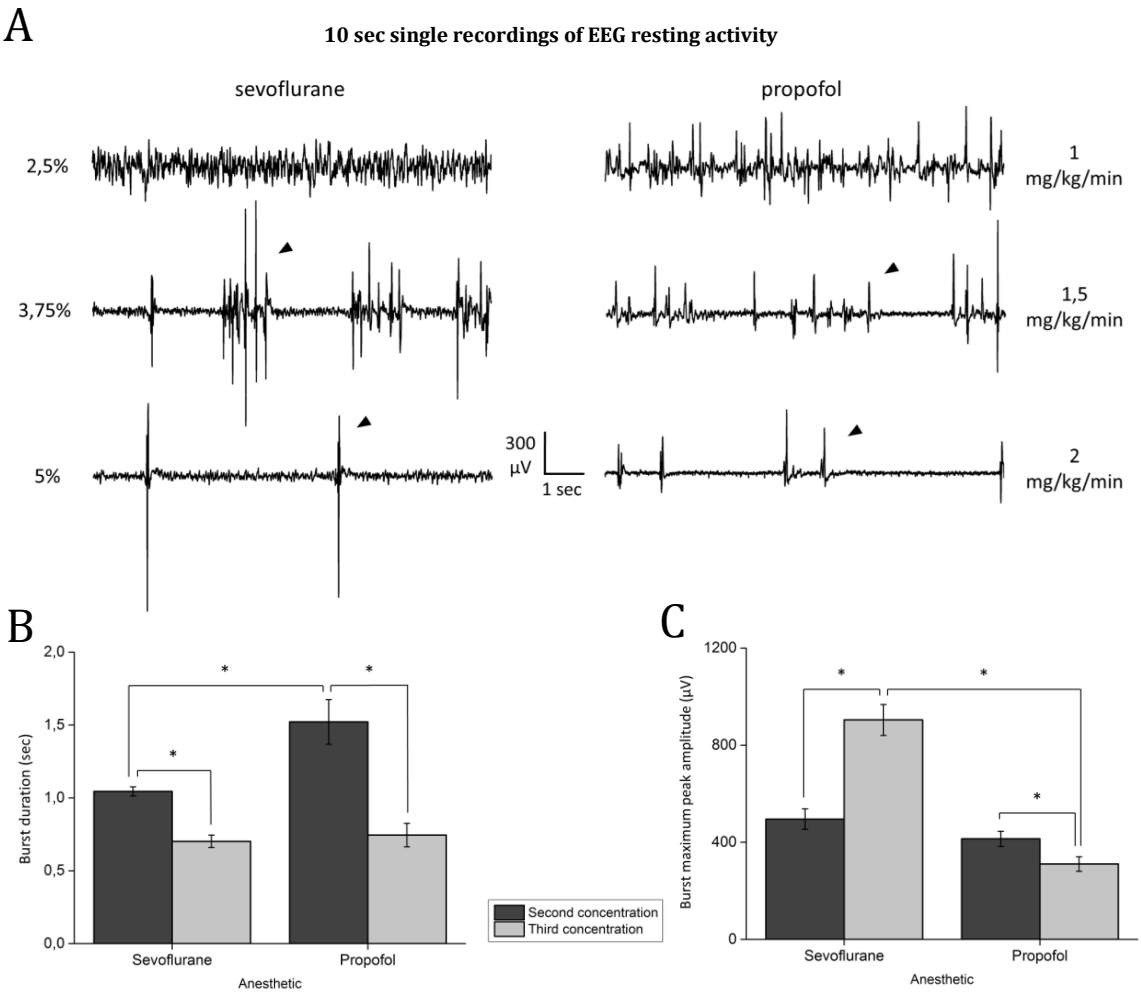

Fig. 23 A) 10 seconds single recordings of resting EEG activity from a representative animal at increasing expiratory concentrations of sevoflurane (2,5%, 3,75%, 5%) (left) and at increasing endovenous concentrations of propofol (1mg/kg/min, 1,5mg/kg/min, 2mg/kg/min) (right). At the higher states of anesthesia, sevoflurane 3,75-5% and propofol 1,5-2mg/kg/min, the EEG activity assumes a burst-suppression pattern, where burst oscillations could be clearly discriminated (arrow tips) from the resting low voltage activity. The burst shape changes between the anesthetics and within them in a dose dependent fashion in 5 rats. **B)** The mean burst duration decreases by augmenting the concentration of both anesthetics and in the condition of sevoflurane 3,75%, it is shorter than in the propofol 1,5mg/kg/min condition. **C)** The maximum peak amplitude of the rectified burst increases by augmenting the concentration of sevoflurane, while decreases by augmenting the dose of propofol; moreover, at the deeper state of anesthesia, the burst maximum peak in sevoflurane conditin is higher than in propofol condition. **D)** The number of bursts (here expressed in frequency, Hz) also changes and seems to decrease by deepening the anesthesia with both drugs, even if no statistical significance is found in sevoflurane condition. Moreover, at the intermediate level of anesthesia, the number of bursts is higher in the propofol condition than in the sevoflurane condition.
(n=5; Wilcox test: $p<0,05$ ∗).

At the 2 higher concentrations, in coincidence to the relative increase of beta power, in both anesthetic conditions, the resting EEG activity assumed a burst-suppression pattern where transient high-voltage oscillations (burst) and intervals of low-voltage resting activity (suppression) followed one another in a quasi-periodic manner (Fig. 23). The number and the shape of bursts changed between sevoflurane and propofol and also between the various concentrations, within each drug condition. During 110 seconds of recording, the number of detected bursts decreased by augmenting the dose of both anesthetics. Nevertheless, in the sevoflurane condition, no significant difference was found, probably because 1 rat on 5 tested animals showed the opposite trend and in that case, the number of bursts increased by augmenting the dose of sevoflurane (Wilcoxon test: prop. 1,5mg/kg/min > prop. 2mg/kg/min p<0,05 z=1,88776). Moreover, at the intermediate level of anesthesia, a higher number of bursts was found in the propofol condition relative to the sevoflurane condition (Wilcoxon test: prop. 1,5mg/kg/min > sev. 3,75% p<0,05 z=1,88776) (Fig. 23-D). These spontaneous oscillations reduced their duration by increasing the dose of both drugs (Wilcoxon test: sev. 3,75% > sev. 5% p<0,05 z=1,88776; prop. 1,5mg/kg/min > prop. 2mg/kg/min p<0,05 z=1,88776) and at the intermediate state of anesthesia, the bursts induced by propofol were longer (Wilcoxon test: prop. 1,5mg/kg/min > sev. 3,75% p<0,05 z=1,88776) (Fig. 23-B). Moreover, the mean amplitude of the maximum peak of the rectified burst was higher in the deeper state of sevoflurane anesthesia (Wilcoxon test: sev. 3,75% < sev. 5% p<0,05 z=-1,88776), while decreased by the enhancement of the concentration of propofol (Wilcoxon test: prop. 1,5mg/kg/min > prop. 2mg/kg/min p<0,05 z=1,88776), resulting in a significant difference between the two drugs at the highest dose (Wilcoxon test: sev. 5% > prop. 2mg/kg/min p<0,05 z=1,88776) (Fig. 23-C).

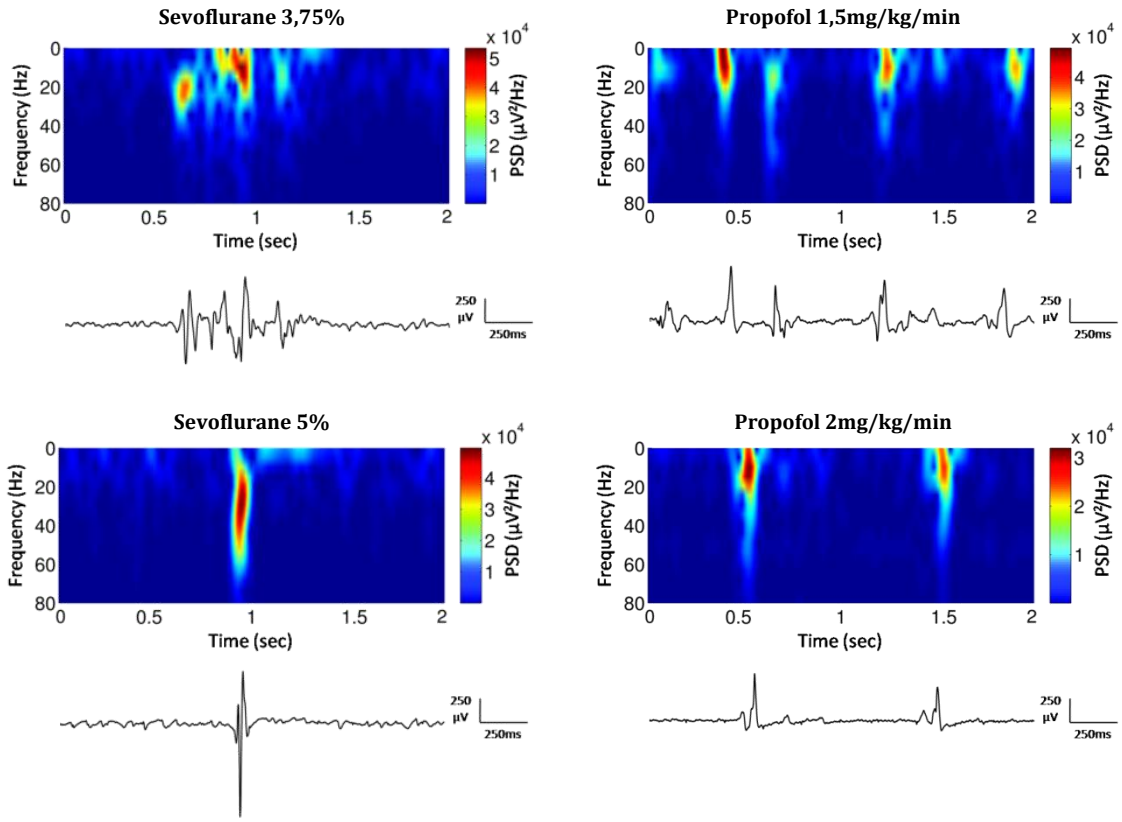

Fig. 24 Spectrograms of bursting epochs and relative raw signals from a representative rat exposed to increasing expiratory concentrations of sevoflurane (3,75 - 5%) and to increasing intravenous concentrations of propofol (1,5 - 2mg/kg/min). The frequency content of the burst changes between the anesthetics and among the concentrations of sevoflurane toward higher frequencies, while no variation is detectable between the 2 states of anesthesia induced by propofol.

The spectral power of the bursts also changed between anesthetic conditions (Fig. 24). The enhancement of the sevoflurane concentration produced an increase in the broadband power of the burst (Wilcoxon test for the total frequency band: sev. 3,75% < sev. 5% p<0,05 z=-1,88776) and the same variation was detected also for beta and gamma powers (Wilcoxon test for beta band: sev. 3,75% < sev. 5% p<0,05 z=-1,88776) (Wilcoxon test for gamma band: sev. 3,75% < sev. 5% p<0,05 z=-1,88776) (Fig. 25-A, B). Otherwise, no variation in the spectral pattern was detected between bursts of the deeper states of propofol anesthesia, while some differences were observed between the two drugs (Fig. 25-C, D). In the intermediate state of anesthesia the relative gamma power was higher in the

sevoflurane condition (Wilcoxon test for gamma band: sev. 3,75% > prop. 1,5mg/kg/min p<0,05 z=1,88776) and the same variation was reported in the deepest state of anesthesia (Wilcoxon test for gamma band: sev. 5% > prop. 2mg/kg/min p<0,05 z=1,88776), where also the relative alpha power changed, by increasing in the propofol condition relative to the sevoflurane anesthesia (Wilcoxon test for alpha band: sev. 5% < prop. 2mg/kg/min p<0,05 z=-1,88776).

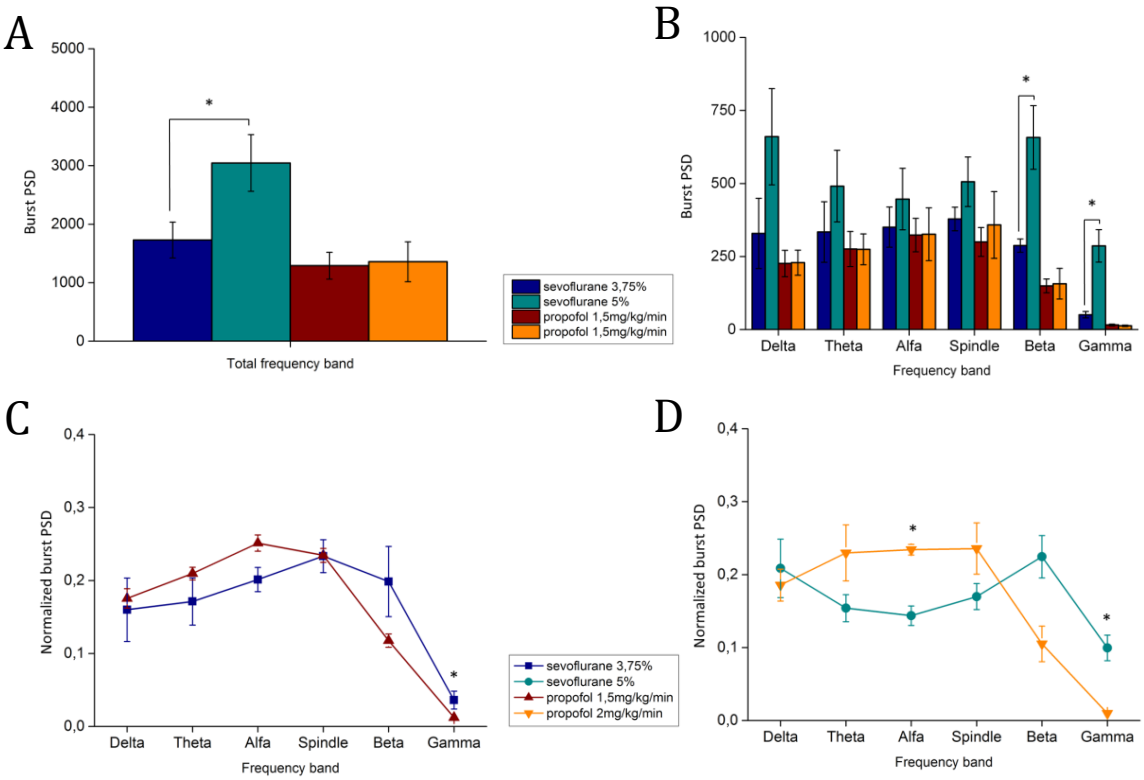

Fig. 25 Power spectral analisys of isolated bursts. These data have been extracted from 5 rats exposed to increasing expiratory concentrations of sevoflurane (3,75%, 5%) and to increasing endovenous concentrations of propofol (1,5mg/kg/min, 2mg/kg/min). **A)** The mean power spectral density (PSD) of the total frequency band (from 2 to 80 Hz) increases in a dose dependent fashion in the sevoflurane condition and **B)** the same variation is been detected also for beta and gamma bands in the same anesthesia conditions. Otherwise none variation is detected between the states of anesthesia induced by propofol. **C)** Moreover, at the intermediate level of anesthesia (sevoflurane 3,75% and propofol 1,5mg/kg/min), the relative gamma band contribution is higher in the sevoflurane condition then in the propofol condition. **D)** At the deeper state of anesthesia, the relative alpha band contribution is higher in the propofol condition then in the sevoflurane condition, whereas the relative gamma power is higher in the sevoflurane condition then in the propofol anesthesia. (n=5; Wilcox test: p<0,05 ∗).

4 DISCUSSION

4.1 TECHNICAL CONSIDERATIONS

The choice to record the cortical behavior by means of two superficial electrodes arose from some properties of this type of bipolar recording, which fit particularly well with the needs of this exploratory study. First of all, this recording strategy with chronically implanted electrodes, permits sequential recordings from the same animal in different time epochs. Moreover, it's been demonstrated in previous studies, that its reproducibility is higher in both inter- and intra-session recordings than other technics (You, et al., 2011). A good recording repeatability in times allows to design repeated measures experiments, which are critical in the comparison of the effects of more than one states of anesthesia induced by different anesthetics. Furthermore, the screw electrodes permit to probe a large area of the cortex simultaneously and because they are grafted into the skull close to the dura mater, the distorting and attenuating effect of the hard tissue is abolished. This ensures a larger amplitude of the signal and a greater resolution for the high-frequency activity patterns compared to the typical scalp EEG (Buzsáki, et al., 2012). The signal to noise ratio of the visual evoked potentials (VEPs) is further enhanced by the position of the screw electrodes. The differential recording between two electrodes placed symmetrically at the level of the primary visual cortexes, allows to cut down the common mode signal, sparing only the VEP signal of the visual cortex which is contralateral to the stimulated eye.

The VEP structure obtained in this report in response to light pulses was already seen in other studies[4], with a good consistency between peak latencies and some interpretations have been proposed, even though the neural generators of the visual evoked response are not completely understood (Creel et al., 1974) (Meeren, et al., 1998) (You et al., 2011). In physiological conditions, P1 is thought

[4] Peaks are been named independently from the literature and all comparison with the wave deflections reported in previous reports, were made on the base of the mean latency of the peaks.

to be closely related to the amount of the thalamic-cortical input, rather than reflecting the resulting excitation of the pyramidal cells of the cortex. In particular, P1 latency could be considered as a marker of the transmission between thalamus and cortex, which is already seen to be strongly dependent on sleep-wake states (P1 latency increases in both REM and non-REM sleep). Whereas, because of the larger variability, the later complex of the VEP has been associated to the higher function of the cortex, from the cortical computation to the cortical-thalamic feedback communications. Because of the putative systemic action of sevoflurane and propofol, a more conservative interpretation of the VEP waves has been preferred for this study and P1 latency has been assessed like a marker of the whole retinal-thalamic functions. While to examine the cortex function in its entirety, the VEP area has been taken into account.

When animals were exposed to light pulses of different brightness, a stimulus-response relation could be evaluated as an index of the computational ability of the first steps of the visual pathway. Therefore, modifications of this function relative to the anesthesia, could reveal how the anesthetics modify the signal processing of these structures. It should be noted that the basal level of darkness of the experimental condition did not change in relation to the different irradiance values, consequently also the contrast increased as the light pulses came brighter. Therefore the stimulus-response relation was actually an index of the ability to discriminate between combinations of brightness and contrast variations. Nevertheless, for reason of simplicity, it has been referred to this relation as a function between the evoked potential and the brightness of the stimulus.

4.2 EFFECTS OF ANESTHETICS ON THE VISUAL EVOKED RESPONSE

A relation between the evoked response and the pulse irradiance could be detected in both the sevoflurane and propofol conditions, but it was modified differently throughout the concentrations and between the two anesthetics. VEP was strictly influenced by the light brightness in both latency and magnitude, for all concentration conditions. P1 latency decreased and the VEP area increased as a

function of the irradiance enhancement. Therefore, even with high doses of anesthetic, the first retinal-thalamic and cortical levels of signal processing maintained their ability to discriminate some basic properties of the stimulus, such as combinations of brightness and contrast, by resulting in different activity patterns (VEP latency and area variations) relative to different stimuli intensities.

P1 latency seemed to be the best marker of the depth of anesthesia, since in both the sevoflurane and propofol conditions, it increased in a concentration dependent fashion. Nevertheless, it should be noted that, when rats were exposed to light pulses of different brightness, in the propofol condition, this concentration effect was less clear and it could be detected only by multiple comparisons between the whole irradiance-response relations. This phenomenon could be ascribed to the lesser VEP magnitude and therefore to the lesser signal to noise ratio observed in the propofol conditions. Indeed, propofol reduced the VEP area in a dose dependent manner especially in response to dim light pulses, while the same plateau level was reached in response to brighter stimuli for all 3 levels of anesthesia. This kind of alteration strongly suggests that propofol induces a rise of the stimulus-detection threshold, rather than a functional modification in the circuitry used to elaborate the light pulse. Consequently, the first stages of the visual system could be more inhibited, but could potentially preserve their physiological ability to discriminate stimuli, as no differences among the concentrations, were detected for light pulses which were bright enough to produce the necessary electrical drive to overstep this putative threshold. Otherwise, VEP area increased its dimension as the sevoflurane anesthesia became deeper, suggesting a hyper-excitable state induced by this drug, which was already seen in relation to other volatile anesthetics (Imas, et al., 2005). Since sevoflurane increased the latency of P1, this enhanced responsive state should be ascribed to a cortical alteration, rather than to thalamic or retinal modifications. Furthermore, if this enhancement concerned only the excitability of the same neuronal ensemble which elaborates the light pulse in physiological conditions, one would expect that even if quicker, the same plateau level related to the VEP area dimension, would be reached in response to brighter stimuli. Indeed, the plateau level represents the saturation point of the neuronal ensemble functioning. Otherwise, a new higher

plateau level was reached for each concentration by suggesting that sevoflurane could modify the recruitment of the neuronal ensemble per se and not only its excitability, apparently enhancing the efficacy whereby the stimulus has been codified and/or increasing the number of neurons which reacted simultaneously to the light pulses.

It is well-known in the literature (Duysens, et al., 1996) that a prolonged light stimulation can reveal another component of the visual evoked response of the cortex, the OFF component of the VEP (VEPOff). It is also known that these two components of the visual response are generated from two very different pathways in the retina, which are composed by specific types of cells with different characteristics. Otherwise, these pathways are not completely independent and interact at various levels. In particular, in the presence of the light, the ON pathway laterally inhibits the OFF pathway through the glycinergic AII amacrine cells (Manookin et al., 2008) (Liang & Freed, 2010). This cross-inhibition possibly improves the OFF pathway ability to detect light to dark contrasts by keeping the membrane potential of the OFF ganglion cells just below the spike threshold and therefore by reducing the number of spikes required to detect dark contrasts and/or the offset of a light pulse (Liang & Freed, 2012). By the administration of the L-AP4, an mGluR6 agonist, the relation of the ON and OFF responses to different pathways is been verified. Moreover, also the OFF response increased its area as a function of the brightness of the stimulus and the VEPOff/VEPOn area ratio did not change relative to the irradiance values. This strongly suggests that the ON cross-inhibition is strictly confined to the duration of the light pulse and/or that the level of the excitation of the ON pathway does not impair the discrimination ability of the OFF pathway. Besides, the smaller magnitude of the OFF response was consistent to previous data which reported a smaller number of cortical cells with OFF circular field (7%) than the number of the cortical cells with ON circular field (25%) in the rodent primary visual cortex (Dräger, 1975).

Like the variations reported for the ON response, P1 latency of the OFF component of the VEP increased as a function of concentration in both anesthetic conditions, confirming that the VEP latency is a good indicator of the depth of anesthesia. Moreover, in the propofol condition the VEPOff area seemed to follow

the same trend as the VEPOn area and its dimension decreased in a dose dependent manner, supporting the previous findings. Concurrently, in the sevoflurane condition, VEPOff area went through an unexpected variation. The OFF response decreased its magnitude as the anesthesia came deeper, until its disappearance at the highest concentration, by following the opposite trend of the ON response. It is important to note that this phenomenon could not be ascribed simply to the level of excitation of the ON pathway and to the subsequent enhancement of the cross-inhibition between the two pathways, as this did not occur when the VEPOn response was enhanced by increasing the light brightness as reported in Fig. 15. The opposite changes of the OFF response could be produced by two alternative events. First, sevoflurane interacts by different mechanisms within the two different pathways, possibly due to variations in the expression of receptors among neurons of the ON and OFF pathways. The other possibility is that the anomalous excited state induced by sevoflurane, leads to a superimposition of the first component of the visual response on the latter component, that is the ON response suppresses the OFF response. This phenomenon could potentially occur at the retinal level, where the cross-inhibition of the ON pathway could prolong the stimulus duration, at the thalamic level or at the cortical level, where the ON and OFF pathway interconnect with each other and converge on single neurons by generating the sub-regions of the receptive field of the simple cells (Schiller, 1982) (Sherk & Horton, 1984) (Hirsch, et al., 1998) (Hirsch & Martinez, 2006). Since at higher concentrations of sevoflurane, P1On latency increased and the variation of the electric field related to the ON response, did not exceed the offset of the light pulse (Fig. 16), the suppression of the OFF response is likely to occur at a cortical level in this latter scenario.

In order to discriminate between these two possibilities, rats were exposed to the same concentrations of sevoflurane and were stimulated by the same light pulses of the experiment reported in Fig. 16-17 immediately after an intravireal injection of L-AP4, by isolating the OFF pathway from the ON one (Fig. 18). If the first scenario were true, the OFF response should be decreased as a function of the concentration of sevoflurane as in Fig. 17. Whereas, if the second scenario were true, the course of the OFF response should be different from that which was

reported in Fig. 17. It was found that, in the absence of the action of the ON pathway, the OFF response increased its area in a concentration dependent fashion by following exactly the same trend which was observed for the ON response reported in Fig. 17. This strongly suggests that at the cortical level, a suppressive effect would occur between the ON and the OFF responses and that the OFF pathway is potentially able to produce the same excitable cortical state induced by sevoflurane. The exciting action of sevoflurane is likely to occur only at the cortical level mostly because of the increased P1 latency (both On and Off) as a function of the anesthetic concentration. This delay should be taken as a sign of the inhibited state of the retinal-thalamic pathway. Indeed, an enhanced retinal or thalamic visual response should carry a higher electrical drive and therefore should produce an earlier variation in the extracellular field recorded at the subsequent station of signal computation, as what occurred for the responses to brighter stimuli reported in Fig. 8 and 11. Moreover, this explanation of the P1 latency variation is consistent with previous reports (Creel et al., 1974)(Meeren et al., 1998). It is well known that at the cortical level, ON and OFF thalamic projections mostly converge on single simple cells, by generating their ON and OFF receptive subfields (Schiller, 1982) (Sherk & Horton, 1984) (Hirsch et al., 1998) (Hirsch & Martinez, 2006). Therefore, the OFF response suppression should occur through mechanisms which act at the single cell level, rather than by means of inhibition mechanisms between independent circuits, like retinal cross-inhibition. One possible explanation is that sevoflurane induces a hyper-excitable state which results in a bi-stable behavior of the cortical cells, where states of strong excitation are followed by states of profound inhibition. In this scenario of all-or-none responsiveness, the OFF component of the VEP could be suppressed only because of timing. Indeed, the membrane potential of the cortical cell could need more time to repolarize after these kinds of strong depolarization and hyperpolarization, thereby failing to generate an OFF response which is temporally too close to an ON response. This hypothesis is even more fascinating since it was shown that an alteration in the inhibition/excitation balance towards excitation, for example by blocking GABA receptors, leads to the destruction of the subfield segregation in the simple cells. In this anomalous hyper-excitable state, even a light pulse projected at

their OFF subfield is able to generate a strong depolarization instead of the physiological inhibition (Sillito, 1975) (Nelson, et al., 1994)(Liu et al., 2010). A similar unstable hyper-excitability of cortical neurons, but not of thalamic cells, was also shown during states of anesthesia induced by isoflurane, another volatile general anesthetic. At high doses isoflurane produced a burst-suppression pattern of cortical resting EEG activity, which was associated with an increased responsiveness of cortical neurons to sensorial stimulations (Detsch, et al., 2002) (Kroeger & Amzica, 2007) (Ferron, et al., 2009). Therefore, the analysis of the resting EEG signal could be helpful in order to clarify some aspects of the previous data.

4.3 EFFECTS OF ANESTHETICS ON THE RESTING EEG ACTIVITY

The conscious experience and the integration of exogenous and endogenous information are likely produced by the activity of several specialized neuronal ensembles whose temporal synchronization and desynchronization generate typical oscillations in the electric field, which can be detected and transposed in the frequency domain. This mathematical operation allows quantification of the frequency content of the oscillations of the electric field and therefore, is widely used as a powerful tool to clarify some aspects of brain functioning, including the loss of consciousness and the states of anesthesia (John & Prichep, 2005). Even if the single derivation used for recording, cannot account for the phase synchrony of the wavebands among brain regions, some differences were found in absolute and relative spectral powers in relation to the anesthetic and to the concentration conditions. The common decrease of the broad band PSD and the same pattern of relative waveband powers observed in the lightest state of anesthesia, would suggest that sevoflurane and propofol shared a similar mechanism by which the anesthesia is induced. Nevertheless at the 2 higher concentrations of anesthetic some differences in the relative alpha and in the relative gamma powers could be detected between the two anesthetics, suggesting different actions. It is important to note that exactly at the two higher concentrations, the resting oscillations

changed into a burst-suppression pattern for both anesthetics. Therefore, the spectral variations detected could be ascribed, or at least influenced, by the frequency content of the bursts. Moreover, the onset of these spontaneous high-voltage activities could explain the relative increase of the beta power in both anesthetic conditions (Fig. 21). The burst-suppression activity has been associated to the comatose brain state and can be induced by high doses of anesthetic. Even if the underlying mechanism is not fully understood, it has been proposed that the bursts could be strictly dependent on glutammatergic synaptic depolarizations of cortical neurons which are in a quiescent and hyper-excitable state. Indeed, bursts are largely spontaneous, but they can also be induced by stimulations which are subliminal during awareness (Lukatch, et al., 2005) (Detsch et al., 2002) (Steriade, et al., 1994) (Kroeger & Amzica, 2007) (Amzica, 2009) (Lewis et al., 2013). Therefore, the shape and the frequency content of the bursts could reflect some characteristics of the anesthetic action on the cortical computation. The variation in shape was reminiscent of the changing VEPs observed in relation to the anesthetic concentrations. Indeed, in the sevoflurane condition, the maximum peak amplitude increased in the deeper anesthesia, while in the propofol condition decreased. Moreover, the faster frequencies increased their power as a function of the concentration of sevoflurane, suggesting a mechanism of action that at least in part, could be concentration-dependent. Otherwise, in the propofol condition, no variation in the spectral pattern could be detected relative to the concentration, but the relative gamma power was always smaller than in the sevoflurane condition. Due to both the lack of a full comprehension of the neural generators and of the exact functional roles of faster rhythms, particular care should be taken in the interpretation of their variations. Nevertheless, the cortical gamma oscillation has been proposed to be a computational mechanism wherein the cyclical inhibitions of fast spiking interneurons on pyramidal cells have a critical role. This inhibitory activity at fast frequencies should create a temporal frame by which the excitatory drives of cortical inputs are selected, to generate the synchronized neuronal assemblies that encode and promote the transmission of the sensory signal throughout the cortical circuits (Fries, et al., 2007) (Fries, 2009) (Buzsáki & Wang, 2012) (Sohal et al., 2009) (Cardin et al., 2009) (Rodriguez et al.,

1999). Due to the important role of the gamma cycle in signal computation, a connection between the enhancement of the VEP magnitudes and the alterations in gamma activity induced by sevoflurane, cannot be excluded. Moreover, similar results have been reported in relation to other volatile anesthetics such halothane, isoflurane and desflurane (Imas, et al., 2005). Nevertheless, my results cannot account for any form of causal relation between these phenomena, therefore other experiments are needed to further clarify the biological mechanisms underlying the action of sevoflurane.

5 CONCLUSIONS

The main result of this study is that sevoflurane and propofol are able to alter the elaboration of the visual signal in two very different manner (Fig. 9-11, 16, 17), suggesting two different mechanisms of action. Nevertheless, both drugs induce analogous trends of hypnotic state throughout the deepening of anesthesia, expressed by a gradual reduction of the overall EEG activity, from high voltage oscillations to a burst-suppression pattern (Fig. 19, 20, 23). Consequently, since loss of consciousness is likely to be produced by profound alterations in the signal processing abilities of the brain (Alkire et al., 2008), it is conceivable that at least two different mechanisms can underlie the same state of unconsciousness.

Interestingly, the sensory processing alterations induced by sevoflurane and propofol, seem to be a local scale reminiscence of the long-range alterations postulated by the "Integrated information theory" developed by Tononi and Edelman, relative to states of loss of consciousness (Tononi & Edelman, 1998). Authors hypothesized that consciousness is strictly dependent on the complexity of a system and that the complexity is a function of the level of integration and of the informative content of the system. If a system is highly integrated but loses its informative content, it will not generate consciousness. Ideally, if it were perturbed, for example by an external stimulation, it would react leading to an all-or-none response, where all components of the system would either assume the same activity state or are silenced at the same time, with no other option. Within this theoretical framework, it could be expected that if the visual system lost its informative content but not its connections, a light pulse stimulation would engage the activation of an aberrant neuronal ensemble, larger than during physiological conditions and possibly also constituted by neurons which should not be able to process that kind of information. This global all-or-none response would generate two main electrophysiological features. First, the magnitude of the evoked potential should be higher, due to the increased number of neurons which would fire in synchrony. Second, the functional specialization of the cortical receptive

fields would be lost, due to the increased responsiveness of neurons. Both alterations are compatible with the two main findings observed during sevoflurane anesthesia: the plateau level of the brightness sensitivity function increased and the ON/OFF dichotomy was gradually suppressed as the anesthesia deepened (Fig. 11, 17). Otherwise, if a system loses its connectivity selectively, the information will not be integrated throughout its elements and consciousness will not be generated as well. This situation could be achieved with the excision of the connections among elements of the system and therefore by isolating them, or by cutting down the efficacy of connections, therefore reducing the probability of communication between elements. If the visual system assumed this latter state of functioning, it would be expected that the visual cortex should potentially maintain its ability to process the information, but the necessary electrical drive to sustain the right elaboration would dramatically increase. Therefore, only stronger light stimulation would generate a cortical response. Propofol seemed to produce compatible effects with this kind of alteration, since the magnitude of evoked potentials generally decreased as the anesthesia deepened. Otherwise, the same plateau of the brightness sensitivity function, relative to responses to brighter light pulses, was always reached and the ON/OFF dichotomy was preserved independently of the level of anesthesia (Fig. 11, 17).

Nevertheless, the exploratory nature of this report, only allows for hypothesis at this stage and other experiments are needed to confirm them. A deeper examination into the alterations of receptive fields of single visual cortical neurons should prove useful. If sevoflurane selectively suppressed the informative content of the signal processing, simple cells would be more excitable then during physiological condition. The orientation selectivity of their receptive field should be suppressed, leading to the same high responsiveness for stimuli of all orientations. Otherwise, if propofol selectively cut down the connectivity of the visual system, simple cells would be less excitable, but their receptive field should maintain its orientation selectivity and possibly it would be strengthened by reducing the spatial extension of the field. In order to test these hypothesis, *in vivo* single unit or patch clamp electrophysiological recordings will be needed. *In vivo* multiple field recordings by means of intra-cortical electrodes should also be

useful to test local phase synchrony of cortical oscillations. In the same hypothetical framework, sevoflurane anesthesia would lead to an enhanced cortical synchronization, while the opposite effect is expected during propofol anesthesia. Moreover, the phase synchronization could uncover some aspects concerning the mechanisms of action of these alterations. For example, if the phase synchrony of gamma frequencies increased throughout the visual cortex during sevoflurane anesthesia, its implications in the action of this drug would be confirmed and a particular role for the gamma oscillation in the engagement of the aberrant neuronal ensemble would be strongly suggested. Hence, the investigation should then focalize on the activity of fast-spiking interneurons and on their network, given their prominent role in the gamma cycle (Fries, 2009) (Buzsáki & Wang, 2012) (Sohal et al., 2009) (Cardin et al., 2009). If the effects of sevoflurane and propofol were compatible with the "Integrated information theory" also at the local scale of the visual cortex, it would help to extend our knowledge about the awake functions and about the mechanisms of loss of consciousness to a more comprehensive level, generating new questions concerning how local scale circuitry and long range information processing influence each other.

6 BIBLIOGRAPHY

Abbott, L. F., & Chance, F. S. (2002). Rethinking the taxonomy of visual neurons Neural stem cells : form and function. *Nature Neuroscience*.

Ahnelt, P., & Kolb, H. (1994). Horizontal cells and cone photoreceptors in human retina: A Golgi-electron microscopic study of spectral connectivity. *The Journal of Comparative Neurology*, *343*(3), 406–427. doi:10.1002/cne.903430306

Alkire, M. T., Hudetz, A. G., & Tononi, G. (2008). Consciousness and anesthesia. *Science*, *322*(5903), 876–80. doi:10.1126/science.1149213

Alkire, M. T., & Miller, J. (2005). General anesthesia and the neural correlates of consciousness. *Progress in Brain Research*, *150*, 229–44. doi:10.1016/S0079-6123(05)50017-7

Amzica, F. (2009). Basic physiology of burst-suppression. *Epilepsia*, *50 Suppl 1*, 38–9. doi:10.1111/j.1528-1167.2009.02345.x

Benito, J., Aguado, D., Abreu, M. B., García-Fernández, J., & Gómez de Segura, I. a. (2010). Remifentanil and cyclooxygenase inhibitors interactions in the minimum alveolar concentration of sevoflurane in the rat. *British Journal of Anaesthesia*, *105*(6), 810–7. doi:10.1093/bja/aeq241

Bertaccini, E. J., & Trudell, J. R. (2012). Induced changes in protein receptors conferring resistance to anesthetics. *Current Opinion in Anaesthesiology*, *25*(4), 405–10. doi:10.1097/ACO.0b013e328354fda8

Bieda, M. C., & MacIver, M. B. (2004). Major role for tonic GABAA conductances in anesthetic suppression of intrinsic neuronal excitability. *Journal of Neurophysiology*, *92*(3), 1658–67. doi:10.1152/jn.00223.2004

Bloomfield, S. a, & Völgyi, B. (2009). The diverse functional roles and regulation of neuronal gap junctions in the retina. *Nature Reviews. Neuroscience*, *10*(7), 495–506. doi:10.1038/nrn2636

Bloomfield, S., & Xin, D. (2000). Surround inhibition of mammalian AII amacrine cells is generated in the proximal retina. *The Journal of Physiology*. Retrieved from http://jp.physoc.org/content/523/3/771.short

Brammer, a, West, C. D., & Allen, S. L. (1993). A comparison of propofol with other injectable anaesthetics in a rat model for measuring cardiovascular parameters. *Laboratory Animals*, *27*(3), 250–7. Retrieved from http://www.ncbi.nlm.nih.gov/pubmed/8366671

Buzsáki, G., Anastassiou, C. a, & Koch, C. (2012). The origin of extracellular fields and currents--EEG, ECoG, LFP and spikes. *Nature Reviews. Neuroscience*, *13*(6), 407–20. doi:10.1038/nrn3241

Buzsáki, G., & Wang, X.-J. (2012). Mechanisms of gamma oscillations. *Annual Review of Neuroscience*, *35*, 203–25. doi:10.1146/annurev-neuro-062111-150444

Buzsáki, G., & Watson, B. O. (2012). Brain rhythms and neural syntax: implications for efficient coding of cognitive content and neuropsychiatric desease. *Dialogues in Clinical Neuroscience*, 345–367.

Cardin, J. a, Carlén, M., Meletis, K., Knoblich, U., Zhang, F., Deisseroth, K., … Moore, C. I. (2009). Driving fast-spiking cells induces gamma rhythm and controls sensory responses. *Nature*, *459*(7247), 663–7. doi:10.1038/nature08002

Coenen, a M. (1995). Neuronal activities underlying the electroencephalogram and evoked potentials of sleeping and waking: implications for information processing. *Neuroscience and Biobehavioral Reviews*, *19*(3), 447–63. Retrieved from http://www.ncbi.nlm.nih.gov/pubmed/7566746

Creel, D., Dustman, R. E., & Beck, E. C. (1974). Intensity of flash illumination and the visually evoked potential of rats, guinea pigs and cats. *Vision Research*, *14*(8), 725–729. doi:10.1016/0042-6989(74)90070-4

Crone, N. E., Korzeniewska, A., & Franaszczuk, P. J. (2011). Cortical γ responses: searching high and low. *International Journal of Psychophysiology : Official Journal of the International Organization of Psychophysiology*, *79*(1), 9–15. doi:10.1016/j.ijpsycho.2010.10.013

De Sousa, S. L., Dickinson, R., Lieb, W. R., & Franks, N. P. (2000). Contrasting synaptic actions of the inhalational general anesthetics isoflurane and xenon. *Anesthesiology*, *92*(4), 1055–66. Retrieved from http://www.ncbi.nlm.nih.gov/pubmed/10754626

Detsch, O., Kochs, E., Siemers, M., Bromm, B., & Vahle-Hinz, C. (2002). Increased responsiveness of cortical neurons in contrast to thalamic neurons during isoflurane-induced EEG bursts in rats. *Neuroscience Letters*, *317*(1), 9–12. Retrieved from http://www.ncbi.nlm.nih.gov/pubmed/11750984

Dhingra, a, Lyubarsky, a, Jiang, M., Pugh, E. N., Birnbaumer, L., Sterling, P., & Vardi, N. (2000). The light response of ON bipolar neurons requires G[alpha]o. *The Journal of Neuroscience : The Official Journal of the Society for Neuroscience*, *20*(24), 9053–8. Retrieved from http://www.ncbi.nlm.nih.gov/pubmed/11124982

Dräger, U. C. (1975). Receptive fields of single cells and topography in mouse visual cortex. *The Journal of Comparative Neurology*, *160*(3), 269–289. doi:10.1002/cne.901600302

Dreosti, E., Esposti, F., Baden, T., & Lagnado, L. (2011). In vivo evidence that retinal bipolar cells generate spikes modulated by light. *Nature Neuroscience*, *14*(8), 951–2. doi:10.1038/nn.2841

Dubin, M. W., & Cleland, B. G. (1977). Organization of visual inputs to interneurons of lateral geniculate nucleus of the cat. *J Neurophysiol*, *40*(2), 410–427. Retrieved from http://jn.physiology.org/content/40/2/410

Duysens, J., Schaafsma, S., & Orban, G. (1996). Cortical OFF response tuning for Stimulus Duration. *Vision Research*. Retrieved from http://www.sciencedirect.com/science/article/pii/0042698996000405

Ferrarelli, F., Huber, R., Peterson, M. J., Massimini, M., Murphy, M., Riedner, B. a, … Tononi, G. (2007). Reduced sleep spindle activity in schizophrenia patients. *The American Journal of Psychiatry*, *164*(3), 483–92. doi:10.1176/appi.ajp.164.3.483

Ferrarelli, F., Massimini, M., Sarasso, S., Casali, A., Riedner, B. a, Angelini, G., … Pearce, R. a. (2010). Breakdown in cortical effective connectivity during midazolam-induced loss of consciousness. *Proceedings of the National Academy of Sciences of the United States of America*, *107*(6), 2681–6. doi:10.1073/pnas.0913008107

Ferron, J.-F., Kroeger, D., Chever, O., & Amzica, F. (2009). Cortical inhibition during burst suppression induced with isoflurane anesthesia. *The Journal of Neuroscience : The Official Journal of the Society for Neuroscience*, *29*(31), 9850–60. doi:10.1523/JNEUROSCI.5176-08.2009

Franks, N. P. (2008, May). General anaesthesia: from molecular targets to neuronal pathways of sleep and arousal. *Nature Reviews. Neuroscience*. doi:10.1038/nrn2372

Fries, P. (2009). Neuronal gamma-band synchronization as a fundamental process in cortical computation. *Annual Review of Neuroscience*, *32*, 209–24. doi:10.1146/annurev.neuro.051508.135603

Fries, P., Nikolić, D., & Singer, W. (2007). The gamma cycle. *Trends in Neurosciences*, *30*(7), 309–16. doi:10.1016/j.tins.2007.05.005

Gazzaniga, M. S. (1995, February). Principles of human brain organization derived from split-brain studies. *Neuron*. Retrieved from http://www.ncbi.nlm.nih.gov/pubmed/7857634

Gordon, A., & Sttyker, P. (1996). Experience-Dependent Primary Visual Cortex Plasticity of Binocular of the Mouse Responses in the. *The Journal of Neuroscience : The Official Journal of the Society for Neuroscience*, *76*(10), 3274–3286.

Hartline, H. K. (1969). Visual receptors and retinal interaction. *Science (New York, N.Y.)*, *164*(3877), 270–8. Retrieved from http://www.ncbi.nlm.nih.gov/pubmed/5776637

Hattar, S., Liao, H.-W., Takao, M., Berson, D. M., & Yau, K.-W. (2002). Melanopsin-Containing Retinal Ganglion Cells: Architecture, Projections, and Intrinsic Photosensitivity. *Science* , *295* (5557), 1065–1070. doi:10.1126/science.1069609

Herold, K. F., & Hemmings, H. C. (2012). Sodium channels as targets for volatile anesthetics. *Frontiers in Pharmacology*, *3*(March), 50. doi:10.3389/fphar.2012.00050

Hirsch, J. a, Alonso, J. M., Reid, R. C., & Martinez, L. M. (1998). Synaptic integration in striate cortical simple cells. *The Journal of Neuroscience : The Official Journal of the Society for Neuroscience*, *18*(22), 9517–28. Retrieved from http://www.ncbi.nlm.nih.gov/pubmed/9801388

Hirsch, J. a, & Martinez, L. M. (2006). Circuits that build visual cortical receptive fields. *Trends in Neurosciences*, *29*(1), 30–9. doi:10.1016/j.tins.2005.11.001

Hollmann, M. W., Liu, H. T., Hoenemann, C. W., Liu, W. H., & Durieux, M. E. (2001). Modulation of NMDA receptor function by ketamine and magnesium. Part II: interactions with volatile anesthetics. *Anesthesia and Analgesia*, *92*(5), 1182–91. Retrieved from http://www.ncbi.nlm.nih.gov/pubmed/11323344

Horton, J. C., & Adams, D. L. (2005). The cortical column: a structure without a function. *Philosophical Transactions of the Royal Society of London. Series B, Biological Sciences*, *360*(1456), 837–62. doi:10.1098/rstb.2005.1623

Huberman, A. D., Clandinin, T. R., & Baier, H. (2010). Molecular and cellular mechanisms of lamina-specific axon targeting. *Cold Spring Harbor Perspectives in Biology*, *2*(3), a001743. doi:10.1101/cshperspect.a001743

Hudetz, A. G., & Imas, O. a. (2007). Burst activation of the cerebral cortex by flash stimuli during isoflurane anesthesia in rats. *Anesthesiology*, *107*(6), 983–91. doi:10.1097/01.anes.0000291471.80659.55

Hudetz, A. G., Vizuete, J. a, & Imas, O. a. (2009). Desflurane selectively suppresses long-latency cortical neuronal response to flash in the rat. *Anesthesiology*, *111*(2), 231–9. doi:10.1097/ALN.0b013e3181ab671e

Imas, O. a, Ropella, K. M., Ward, B. D., Wood, J. D., & Hudetz, A. G. (2005). Volatile anesthetics enhance flash-induced gamma oscillations in rat visual cortex. *Anesthesiology*, *102*(5), 937–47. Retrieved from http://www.ncbi.nlm.nih.gov/pubmed/15851880

Imas, O. a, Ropella, K. M., Wood, J. D., & Hudetz, A. G. (2006). Isoflurane disrupts anterio-posterior phase synchronization of flash-induced field potentials in the rat. *Neuroscience Letters*, *402*(3), 216–21. doi:10.1016/j.neulet.2006.04.003

Jacobs, G. (2001). Cone-based vision of rats for ultraviolet and visible lights. *Journal of Experimental Biology*, *2446*, 2439–2446. Retrieved from http://jeb.biologists.org/content/204/14/2439.short

John, E. R., & Prichep, L. S. (2005). The anesthetic cascade: a theory of how anesthesia suppresses consciousness. *Anesthesiology*, *102*(2), 447–71. Retrieved from http://www.ncbi.nlm.nih.gov/pubmed/15681963

Kaisti, K. K., Långsjö, J. W., Aalto, S., Oikonen, V., Sipilä, H., Teräs, M., … Scheinin, H. (2003). Effects of sevoflurane, propofol, and adjunct nitrous oxide on regional cerebral blood flow, oxygen consumption, and blood volume in humans. *Anesthesiology*, *99*(3), 603–13. Retrieved from http://www.ncbi.nlm.nih.gov/pubmed/12960544

Kajimura, N., Uchiyama, M., Takayama, Y., Uchida, S., Uema, T., Kato, M., … Takahashi, K. (1999). Activity of midbrain reticular formation and neocortex during the progression of human non-rapid eye movement sleep. *The Journal of Neuroscience : The Official Journal of the Society for Neuroscience*, *19*(22), 10065–73. Retrieved from http://www.ncbi.nlm.nih.gov/pubmed/10559414

Kandel, E. R., Schwartz, J. H., & Jessell, T. M. (2000). *Principle of neuroscience*. *New York: McGraw-Hill* (4th ed., Vol. 4th ed.). New York: McGraw-Hill.

Kim, I.-J., Zhang, Y., Meister, M., & Sanes, J. R. (2010). Laminar restriction of retinal ganglion cell dendrites and axons: subtype-specific developmental patterns revealed with transgenic markers. *The Journal of Neuroscience : The Official Journal of the Society for Neuroscience*, *30*(4), 1452–62. doi:10.1523/JNEUROSCI.4779-09.2010

Kodama, K., Goto, T., Sato, A., Sakai, K., Tanaka, Y., & Hongo, K. (2010). Standard and limitation of intraoperative monitoring of the visual evoked potential. *Acta Neurochirurgica*, *152*(4), 643–648. doi:10.1007/s00701-010-0600-2

Koike, C., Obara, T., Uriu, Y., Numata, T., Sanuki, R., Miyata, K., … Furukawa, T. (2010). TRPM1 is a component of the retinal ON bipolar cell transduction channel in the mGluR6 cascade. *Proceedings of the National Academy of*

Sciences of the United States of America, *107*(1), 332–7. doi:10.1073/pnas.0912730107

Kolb, H. (1974). The connections between horizontal cells and photoreceptors in the retina of the cat: Electron microscopy of Golgi preparations. *The Journal of Comparative Neurology*, *155*(1), 1–14. doi:10.1002/cne.901550102

Kolb, H., Cuenca, N., Wang, H.-H., & Dekorver, L. (1990). The synaptic organization of the dopaminergic amacrine cell in the cat retina. *Journal of Neurocytology*, *19*(3), 343–366. doi:10.1007/BF01188404

Kroeger, D., & Amzica, F. (2007, September 26). Hypersensitivity of the anesthesia-induced comatose brain. *The Journal of Neuroscience : The Official Journal of the Society for Neuroscience*. doi:10.1523/JNEUROSCI.3440-07.2007

Kuroda, K., Fujiwara, A., Takeda, Y., & Kamei, C. (2009). Effects of narcotics, including morphine, on visual evoked potential in rats. *European Journal of Pharmacology*, *602*(2-3), 294–7. doi:10.1016/j.ejphar.2008.11.048

Långsjö, J. W., Maksimow, A., Salmi, E., Kaisti, K., Aalto, S., Oikonen, V., … Scheinin, H. (2005). S-ketamine anesthesia increases cerebral blood flow in excess of the metabolic needs in humans. *Anesthesiology*, *103*(2), 258–68. Retrieved from http://www.ncbi.nlm.nih.gov/pubmed/16052107

Lewis, L. D., Ching, S., Weiner, V. S., Peterfreund, R. a, Eskandar, E. N., Cash, S. S., … Purdon, P. L. (2013). Local cortical dynamics of burst suppression in the anaesthetized brain. *Brain : A Journal of Neurology*, *136*(Pt 9), 2727–37. doi:10.1093/brain/awt174

Liang, Z., & Freed, M. a. (2010). The ON pathway rectifies the OFF pathway of the mammalian retina. *The Journal of Neuroscience : The Official Journal of the Society for Neuroscience*, *30*(16), 5533–43. doi:10.1523/JNEUROSCI.4733-09.2010

Liang, Z., & Freed, M. a. (2012). Cross inhibition from ON to OFF pathway improves the efficiency of contrast encoding in the mammalian retina. *Journal of Neurophysiology*, *108*(10), 2679–88. doi:10.1152/jn.00589.2012

Liu, B., Li, P., Sun, Y. J., Li, Y., Zhang, L. I., & Tao, H. W. (2010). Intervening inhibition underlies simple-cell receptive field structure in visual cortex. *Nature Neuroscience*, *13*(1), 89–96. doi:10.1038/nn.2443

Liu, C., Au, J. D., Zou, H. L., Cotten, J. F., & Yost, C. S. (2004). Potent activation of the human tandem pore domain K channel TRESK with clinical concentrations of volatile anesthetics. *Anesthesia and Analgesia*, *99*(6), 1715–22, table of contents. doi:10.1213/01.ANE.0000136849.07384.44

Liu, H. T., Hollmann, M. W., Liu, W. H., Hoenemann, C. W., & Durieux, M. E. (2001). Modulation of NMDA receptor function by ketamine and magnesium: Part I. *Anesthesia and Analgesia*, *92*(5), 1173–81. Retrieved from http://www.ncbi.nlm.nih.gov/pubmed/11323344

Lukatch, H. S., Kiddoo, C. E., Maciver, M. B., & Program, S. N. (2005). Anesthetic-induced Burst Suppression EEG Activity Requires Glutamate-mediated Excitatory Synaptic Transmission, *3*(September). doi:10.1093/cercor/bhi015

Maclver, M. B., Mikulec, a a, Amagasu, S. M., & Monroe, F. a. (1996, October). Volatile anesthetics depress glutamate transmission via presynaptic actions. *Anesthesiology*. Retrieved from http://www.ncbi.nlm.nih.gov/pubmed/8873553

Manookin, M. B., Beaudoin, D. L., Ernst, Z. R., Flagel, L. J., & Demb, J. B. (2008). Disinhibition combines with excitation to extend the operating range of the OFF visual pathway in daylight. *The Journal of Neuroscience : The Official Journal of the Society for Neuroscience*, *28*(16), 4136–50. doi:10.1523/JNEUROSCI.4274-07.2008

Maquet, P., Laureys, S., Peigneux, P., Fuchs, S., Petiau, C., Phillips, C., … Cleeremans, a. (2000, August). Experience-dependent changes in cerebral activation during human REM sleep. *Nature Neuroscience*. doi:10.1038/77744

Markowitsch, H. J., & Kessler, J. (2000). Massive impairment in executive functions with partial preservation of other cognitive functions: the case of a young patient with severe degeneration of the prefrontal cortex. *Experimental Brain Research*, *133*(1), 94–102. doi:10.1007/s002210000404

Masland, R. (1988). Amacrine cells. *Trends in Neurosciences*, *11*(9), 405–410. doi:10.1016/0166-2236(88)90078-1

Massimini, M., & Amzica, F. (2001). Extracellular calcium fluctuations and intracellular potentials in the cortex during the slow sleep oscillation. *Journal of Neurophysiology*, 1346–1350. Retrieved from http://jn.physiology.org/content/85/3/1346.short

Massimini, M., Ferrarelli, F., Esser, S. K., Riedner, B. a, Huber, R., Murphy, M., … Tononi, G. (2007). Triggering sleep slow waves by transcranial magnetic stimulation. *Proceedings of the National Academy of Sciences of the United States of America*, *104*(20), 8496–501. doi:10.1073/pnas.0702495104

Massimini, M., Ferrarelli, F., Huber, R., Esser, S. K., Singh, H., & Tononi, G. (2005). Breakdown of cortical effective connectivity during sleep. *Science (New York, N.Y.)*, *309*(5744), 2228–32. doi:10.1126/science.1117256

Mayer, B., & Fink, H. (2001). Inflammatory liver disease shortens atracurium-induced neuromuscular blockade in rats. *European Journal of Anaesthesiology*, 599–604. Retrieved from http://onlinelibrary.wiley.com/doi/10.1046/j.1365-2346.2001.00897.x/full

Meeren, H. K., Van Luijtelaar, E. L., & Coenen, a M. (1998). Cortical and thalamic visual evoked potentials during sleep-wake states and spike-wave discharges in the rat. *Electroencephalography and Clinical Neurophysiology*, *108*(3), 306–19. Retrieved from http://www.ncbi.nlm.nih.gov/pubmed/9607520

Mhuircheartaigh, R. N., Rosenorn-Lanng, D., Wise, R., Jbabdi, S., Rogers, R., & Tracey, I. (2010). Cortical and subcortical connectivity changes during decreasing levels of consciousness in humans: a functional magnetic resonance imaging study using propofol. *The Journal of Neuroscience : The Official Journal of the Society for Neuroscience*, *30*(27), 9095–102. doi:10.1523/JNEUROSCI.5516-09.2010

Mihic, S. J., Ye, Q., Wick, M. J., Koltchine, V. V, Krasowski, M. D., Finn, S. E., … Harrison, N. L. (1997). Sites of alcohol and volatile anaesthetic action on GABA(A) and glycine receptors. *Nature*, *389*(6649), 385–9. doi:10.1038/38738

Mostany, R., & Portera-Cailliau, C. (2008). A craniotomy surgery procedure for chronic brain imaging. *Journal of Visualized Experiments : JoVE*.

Murphy, M., Bruno, M.-A., Riedner, B. a, Boveroux, P., Noirhomme, Q., Landsness, E. C., … Boly, M. (2011). Propofol anesthesia and sleep: a high-density EEG study. *Sleep*, *34*(3), 283–91A. Retrieved from http://www.pubmedcentral.nih.gov/articlerender.fcgi?artid=3041704&tool=pmcentrez&rendertype=abstract

Nakajimas, Y., Iwakabes, H., Akazawas, C., Shigemotoll, R., & Mizunoll, N. (1993). Molecular Characterization of a Novel Retinal Metabotropic Glutamate Receptor mGluR6 with a High Agonist Selectivity for. *The Journal of Biological Chemistry*, 11868–11873.

Nelson, S., Toth, L., Sheth, B., & Sur, M. (1994). Orientation selectivity of cortical neurons during intracellular blockade of inhibition. *Science* , *265* (5173), 774–777. doi:10.1126/science.8047882

Niell, C. M., & Stryker, M. P. (2008). Highly selective receptive fields in mouse visual cortex. *The Journal of Neuroscience : The Official Journal of the Society for Neuroscience*, *28*(30), 7520–36. doi:10.1523/JNEUROSCI.0623-08.2008

Nishikawa, K., & MacIver, M. B. (2001). Agent-selective Effects of Volatile Anesthetics on GABA A Receptor – mediated Synaptic Inhibition in Hippocampal Interneuron. *Anesthesiology*, (2), 340–347.

Ota, T., Kawai, K., Kamada, K., Kin, T., & Saito, N. (2010). Intraoperative monitoring of cortically recorded visual response for posterior visual pathway. *Journal of Neurosurgery*, *112*(2), 285–94. doi:10.3171/2009.6.JNS081272

Pascual-Leone, A., & Walsh, V. (2001). Fast Backprojections from the Motion to the Primary Visual Area Necessary for Visual Awareness. *Science* , *292* (5516), 510–512. doi:10.1126/science.1057099

Paxinos, G. (2004). *The rat nervous system* (3rd ed.). San Diego, California, USA; London, UK: Elsevier Academic Press. Retrieved from http://books.google.com/books?hl=en&lr=&id=F5xkDtDL4AUC&oi=fnd&pg=PP2&dq=The+rat+nervous+system&ots=apg79fxh0c&sig=faXQt29uMoXatzksR4ir4qimKwU

Paxinos, G., & Watson, C. (2007). *The rat brain in stereotaxic coordinates*. (A. Press, Ed.) (Sixth edit.). Elsevier Inc.

Pourcho, R. G., & Goebel, D. J. (1988). Colocalization of substance P and γ-aminobutyric acid in amacrine cells of the cat retina. *Brain Research*, *447*(1), 164–168. doi:10.1016/0006-8993(88)90979-1

Protti, D. a, Flores-Herr, N., & von Gersdorff, H. (2000). Light evokes Ca2+ spikes in the axon terminal of a retinal bipolar cell. *Neuron*, *25*(1), 215–27. Retrieved from http://www.ncbi.nlm.nih.gov/pubmed/10707985

Purves, D., Augustine, G. J., Fitzpatrick, D., Hall, W. C., LaMantia, A.-S., McNamara, J. O., & Williams, S. M. (2004). *Neuroscience* (3rd ed.). Sunderland: Sinauer Associates, Inc.

Rodieck, R. W. (1973, November 1). The Vertebrate Retina. Principles of Structure and Function. *British Journal of Ophthalmology*. Oxford: W. H. Freeman. doi:10.1136/bjo.58.11.948-c

Rodriguez, E., George, N., Lachaux, J.-P., Martinerie, J., Renault, B., & Varela, F. J. (1999). Perception's shadow: long-distance synchronization of human brain activity. *Nature*, *397*(February). Retrieved from http://www.nature.com/nature/journal/v397/n6718/abs/397430a0.html

Sanchez-Vives, M. V, & McCormick, D. a. (2000, October). Cellular and network mechanisms of rhythmic recurrent activity in neocortex. *Nature Neuroscience*. doi:10.1038/79848

Schiller, P. H. (1982). Central connections of the retinal ON and OFF pathways. *Nature*.

Schuett, S., Bonhoeffer, T., & Hübener, M. (2002). Mapping retinotopic structure in mouse visual cortex with optical imaging. *The Journal of Neuroscience : The Official Journal of the Society for Neuroscience*, *22*(15), 6549–59. doi:20026635

Sergent, C., Baillet, S., & Dehaene, S. (2005, October). Timing of the brain events underlying access to consciousness during the attentional blink. *Nature Neuroscience*. doi:10.1038/nn1549

Sherk, H., & Horton, C. (1984). Receptive Field Properties In The Cat's Area 17 In The Absence Of On-Center Geniculate Input. *The Journal of Neuroscience : The Official Journal of the Society for Neuroscience*.

Shmuel, A., Yacoub, E., Pfeuffer, J., Van de Moortele, P. F., Adriany, G., Hu, X., & Ugurbil, K. (2002). Sustained negative BOLD, blood flow and oxygen consumption response and its coupling to the positive response in the human brain. *Neuron*, *36*(6), 1195–210. Retrieved from http://www.ncbi.nlm.nih.gov/pubmed/12495632

Sillito, A. (1975). The contribution of inhibitory mechanisms to the receptive field properties of neurones in the striate cortex of the cat. *The Journal of Physiology*, 305–329. Retrieved from http://jp.physoc.org/content/250/2/305.short

Slaughter, M. M., & Miller, R. F. (1981). 2-amino-4-phosphonobutyric acid: a new pharmacological tool for retina research. *Science*, *211*(4478), 182–185. doi:10.1126/science.6255566

Sohal, V. S., Zhang, F., Yizhar, O., & Deisseroth, K. (2009). Parvalbumin neurons and gamma rhythms enhance cortical circuit performance. *Nature*, *459*(7247), 698–702. doi:10.1038/nature07991

Solt, K., Eger, E. I., & Raines, D. E. (2006). Differential modulation of human N-methyl-D-aspartate receptors by structurally diverse general anesthetics. *Anesthesia and Analgesia*, *102*(5), 1407–11. doi:10.1213/01.ane.0000204252.07406.9f

Sporns, O. (2003). Network Analysis, Complexity, and Brain Function. *Complexity*, *8*(1).

Sporns, O., & Tononi, G. (2002). Classes of Network Connectivity and Dynamics. *Complexity*, *7*(1), 28–38.

Sporns, O., Tononi, G., & Edelman, G. M. (2000, February). Theoretical neuroanatomy: relating anatomical and functional connectivity in graphs and cortical connection matrices. *Cerebral Cortex (New York, N.Y. : 1991)*. Retrieved from http://www.ncbi.nlm.nih.gov/pubmed/10667981

Sporns, O., Tononi, G., & Edelman, G. M. (2002). Theoretical neuroanatomy and the connectivity of the cerebral cortex. *Behavioural Brain Research*, *135*(1-2), 69–74. Retrieved from http://www.ncbi.nlm.nih.gov/pubmed/12356436

Steriade, M. (2006). Grouping of brain rhythms in corticothalamic systems. *Neuroscience*, *137*(4), 1087–106. doi:10.1016/j.neuroscience.2005.10.029

Steriade, M., Amzica, F., & Contreras, D. (1994). Cortical and thalamic cellular correlates of electroencephalographic burst-suppression. *Electroencephalography and Clinical Neurophysiology*, *90*(1), 1–16. doi:http://dx.doi.org/10.1016/0013-4694(94)90108-2

Steriade, M., McCormick, D. a, & Sejnowski, T. J. (1993). Thalamocortical oscillations in the sleeping and aroused brain. *Science (New York, N.Y.)*, *262*(5134), 679–85. Retrieved from http://www.ncbi.nlm.nih.gov/pubmed/8235588

Steriade, M., Nuñez, A., & Amzica, F. (1993). Intracellular analysis of relations between the slow (< 1 Hz) neocortical oscillation and other sleep rhythms of the electroencephalogram. *The Journal of Neuroscience*, *73*(August). Retrieved from http://www.jneurosci.org/content/13/8/3266.short

Strettoi, E., Raviola, E., & Dacheux, R. F. (1992). Synaptic connections of the narrow-field, bistratified rod amacrine cell (AII) in the rabbit retina. *The Journal of Comparative Neurology*, *325*(2), 152–168. doi:10.1002/cne.903250203

Su, J., Haner, C. V, Imbery, T. E., Brooks, J. M., Morhardt, D. R., Gorse, K., … Fox, M. a. (2011). Reelin is required for class-specific retinogeniculate targeting. *The Journal of Neuroscience : The Official Journal of the Society for Neuroscience*, *31*(2), 575–86. doi:10.1523/JNEUROSCI.4227-10.2011

Supèr, H., Spekreijse, H., & Lamme, V. a. (2001, March). Two distinct modes of sensory processing observed in monkey primary visual cortex (V1). *Nature Neuroscience*. doi:10.1038/85170

Thompson, E., & Varela, F. J. (2001). Radical embodiment: neural dynamics and consciousness. *Trends in Cognitive Sciences*, *5*(10), 418–425. Retrieved from http://www.ncbi.nlm.nih.gov/pubmed/11707380

Tononi, G., & Edelman, G. M. (1998). Consciousness and Complexity. *Science*, *282*(5395), 1846–1851. doi:10.1126/science.282.5395.1846

Vanderwolf, C. H. (2000). Are neocortical gamma waves related to consciousness? *Brain Research*, *855*(2), 217–224. doi:http://dx.doi.org/10.1016/S0006-8993(99)02351-3

Vardi, N. (1998). Alpha subunit of Go localizes in the dendritic tips of ON bipolar cells. *The Journal of Comparative Neurology*, *52*(February 1997), 43–52. Retrieved from http://retina.anatomy.upenn.edu/pdfiles/4157.pdf

Vardi, N., Duvoisin, R., Wu, G., & Sterling, P. (2000). Localization of mGluR6 to dendrites of ON bipolar cells in primate retina. *The Journal of Comparative Neurology*, *423*(3), 402–412. doi:10.1002/1096-9861(20000731)423:3<402::AID-CNE4>3.0.CO;2-E

Varela, F., Lachaux, J., Rodriguez, E., & Martinerie, J. (2001). The Brainweb : Phase Large-Scale Integration. *Nature Reviews Neuroscience*, *2*(April).

Waêssle, H., & Boycott, B. B. (1991). Functional architecture of the mammalian retina. *Physiological Reviews*, *71*(2), 447–480. Retrieved from http://books.google.com/books?hl=en&lr=&id=F5xkDtDL4AUC&oi=fnd&pg=PP2&dq=The+rat+nervous+system&ots=apg79fxg_i&sig=ySoWGV90VifboIc5dReT-S6hHrs

Wassle, H., Peichl, L., & Boycott, B. B. (1981). Morphology and Topography of on- and off-Alpha Cells in the Cat Retina. *Proceedings of the Royal Society of London. Series B. Biological Sciences* , *212* (1187), 157–175. doi:10.1098/rspb.1981.0032

Wu, S. M., Gao, F., & Maple, B. R. (2000). Functional architecture of synapses in the inner retina: segregation of visual signals by stratification of bipolar cell axon terminals. *The Journal of Neuroscience : The Official Journal of the Society for Neuroscience*, *20*(12), 4462–70. Retrieved from http://www.ncbi.nlm.nih.gov/pubmed/10844015

Xu, Y., Dhingra, A., Fina, M. E., Koike, C., Furukawa, T., & Vardi, N. (2012). mGluR6 deletion renders the TRPM1 channel in retina inactive. *Journal of Neurophysiology*, *107*(3), 948–57. doi:10.1152/jn.00933.2011

Yamada, E. (1969). Some structural features of the fovea centralis in the human retina. *Archives of Ophthalmology*, *82*(2), 151–159. Retrieved from http://dx.doi.org/10.1001/archopht.1969.00990020153002

You, Y., Klistorner, A., Thie, J., & Graham, S. (2011). Improving reproducibility of VEP recording in rats: electrodes, stimulus source and peak analysis. *Documenta Ophthalmologica*, 109–119. doi:10.1007/s10633-011-9288-8

ACKNOWLEDGEMENTS

Il primo sentito ringraziamento va al Capo, Antonio Malgaroli, che mi ha dato la possibilità e gli strumenti per muovere i primi passi nel mondo della ricerca. Quindi ringrazio i compagni della barca, quelli con cui cresci e ti sostieni quotidianamente, confrontandoti e affrontando le gioie, ma sopratutto le difficoltà di questo lavoro. Grazie di cuore a Jacopo, Maddy, Mattia, Sara, Gabry, AleA, Carley, Generale e naturalmente, ultimo, ma non meno importante, grazie a Radio Montesano che ci tiene sempre compagnia. Un sentito ringraziamento va anche all'intero gruppo di Anestesia e Rianimazione – Testa-Collo dell'Ospedale San Raffaele per il supporto tecnico ed in particolare a Marco Gemma, per la sua disponibilità, l'aiuto e le interessanti chiacchierate. Grazie anche a Giuliano Ravasio, indispensabile per lo sviluppo di alcune fondamentali abilità veterinarie. Poi ringrazio i miei genitori, che hanno sempre creduto in me, dandomi la forza di andare avanti. A loro devo ogni cosa. Ringrazio anche la restante parte di famiglia, tutta, ristretta e allargata, che mi ha sempre sostenuto e su cui posso sempre contare nei momenti di difficoltà. Quindi un grazie va ai nonni (anche a chi non è più qui) e poi a Barbara, Domenico, Rosanna, Diego e ovviamente alla nuova arrivata, Martina, che non dice ancora molto e quando mi guarda più che altro ride e vomita con un fare un po' punk. Ringrazio la mia tenacia. Ringrazio gli amici, con cui ho condiviso la vita e le esperienze più importanti. È anche grazie a loro se sono diventato quello che sono; davvero grazie Mark, Loca, Buz, Teo, Roby, Gabo, Lore, Gio, Carlo, Feller, Marche, Paga, naturalmente Vinz e tutti coloro che nel bene o nel male hanno orbitato e orbitano ancora attorno a me. Grazie.